DEVELOPMENT OF A TEST PROTOCOL FOR
CYCLIC PULLOUT OF GEOSYNTHETICS
IN ROADWAY BASE REINFORCEMENT

by

Timothy Michael Holley

A thesis submitted in partial fulfillment
of the requirements for the degree

of

Master of Science

in

Civil Engineering

MONTANA STATE UNIVERSITY
Bozeman, Montana

May 2009

APPROVAL

of a thesis submitted by

Timothy Michael Holley

This thesis has been read by each member of the thesis committee and has been found to be satisfactory regarding content, English usage, format, citation, bibliographic style, and consistency, and is ready for submission to the Division of Graduate Education.

Dr. Steven Perkins

Approved for the Department of Civil Engineering

Dr. Brett Gunnink

Approved for the Division of Graduate Education

Dr. Carl A. Fox

STATEMENT OF PERMISSION TO USE

In presenting this thesis in partial fulfillment of the requirements for a master's degree at Montana State University, I agree that the Library shall make it available to borrowers under rules of the Library.

If I have indicated my intention to copyright this thesis by including a copyright notice page, copying is allowable only for scholarly purposes, consistent with "fair use" as prescribed in the U.S. Copyright Law. Requests for permission for extended quotation from or reproduction of this thesis in whole or in parts may be granted only by the copyright holder.

Timothy Michael Holley

May 2009

TABLE OF CONTENTS

TABLE OF CONTENTS - CONTINUED

LIST OF TABLES

Table Page

LIST OF FIGURES

Figure Page

LIST OF FIGURES - CONTINUED

Figure Page

LIST OF FIGURES - CONTINUED

Figure Page

LIST OF FIGURES - CONTINUED

Figure Page

ABSTRACT

Geosynthetics, or manmade materials used in soils engineering, have successfully been used as base reinforcement of pavements for over 40 years. Use of geosynthetics can result in cost savings by allowing the aggregate base layer to be reduced in thickness and/or the service life of the pavement to be extended. Design methods for this type of reinforcement have typically been developed by individual manufacturers for specific products. These methods are not widely used by state transportation agencies because 1) they are proprietary, 2) they are empirically based, and 3) they lack compatibility with the current national trend towards mechanistic-empirical pavement design procedures. This project was initiated to develop testing methods to determine one of the critical material properties needed for mechanistic-empirical base-reinforced pavement design, namely, the resilient interface shear stiffness. This property describes the interaction, in particular the shear stiffness, between the geosynthetic and the surrounding aggregate. This new test protocol closely mimics vehicular load patterns, resulting in design parameters pertinent to the use of the geosynthetics to reinforce the base course. A study was conducted to evaluate the repeatability of these tests and to develop a standardized test method. Specific parameters under investigation include load pulse and rest period duration, embedment length of the geosynthetic, and differences in results using different soils and types of geosynthetics.

Some parameters seemed to have little effect on values of resilient interface shear stiffness, while others vastly impacted the results. Load pulse and rest period durations did not affect output results significantly. Maintaining a constant confinement or shear stress during the test duration produced higher repeatability and correlated well to the adapted resilient modulus equation. Three-aperture length tests on polyester geogrid also correlated well with this equation, however repeatability was moderately low. Polypropylene geogrid and a woven geotextile confined in Ottawa sand displayed low correlation to this equation. During testing, very small displacements occur, and therefore, every effort should be made to ensure that these measurements are accurate and not skewed by electrical noise and interference.

INTRODUCTION

Design of geosynthetic reinforcement for roadways currently requires the use of factors and design charts, which have been developed by empirical methods. The design parameters have been developed by Individual highway departments and engineers through construction of test tracks or test sections of roadways to test out the behavior of geosynthetic reinforcement for certain projects. Consequently, these design methods are regionally developed, and applicable only to the specific areas and soil conditions they were developed for. In other words, a geosynthetic reinforcement design that worked at one site may not work as well on another site. Developing a purely empirical design method usually requires considerable trial and error, or construction of test tracks. Both methods require substantial funding to develop, and only lead to an understanding of how the reinforcement behaves in specific conditions.

Highway design is currently moving away from solely empirical design towards a more mechanistic-empirical (M-E) approach. This method allows for more standardized methods to be applied to a variety of conditions, since it will be based on mechanisms that work within the pavement system. The National Cooperative Highway Research Program (NCHRP) has been developing a Mechanistic-Empirical Pavement Design Guide (ME-PDG), which is designed to create nationalized M-E design methods.

As of yet, the ME-PDG does not incorporate geosynthetics for base reinforcement. In order to include geosynthetics in the M-E design process, a greater understanding of the soil-geosynthetic interaction is required. Progress is currently being made to develop mechanistic response models for geosynthetics as reinforcement, such as finite element analyses. Perkins, et al. (2004) began developing these type of models, which include parameters that describe the geosynthetic-soil interaction mechanisms. A good mechanical model of the interaction between the soil and the geosynthetic can aid in optimization of the design. However, as in any type of design, the model's accuracy and the user's understanding of the input parameters can greatly affect the output. Without an understanding of these parameters, the results of the analysis are difficult to interpret. The inputs then become random values that may or may not reflect reality, and garbage in will yield garbage out. Any model is only as good as the parameters and the values that are involved.

For the most part, the interaction between a geosynthetic and soil has been determined by use of monotonic pullout testing. While this method represents the behavior of geosynthetics used in retaining walls, slopes, and other static structures under the limit state, it does not directly portray the behavior of geosynthetics used for base reinforcement in highways. Perkins, et al. (2004) proposed using cyclic pullout tests to model a parameter termed the resilient interface shear stiffness, or G_i. This parameter is related to the M_R, the resilient modulus of unbound aggregates (NCHRP, 2004) as it is also dependent on confinement and shear stress. With respect to traffic, a cyclic loading sequence also better represents load conditions experienced by a pavement system, and therefore would be more directly applicable to geosynthetics used in roadway applications than simple monotonic testing.

This study focused on development of a test protocol to determine soil-geosynthetic interaction. A literature review was conducted to determine the types of testing methods and equipment that has been used to analyze the effect of geosynthetics in soil. A pullout box was then used to test samples of geosynthetics confined by soils. The testing regimen was designed, and then developed to assess different aspects of the materials and the test protocol itself. Finally, the data from the testing regimen was analyzed, and compiled for this thesis.

The main objectives for testing were to: refine the test protocol with respect to load pulse and rest period duration, evaluate the effects of sample length, different geosynthetics and confining aggregates on test results, evaluate repeatability between test replicates, and compare measured results to calculated results using an equation with regression constants. The testing regimen consisted of: modified test protocols, tests using two different confining soils, and timing testing. The modified test protocol aimed to single out aspects of the test protocol, such as confining stress and shear stress in order to analyze these components. Tests conducted using two different confining soils sought to analyze the affect of confining soils on test results. Finally, the timing testing aimed to isolate the rest period and load period aspects of the load pulse frequency utilized to deliver the cyclic load to the geosynthetic.

LITERATURE REVIEW

This project focused mainly on geosynthetic behavior under cyclic traffic loadings. In order to better understand the behavior of geosynthetics in soil, traditional monotonic testing was reviewed, with an emphasis on interaction parameters derived from these tests. Several different methods have been employed in attempts to determine the interaction between soils and geosynthetics. Large-scale triaxial tests, direct shear, and pullout tests comprise the most common methods. Each method has its own advantages and disadvantages, discussed below.

Methods for Determining Geosynthetic-Soil Interaction

Triaxial Testing

Eiksund et al. (2004) conducted large-scale resilient modulus tests on reinforced base course aggregate. Samples for these tests were 300 mm in diameter and 600 mm in height, with the geosynthetic placed at mid-height. Four materials were used, consisting of a polypropylene geogrid, a woven polypropylene film, a PVC coated woven polyester grid, and composite polyester grid and non-woven polypropylene. Results from these tests did not display a significant difference in resilient modulus between geosynthetic-reinforced and unreinforced aggregates. Permanent deformation results were relatively variable, and may have been influenced by small variations in properties between samples. The study also concluded that reinforcement has a lesser effect when confinements are relatively high. The study showed that the reinforcement restrained lateral strain above and below the geosynthetic by a distance of 150 mm.

The triaxial test has the potential to be most representative of field conditions (Lee and Manjunath, 2000), with the ability to vary confinement and load initiated at the top of the soil specimen. The resilient modulus test for unbound aggregates is already standardized, and cyclic triaxial testing of reinforced aggregate closely resembles the established test procedure. This type of testing describes the interaction between a column of soil and geosynthetic reinforcement, and yields a resilient stiffness of the soil column. Problems inherent with this method arise with partial apertures for geogrids puncturing the rubber membrane, creation of a circular sample, and an issue of dealing with the partial apertures in calculations.

Direct Shear Testing

Direct shear testing of the soil/ geosynthetic interface has received more attention than the triaxial test method. Traditional, relatively small-scale direct shear devices were unable to accommodate geosynthetic testing (Ingold, 1982), requiring a larger scale device. For direct shear tests involving a geosynthetic in between soil, sagging from the confinement load placed on top of the specimen is likely, and would yield inaccurate test results. Therefore, most direct shear tests are conducted using a geosynthetic sample secured to a rigid block or spacer (Lee and Manjunath, 2000) in order to avoid complications caused by sagging geosynthetics. Figure 1 shows the general arrangement of a large scale direct shear test. Since these tests are conducted with a rigid block on one side of the geosynthetics, the test can only measure frictional resistance of the top of the sample. In reality, and in pullout testing, both sides of the geosynthetic resist movement, along with bearing resistance of transverse ribs in geogrids. Strength properties from direct shear testing yield lower results than that of pullout testing due to neglecting this bearing resistance (Nejad and Small, 2005).

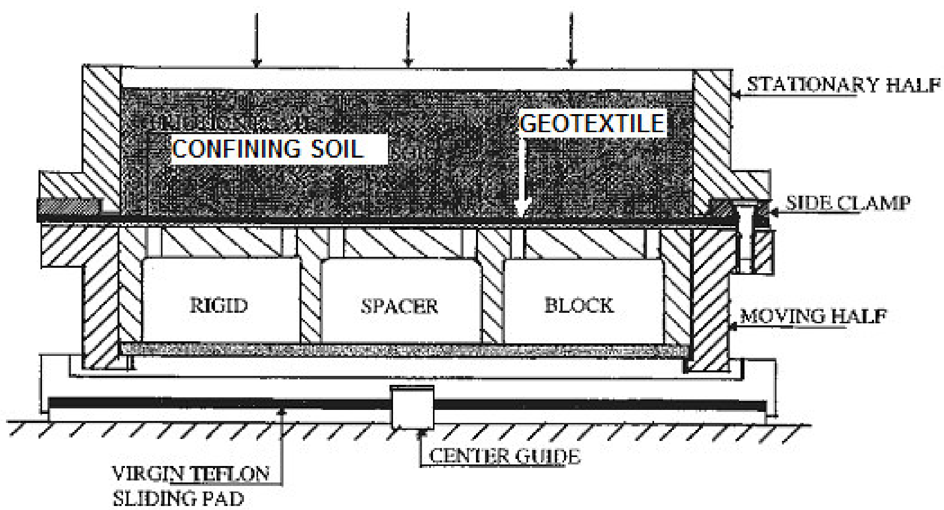

Figure 1. Large-scale direct shear test apparatus cross section (Lee and Manjunath, 2000).

Pullout Testing

For many years, pullout testing has been used to analyze the interaction between soils and geosynthetics. This method allows the geosynthetic sample to be confined completely by soil, unlike most direct shear testing that has been conducted. Jewell et al. (1984) presented three main geosynthetic/ soil interaction mechanisms that occur:

1. Frictional resistance from shear between the soil and planar surfaces of the geosynthetic along the direction of movement,
2. Passive Bearing resistance from geosynthetics with material normal to the direction of movement (i.e., geogrids), and
3. Soil-on-soil shear resistance within apertures/ openings

Pullout testing allows these three interaction mechanisms to develop, and may expedite their development by applying loading directly to the geosynthetic rather than the soil. The inclusion of mechanisms 2 and 3 results in much greater values of strength properties from pullout testing than large scale direct shear testing of the soil/ geosynthetic interface.

The majority of pullout tests performed have been in a monotonic fashion. These types of tests represent a load in a single direction, such as frictional reinforcement for retaining walls. A testing standard, ASTM D6706 (2004), has been developed to standardize this method of testing. Cyclic pullout testing has received some attention, but mainly for analysis of seismic loading in retaining walls. Limited cyclic pullout testing has been conducted to determine the behavior of geosynthetics used in roadway applications.

Pullout Testing Apparatus

Pullout Box

Most pullout testing mentioned herein utilized relatively large scale equipment for testing. Outer dimensions of these pullout boxes ranged from approximately 0.6 x 0.4 x 0.4 m (Ochiai et al., 1996) to 1 x 1 x 1 m (Palmeira and Milligan, 1989). The geosynthetic sample and clamping device extend through a slit from the front, and non-extensible wires attached to the embedded geosynthetic exit through a slit in the back to some type of displacement measuring device. The geosynthetic is confined by soil above and below, with additional confinement provided through an expandable bladder and reaction frame. A typical layout of a pullout box is displayed as Figure 2, with components identified as: (1) frame; (2) steel plate; (3) air bag; (4) electric engine; (5) reducer; (6) load cell; and (7) electric jack.

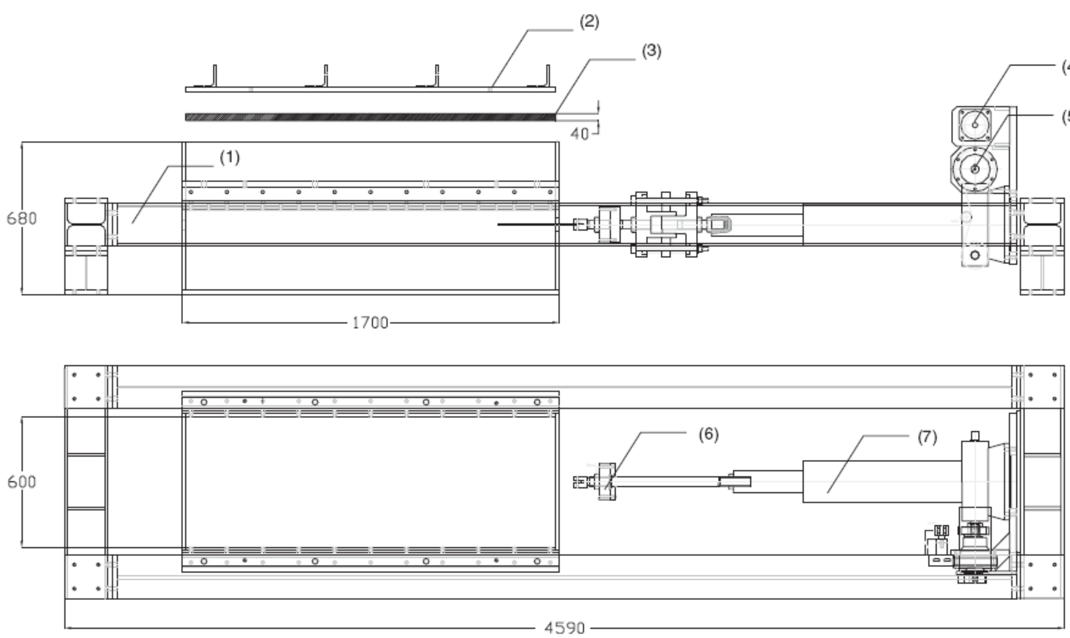

Figure 2. Typical pullout test apparatus (Moraci and Recalcati, 2006)

Cuelho and Perkins (2005) modified a large-scale pullout box to enable use of smaller geosynthetic samples and less confining soil. The soil volume was reduced to 90 cm wide, 60 cm long by 30 cm high. Use of a smaller geosynthetic sample should allow the entire sample to be engaged during cyclic loading, without developing large strains that occur during monotonic testing, to ensure that the sample exhibits elastic behavior. Large strains and plastic behavior of the geosynthetic would lead to failure of the specimen, and difficulty in repeatability. A reduction in soil volume also reduces test preparation time. Figure 3 shows a cross-section of the modified pullout box used by Cuelho and Perkins (2005).

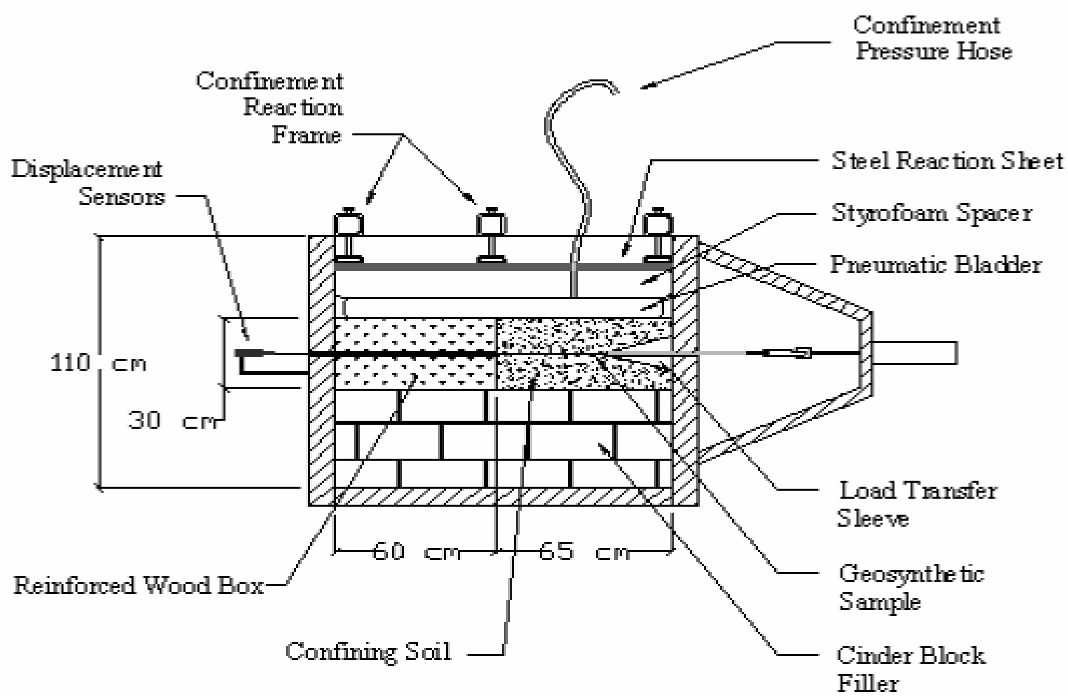

Figure 3. Cross-sectional view of modified pullout box (Cuelho and Perkins, 2005).

Loading Device

The majority of pullout tests conducted have been in monotonic fashion. Since these types of tests require a steady rate of displacement in only one direction, a screw- driven or electric jack type of loading device seems to be the most common (Alagiyawanna et al., 2001; Cuelho, 1998; Moraci and Recalcati, 2006; Yasuda et al., 1992.) A pneumatic type of load applicator was used by Cuelho and Perkins (2005), and some studies incorporated a servo-hydraulic loading apparatus, which is able to provide better control for cyclic and/ or monotonic loading (Raju and Fannin, 1998,Aloabadi et al., 1997.).

For cyclic pullout testing, the type of loading device utilized should be able to produce a steady load pulse during both loading and unloading. Screw-drive and electric jack type systems may be able to apply a steady load at slow frequencies, but could be uneven at higher frequencies. Pneumatic load devices should be able to apply a more rapid load cycle, but could also be prone to a more erratic application, depending on the internal components. A servo-hydraulic cylinder provides the most consistent cyclic load application among the types of load devices encountered (Raju and Fannin, 1998).

<u>Clamping Device</u>

Various clamping devices have been used to connect the geosynthetic specimen to the actuator. Three example types are listed below.

1. Geosynthetic extends from inside the box and clamp is mounted directly to the geosynthetic (Raju and Fannin; 1998, Lopes and Ladeira; 1996; and Voottipruex et al, 2000).

2. Clamp mounted inside the box and attached directly to the geosynthetic (Alfaro et al, 1995; Farrag et al.;1993, Moraci and Recalcati, 2006; Moraci et al., 2004).
3. Geosynthetic is glued to sheet metal plates which extend from inside the pullout device to the loading device (Cuelho 1998; Cuelho and Perkins 2004; Min 1995; and Wilson-Fahmy 1994).

Clamp style 1 creates a simple connection between the load actuator and the geosynthetic sample. With this method, the geosynthetic extends beyond the soil confinement. Due to the extensibility of geosynthetics, the load applied to the embedded sample is likely less than that applied to the sample at the clamp in-air. This method seems more suitable for monotonic testing, as the possibility of engaging the entire embedded sample is more likely, as the sample is loaded at a constant rate in a single direction. For cyclic testing, however, it could be difficult to engage the embedded sample completely as the sample loads and unloads, dependent on the magnitude and rapidity of the load application.

The second clamp style has two distinct advantages, in that it assures a constant embedment length for the duration of the test, and yields direct measurement of the front of the sample as measured at the clamp (Moraci and Recalcati, 2006). Due to the clamp also being confined by soil, preliminary tests must be conducted for calibration, so that the frictional resistance of the clamp is not included in determination of the soil/ geosynthetic interaction properties. This type of device has been used only for monotonic testing. For cyclic testing, calibration of the internal clamping device may prove more difficult, as well as disturbing the confining soil greatly.

The third method was employed for this study, continuing from Cuelho and Perkins (2004). By bonding the geosynthetic between two thin metal plates, the specimen can be aligned so that the entire exposed geosynthetic is embedded in the confining soil at the beginning of the test. The metal plates should be rigid enough to transfer loading energy directly to the geosynthetic. Also, with the entire geosynthetic initially confined by soil, measurements at the leading edge of the metal plates can be used to determine the loss of geosynthetic area due to amassed unrecoverable pullout.

Cyclic Pullout Testing

Test protocols for most of the studies evaluating the pullout of geosynthetics under cyclic loading have mostly reflected that of monotonic testing. The main difference encountered is that the cyclic loading then results in a change from a displacement-controlled test to a load-controlled test. The geosynthetic is then loaded in increasing stress increments until failure occurs, while maintaining a single constant confinement pressure.

Load Pulse Duration

Raju and Fannin (1998) applied loads at 0.1 and 0.01 Hz. These load pulses are much slower than those measured from traffic loads. The slow rates used appear to be due to equipment limitations, and mainly for primary investigation of cyclic pullout behavior. Ten cycles of loading were applied at a constant level, then loading was increased, and ten more cycles of loading applied to the sample, continuing until the geosynthetic sample ruptured. A sinusoidal wave function was used to control the load pulse, with no rest in between load applications. The cyclic loading process used is depicted in Figure 4. They concluded that pullout resistance under cyclic loading may be independent of frequency. However, their data was limited to two relatively slow load frequencies. Ashmawy and Bourdeau (1996) stated that load frequency should affect the stress-strain response of geosynthetics in soil, due to a viscous, time-dependent behavior inherent in these materials.

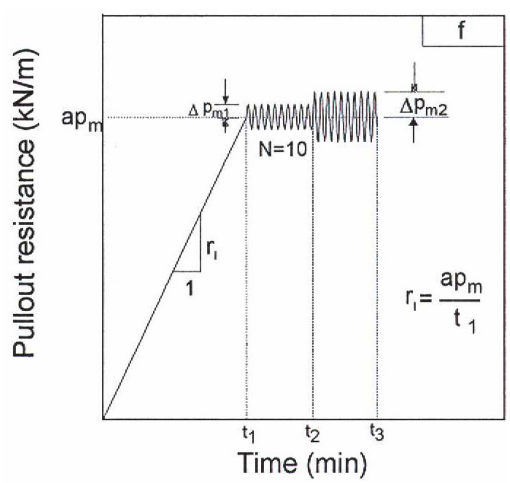

Figure 4. Loading schematic for cyclic loading (Raju and Fannin, 1998).

Yasuda et al. (1992) also conducted pullout tests on geogrids with different confining soils to compare to seismic action. The load frequency utilized in the study was not mentioned. Similar to Raju and Fannin (1998), loads were applied at twenty cycles per amplitude. Load amplitude was then increased until the geogrid pulled out or was torn.

The test method developed by Cuelho and Perkins (2005) attempted to incorporate a load pulse similar to that used in the resilient modulus test, a haversine shape. The pulse shape was determined by Barksdale (1971) and later confirmed by the Virginia Smart Roads project (Al Qadi et al., 2004) to be representative of induced stresses in a road subgrade subjected to traffic loading. The haversine equation is:

$$y(t) = \sin^2\left(\frac{\pi}{2} + \pi * \frac{t}{d}\right) \qquad (1)$$

where t is time, and d is the duration of the pulse (Al-Qadi et al., 2004).
The load pulse is depicted graphically in Figure 5. There is a load pulse duration, consisting of an increase in load with a haversine shape, increasing from $P_{contact}$ to P_{cyclic} and then reducing back to $P_{contact}$, at which point a rest period begins while $P_{contact}$ is maintained. For the base/ subbase, a load pulse duration of 0.1 seconds was specified, and a load pulse duration of 0.2 seconds for subgrade materials. A rest period was added to each load pulse to equal a complete cycle time of 1 second, i.e. 0.1 second load, 0.9 second rest. For granular materials with no plasticity, the rest period may be reduced to 0.4 seconds to reduce testing time (NCHRP, 2004).

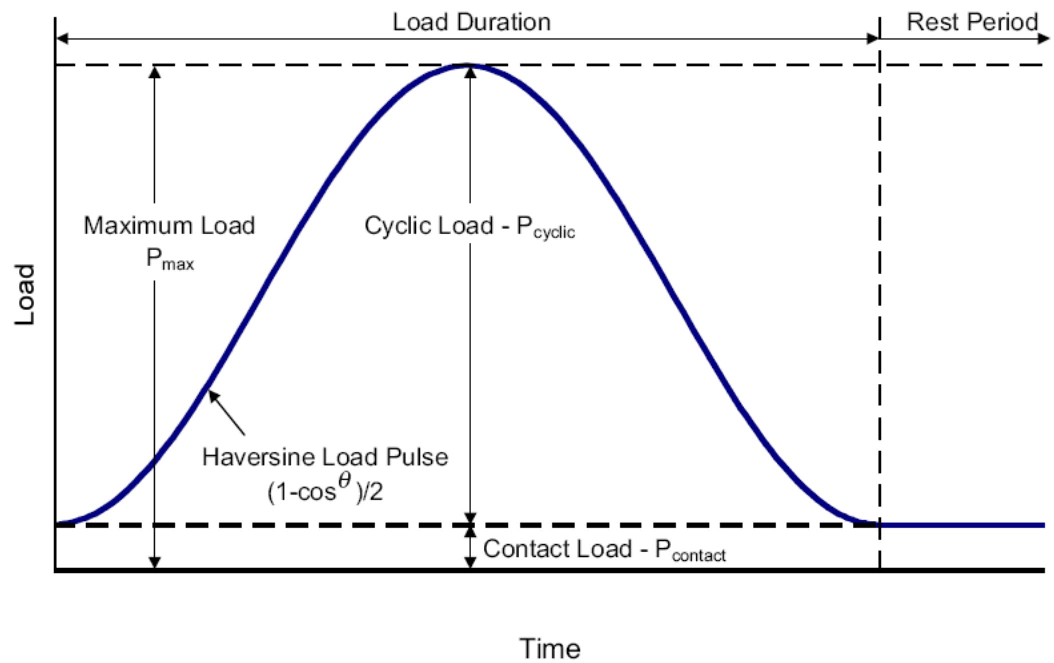

Figure 5. Definition of load pulse (NCHRP, 2004).

Due to complications with the original pneumatic loading apparatus, a 0.2 second load pulse akin to the resilient modulus test was not attained by Cuelho and Perkins (2005). Load pulses were then developed that most closely reflected a haversine-type shape. For the most part, a load pulse duration of 1.3 seconds was applied.

Rest Period Duration

The majority of cyclic pullout tests conducted in the literature utilized sinusoidal load pulses. These pulses did not incorporate a rest period as discussed above. The only testing encountered that included a rest period was conducted by Cuelho and Perkins (2005). A rest period of 0.5 seconds was generally used for testing. This rest period was deemed acceptable on the basis that they used a relatively large, poorly graded aggregate ($^3/_4$ inch washed rock). This aggregate was compacted dry, so therefore additional rest time was not necessary to allow soil pore water pressures to stabilize.

Geosynthetic-Soil Interaction Properties

Monotonic Pullout Interaction

ASTM D6706 (2004) establishes use of pullout resistance for monotonic testing. The standard uses two equations for this parameter, one for geosynthetics without apertures (geotextiles, geomembranes, reinforcing strips), and one for geosynthetics with gridlike structures (geogrids and similar). The need for two equations results from variations among gridlike geosynthetics with regard to the amount and orientation of ribs in the sample affecting its pullout behavior.

For geotextiles and geomebranes, pullout resistance is calculated as:

$$P_r = \frac{F_p}{W_g} \tag{2}$$

For geogrids, etc:

$$P_r = \frac{F_p \times n_g}{N_g} \tag{3}$$

where:

P_r = pullout resistance, kN/m,

F_p = pullout force, kN,

W_g = width of geosynthetics, m,

n_g = number of ribs per unit width of geogrid in the direction of the pullout force, and

N_g = number of ribs of geogrid test specimen in the direction of the pullout force

An interaction shear modulus (G) has also been used to quantify the soil geosynthetic interaction by Cuelho (1998). This parameter is derived from the slope of the shear stress versus shear displacement, and calculated as follows:

$$G = \frac{\Delta\tau}{\Delta(\Delta_t)} \quad (4)$$

$\Delta\tau$ = change in shear stress, and

$\Delta(\Delta_t)$ is the change in shear displacement.

<u>Cyclic Pullout Interaction</u>

Results from both displacement controlled tests in monotonic fashion, and load controlled tests in cyclic fashion from Raju and Fannin (1998) are shown in Figure 6. It should be noted that the displacements were measured at the clamp outside of the pullout box, so that the geosynthetic was partially buried within the box, and partially extended outside of the box. From this data, it was concluded that the maximum pullout resistance during cyclic loading was approximately 20% less than that in monotonic loading.

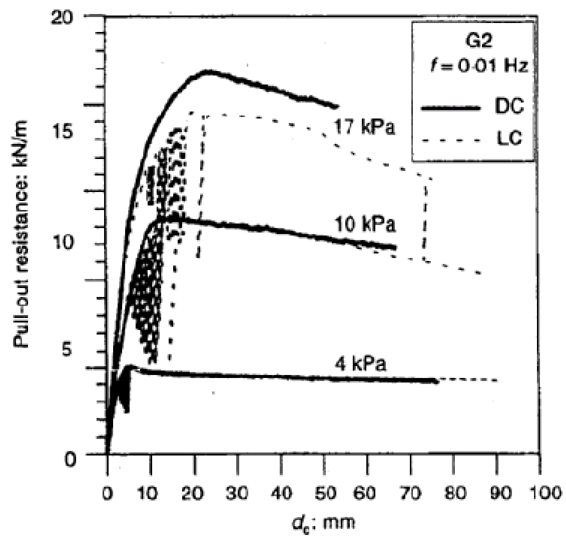

Figure 6. Cyclic Load-Control (LC) and Displacement Control (DC) results. (Raju and Fannin, 1998).

From Figure 6, a resilient stiffness can be calculated by using the slope of the loading and unloading curves. The pullout resistance in kN/m was converted to a stress, dividing by the specimen width of 0.5 m. This then results in resilient stiffnesses of 2.50 E+6 kPa/m, 8.00 E+6 kPa/m, and 10.0 E+6 kPa/m for confinements of 4, 10, and 17 kPa, respectively. Comparison was also made between the displacement at the clamp (Figure 7), and displacement of the embedded sample. The results showed a lag in displacement of the embedded sample, and then a generally linear relationship as the sample was engaged in the soil. During this lagging period, the behavior being described could be more the behavior of the geosynthetic outside the box, and less the actual behavior of the embedded geosynthetic.

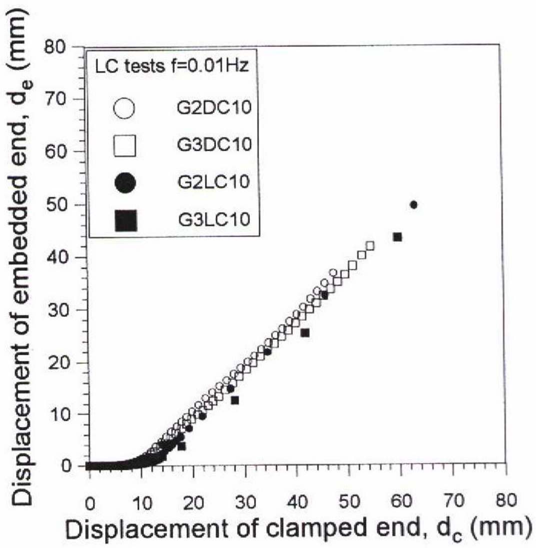

Figure 7. Comparison of displacement at the clamped end and embedded end of two geogrids (Raju and Fannin, 1998).

Yasuda et al. (1992) compared the maximum pullout force under cyclic loading to the maximum pullout force from monotonic tests in order to assess the difference in strength properties between the two conditions. Test results were expressed as ratios, with the maximum dynamic pullout force, Tdf,h divided by the maximum pullout force in monotonic testing, Tsf versus the initial pulling load, Ti divided by Tsf. Typical results for these tests are shown in Figure 8. Contrary to Raju and Fannin's (1998) findings, the maximum pullout force in cyclic loading appears greater than that of the maximum pullout force in monotonic loading. The more dense sample (SR-2) appears to have a lower maximum dynamic pullout force as compared to the sample at a relative density of 30%, SS-2. This may have been due to soil particles in the less dense sample rearranging and developing more inter-particle friction, while the more dense sample's soil particles were less likely to move, and failure developed more plastically.

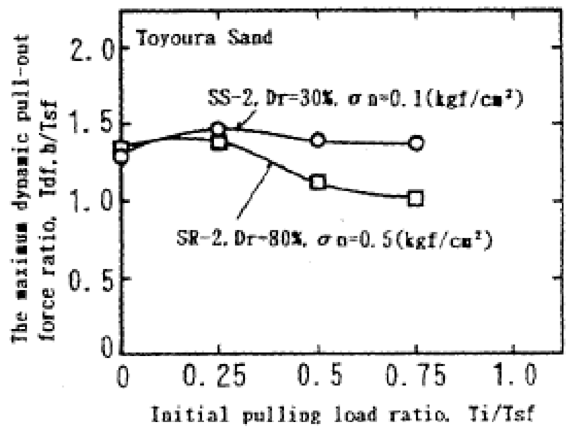

Figure 8. Typical test results under cyclic loading (Yasuda et al., 1992).

A resilient interface shear modulus, G_i, was calculated by Cuelho and Perkins (2005). This parameter is related to M_R , the resilient modulus for unbound aggregates, and is calculated by dividing the cyclic shear stress at the soil-geosynthetic interface by the relative resilient displacement of the geosynthetic in the last 10 cycles of load application for each load step. Figure 9 depicts the calculation inputs for G_i graphically.

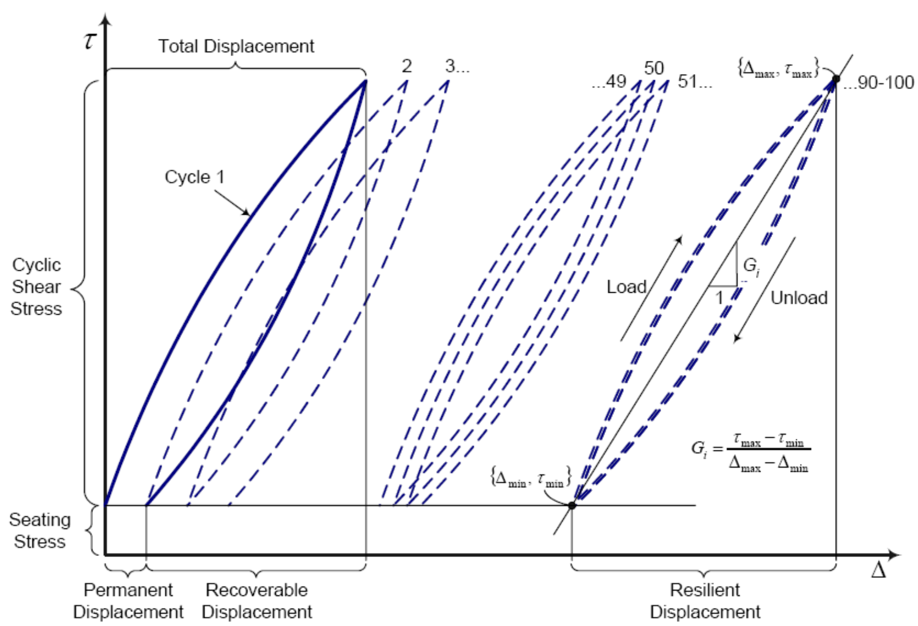

Figure 9. Illustrated calculation of G_i (Cuelho and Perkins, 2005).

At low shear loads, results for G_i were very large, mostly due to the very small magnitude of the sample displacements. Due to these small displacements, any error in measurement could greatly affect the results. Figure 10 shows results of G_i versus shear stress by each confinement level. These results are approximately one order of magnitude less than those calculated above using Raju and Fannin's (1998) data.

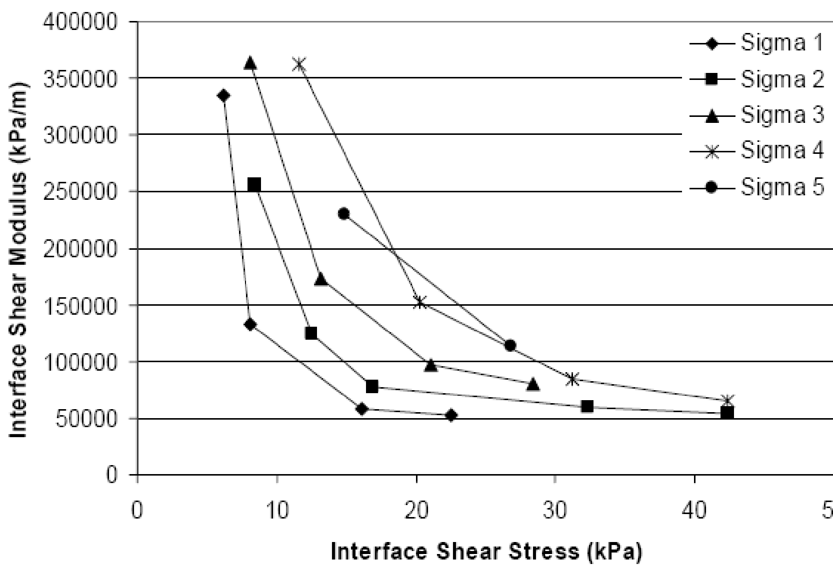

Figure 10. Interface shear modulus vs. interface shear stress for various confinements (Cuelho and Perkins, 2005).

Cuelho and Perkins (2005) also adapted the resilient modulus equation, shown below, in order to further investigate the soil-geosynthetic interaction.

$$M_R = k_1 \cdot p_a \cdot \left(\frac{\theta}{p_a} \right)^{k_2} \cdot \left(\frac{\tau_{oct}}{p_a} + 1 \right)^{k_3} \qquad (5)$$

In this equation, p_a is the atmospheric pressure (101.3 kPa), θ is the bulk stress ($\sigma_1 + 2\sigma_3$), τ_{oct} is the octahedral shear stress $\left(\sqrt{2}/3\right) \cdot (\sigma_1 - \sigma_3)$, and k_1, k_2, and k_3 are dimensionless regression constants corresponding to material properties, where k_1 and $k_2 \geq 0$ and $k_3 \leq 0$. The equation used for G_i is very similar, except that σ_i, the normal stress on the soil-geosynthetic interface replaces the bulk stress, and τ_i, the interface shear stress, replaces the octahedral shear stress. The initial p_a term becomes P_a, atmospheric pressure divided by a unit length of 1 meter, or 101.3 kPa/m to ensure consistent units throughout the equation (Cuelho and Perkins, 2005). This results in:

$$G_i = k_1 \cdot P_a \cdot \left(\frac{\sigma_i}{P_a}\right)^{k_2} \cdot \left(\frac{\tau_i}{P_a} + 1\right)^{k_3} \tag{6}$$

Test results were then used to optimize k_1, k_2 and k_3 for each test by using a statistical regression. A comparison of the calculated and measured values of G_i for one test on one geosynthetic is shown in Figure 11. Cuelho and Perkins stated that the adapted equation for G_i showed good promise to be useful for determining the soil-geosynthetic interface interaction property.

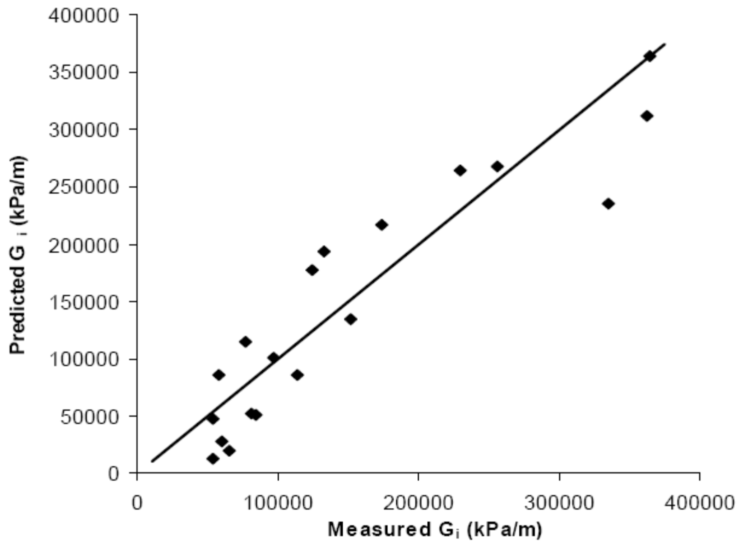

Figure 11. Predicted vs. Measured G_i (Cuelho and Perkins, 2005).

EQUIPMENT

Pullout Box Apparatus

The pullout box is a large steel box with walls of reinforced steel, designed originally for full-size pullout testing of geosynthetics. Currently, the interior of the box is filled with bricks on the bottom and a wooden box in the back to reduce the interior dimensions. Figure 12 shows a side view of the pullout box, and Figure 13 shows the pullout box in plan view.

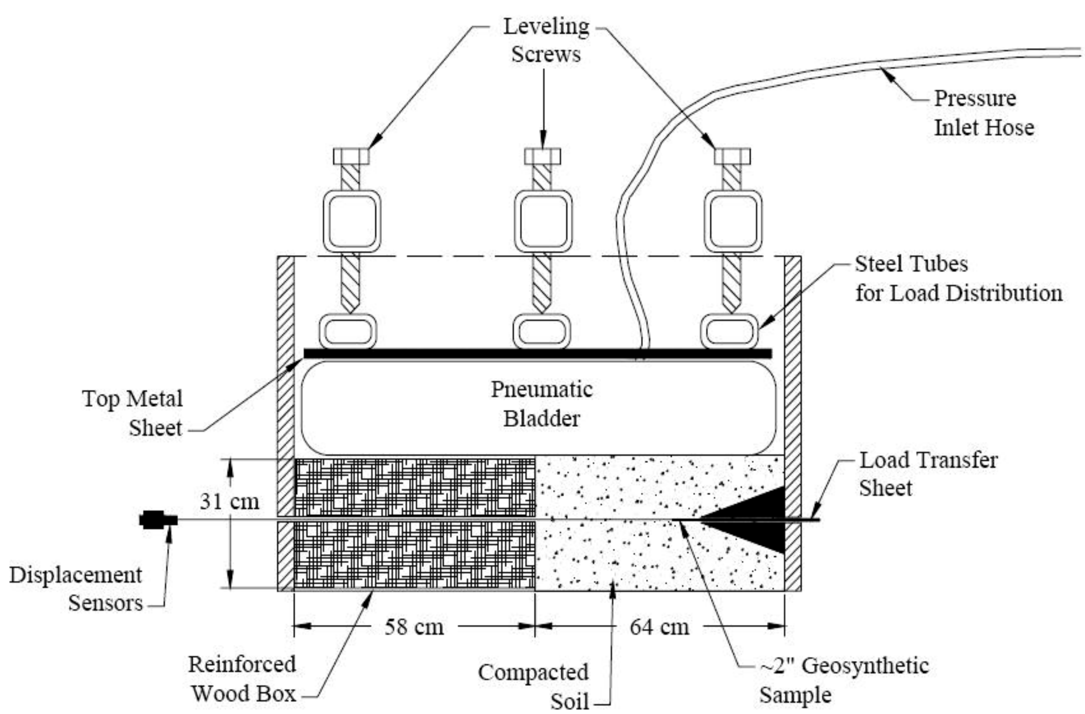

Figure 12. Cross-sectional side view of pullout box.

A pneumatic bladder is placed between the top metal sheet and the soil to provide confinement to the soil and a reaction frame consisting of rectangular steel tubing with leveling screws atop the box. A slit on the front of the box at mid-height allows insertion of the sample, and at the mid-height rear of the box is another slit to accommodate lead wires attached to the geosynthetic, and used to measure displacement.

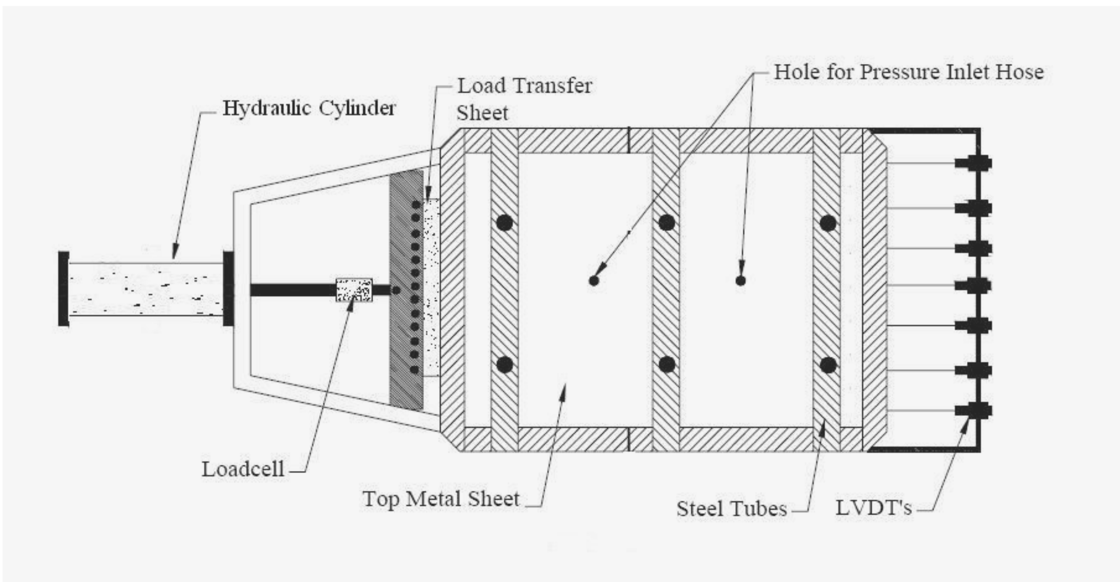

Figure 13. Plan view of pullout box.

The angle brace at the front of the pullout box can accommodate several different loading devices. For the testing conducted in this thesis, a servo-hydraulic cylinder (MTS 244.21S), shown in Figure 14, was used. This cylinder was capable of applying loads accurately at a more rapid pace (at a rate of 34 in/sec and maximum 40,000 psi) than the previous systems, which consisted of either a screw-type jack or a pneumatic cylinder. A Hydraulic Power Unit (HPU) provides hydraulic pressure needed to operate the cylinder.

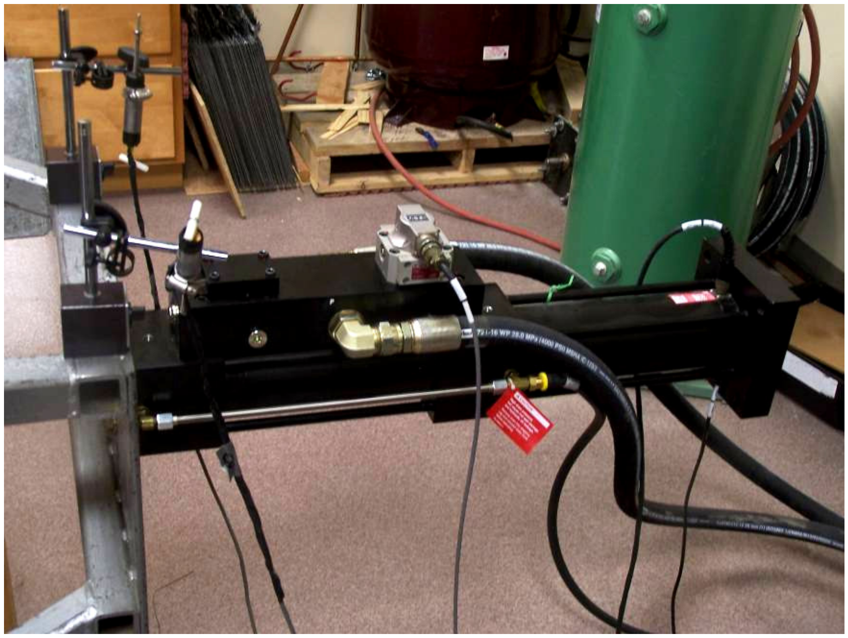

Figure 14. Servo-hydraulic load cylinder.

Instrumentation

Data collection was coordinated through a dedicated Personal Computer (PC) loaded with software to control the servo-hydraulic cylinder. A controller coordinated and conditioned signals from various sensors incorporated into the test. These sensors are: Linear Variable Displacement Transducers (LVDTs) that measure displacements of the geosynthetic, an Electro Pneumatic Regulator (EPR) which controls the air pressure to the pneumatic bladder, load from the load cell attached to the hydraulic ram, and displacement measured from the servo-hydraulic cylinder's position sensor. During load-control tests conducted for this research, the controller monitored signals from the 10,000 pound capacity load cell and adjusted the signal to the servo-hydraulic cylinder. This load cell has an accuracy to within 10 pounds, and is relatively stout for the loads applied in normal testing, however, stiffer geosynthetic-soil interactions may require greater loads to develop stresses along the sample. Applied loads are also generally greater than the sensitivity of the load cell. Stainless steel lead wires attached to the geosynthetic were run to the LVDTs in the rear of the box. Small diameter brass tubes housed the lead wires from the sample to the rear of the box to maintain a straight line between the LVDT and the geosynthetic, while allowing the wires to move freely. Without these tubes, the lead wires would be distorted by the stresses in the confining soil. The LVDTs were attached to magnetic bases (Figure 15) to allow for ease of adjustment, by simply moving the base toward or away from the pullout box in order to set the LVDT within testing ranges.

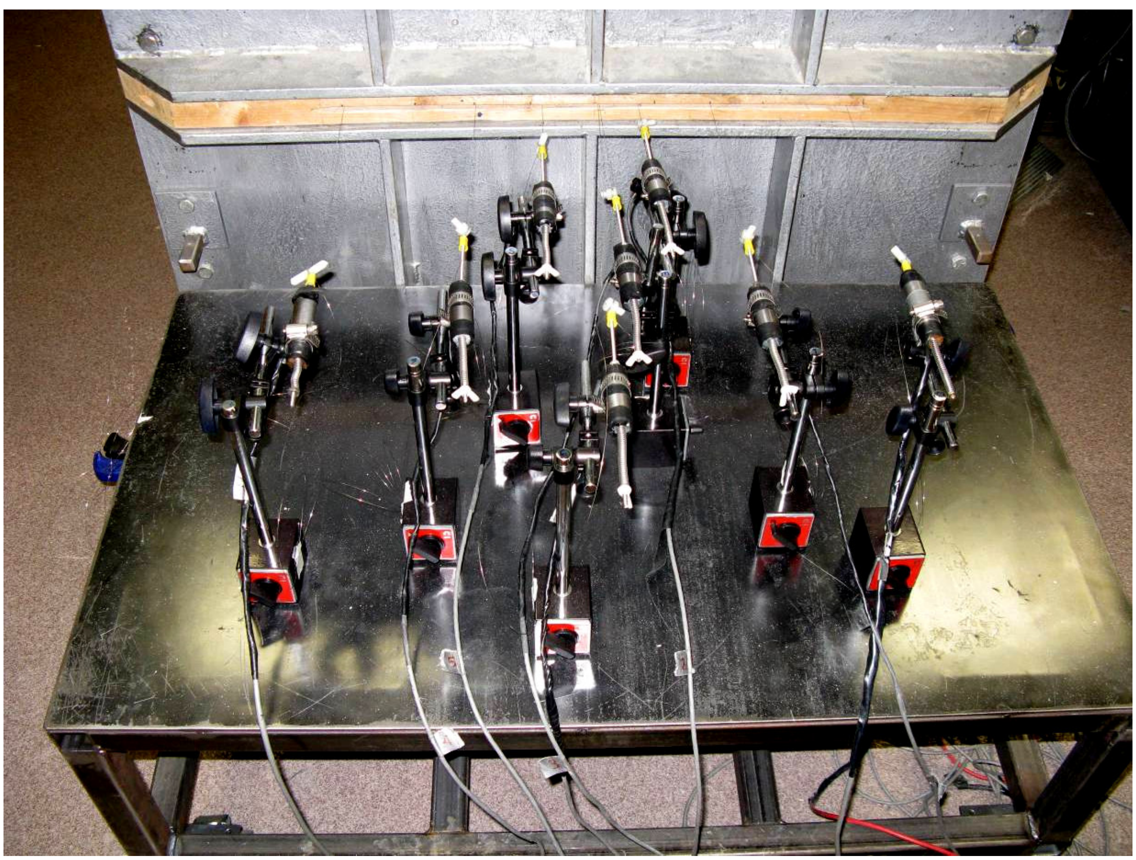

Figure 15. LVDTs with magnetic bases and cart.

The LVDT signals were run through conditioning boxes prior to reaching the controller, and calibrated for a small range of displacement. This results in each LVDT having a sensitivity to 0.001 mm, in order to measure the very small displacements that develop at the rear of the sample during testing. Both the LVDTs and EPR have power distributed via circuits in an electrical box (Figure 16).

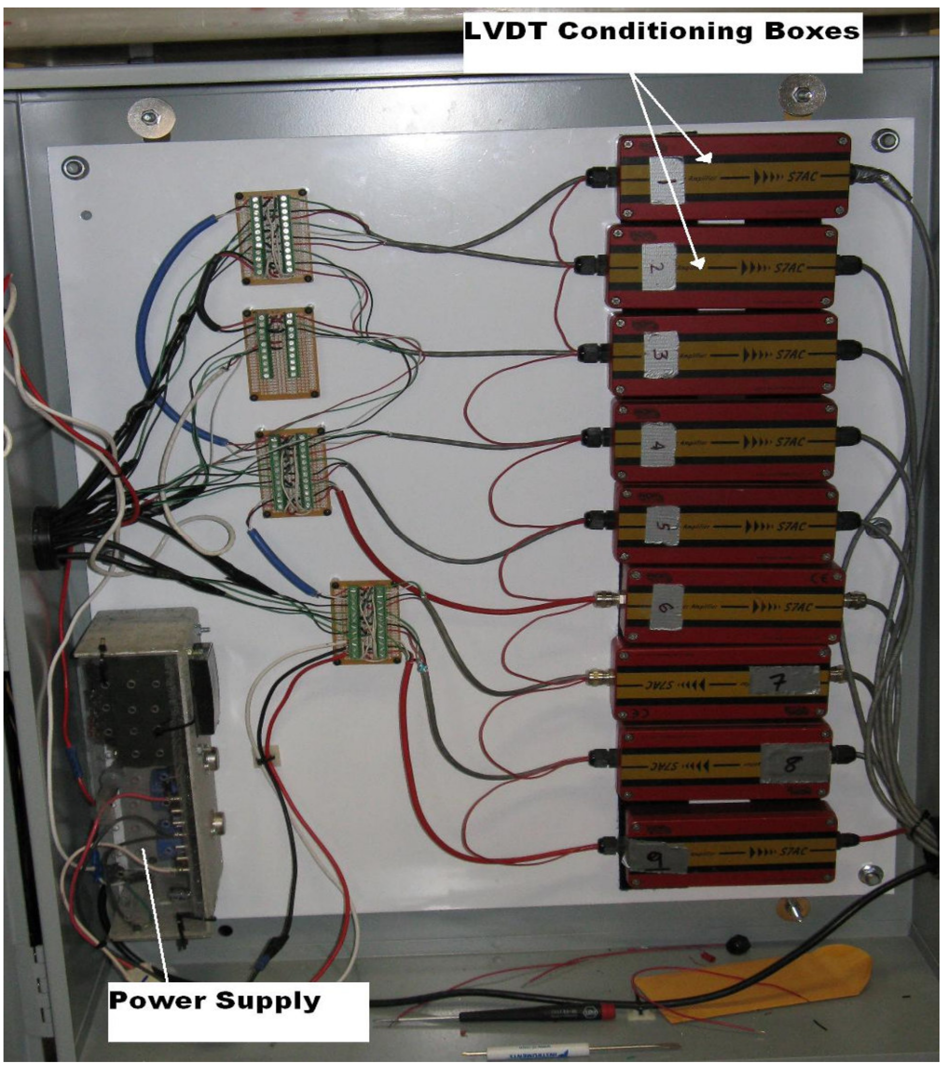

Figure 16. LVDT Conditioners and Electrical Box.

Soils and Soil Preparation

To compact the soil, a 10”x10” pneumatic plate compactor was used. The soils were compacted in a dry state to reduce the influence of fluctuating moisture content. Both soils used in testing were tested for density in a smaller box using the plate compactor, and in a loose state. Aggregate 1, an Ottawa Sand, had a loose density of 100 pcf and dry compacted density of 110 pcf, with a gradation as shown in Figure 17. Aggregate 2, a coarser sand denoted as golf chips aggregate, had a loose density of 103 pcf and a dry compacted density of 118 pcf. The gradation for this soil is shown in Figure 18. Since the soils were compacted in a dry state for testing, maximum density testing (which requires moistening of the sample) was not performed. Finally, to facilitate easier extraction of the soil with less risk of damage to the embedded geosynthetic, an industrial vacuum with a HEPA filter attachment was used. The HEPA filter helps reduce the amount of fine particles released into the air as the soil is evacuated.

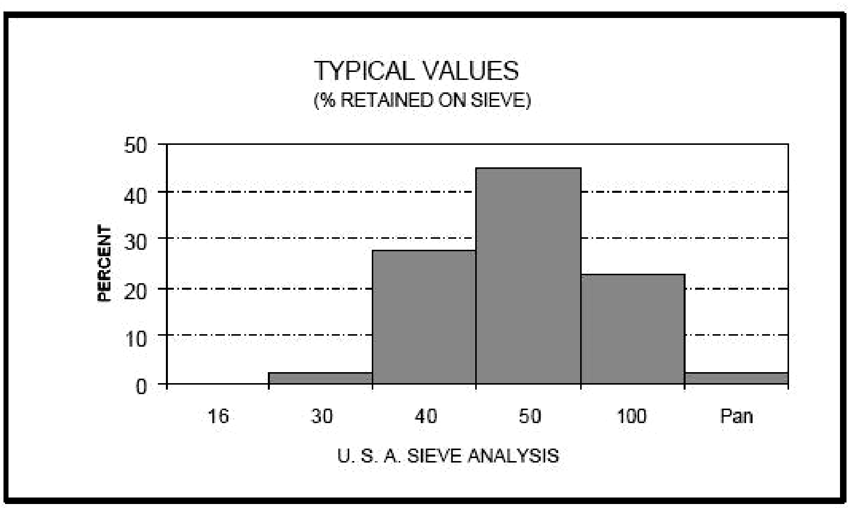

Figure 17. Aggregate 1 gradation.

Aggregate 1 was composed mainly of rounded silica particles. The Ottawa sand was obtained from Ottawa, Illinois, and designated as ASTM Graded Ottawa Sand. This aggregate is readily available as testing sand for tests such as sand cone density, so a test protocol utilizing the Ottawa sand may increase uniformity between testing facilities. The coefficient of uniformity (Cu), a measure of the uniformity of a soil gradation, was 1.9 for the Ottawa sand, indicating a uniform gradation. The friction angle for this soil was 30 degrees.

Aggregate 2 was composed of angular crushed gravels. The “golf chips” aggregate (Aggregate 2) is so named as it is a byproduct from production of golf sand for golf courses. Golf chips were obtained from Knife River Corporation in Bozeman, MT.This aggregate had a Cu of 6.7, indicating a nonuniform gradation. A larger particle size was hoped to provide more frictional resistance at the soil-geosynthetic interface, and the presence of some fines in the gradation was hoped to result in a more dense confining soil than the Ottawa sand. Direct shear testing of this soil produced a friction angle of approximately 52 degrees. This value seems fairly high, but it was likely a product of the larger particles becoming wedged in the apparatus, which would restrict movement of the shear box and result in a greater value.

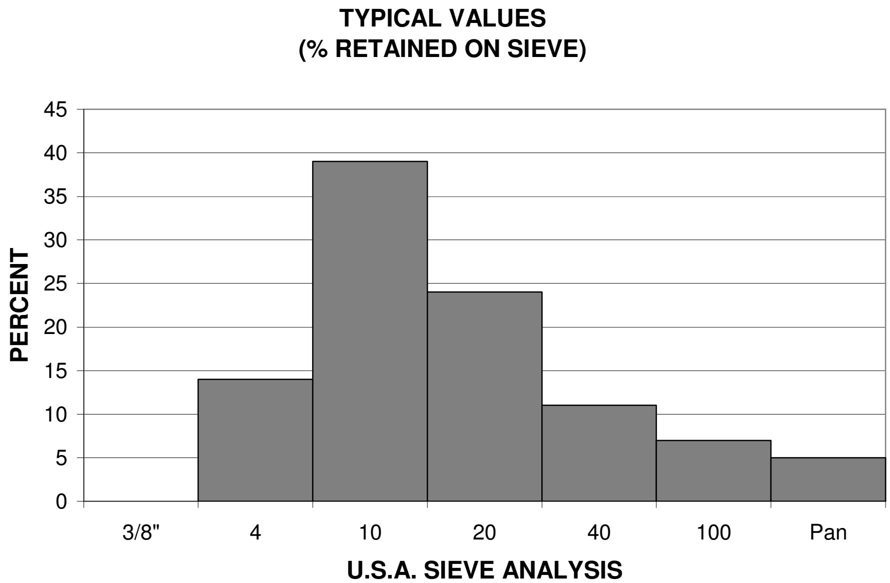

Figure 18. Aggregate 2 gradation.

Geosynthetic Materials and Sample Preparation

Three geosynthetics were utilized in this study, two biaxial geogrids and one woven geotextile. Properties of these materials are shown below in Table 1.

Table 1. Geosynthetic material properties.

Product	Type	Composition	Aperture Size (mm)	Tensile Strength (kN/m)		
				2% Strain	5% Strain	Ultimate
Secugrid 30 30 Q1	Vibration-welded Biaxial Geogrid	Polypropylene (PP)	32x32	12	24	30
Secugrid 30 30 Q6	Vibration-welded Biaxial Geogrid	Polyester (PET)	32x32	13.5	24	30
Mirafi HP 570	Woven Geotextile	Polypropylene (PP)	0.6	14	35	70

Samples were cut from the rolls in the cross-machine direction (XMD) with the reasoning that in a roadbed, this would be the direction experiencing the majority of the load applied by traffic. Geogrid samples were cut to widths of 13 apertures (approximately 480-490 mm) and approximately 350 mm in length. Geotextiles were cut to 500 mm in width, and approximately 400 mm in length. The samples were then glued to sheets of 20 gauge steel, in a manner so that either 2 or 3 apertures of the geogrid (80 or 120 mm), or 80 mm for the geotextile extended beyond the long edge of the sheet. Stainless steel lead wires were then attached to the geosynthetic through small holes hand-drilled into the sample. These wires were then turned back on themselves and secured with conduit to ensure a rigid, stable connection. A typical sample layout is shown in Figure 19.

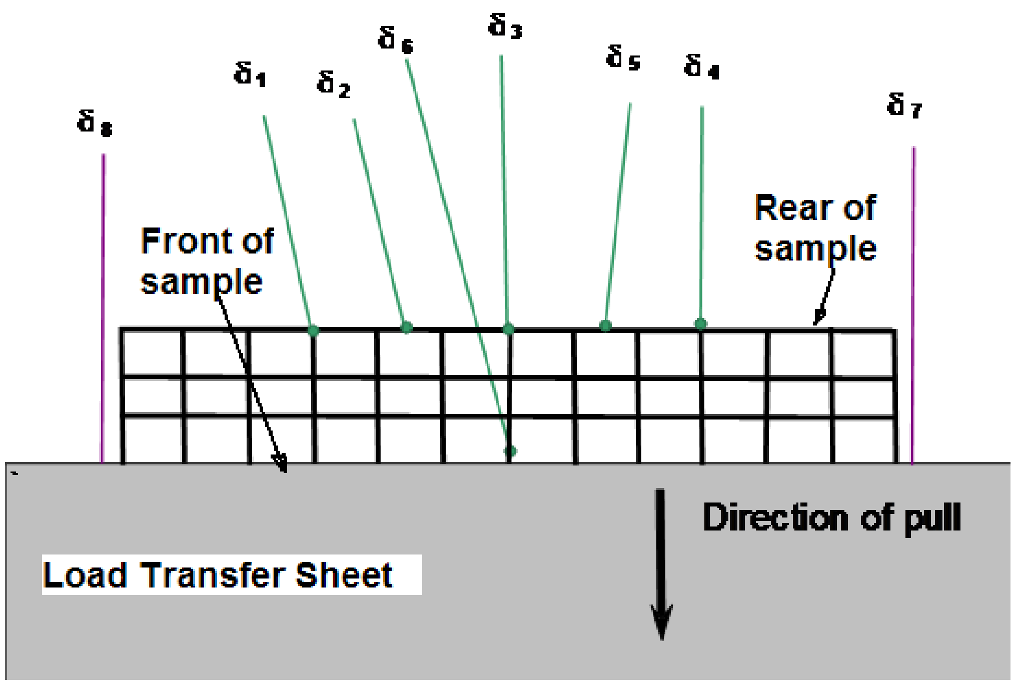

Figure 19. Typical sample layout.

Two LVDTs, δ_7 and δ_8, are attached to the sheet metal to measure the displacement at the very front of the sample. Of the remaining six LVDTs (δ_1 to δ_6), five are attached to the back of the sample. Displacement of the rear of the sample should indicate full engagement of the geosynthetic. The remaining

LVDT , δ_6, is attached to the middle of the sample just rearward of the sheet metal. This allows measurement of the strain between the sheet metal and the very front of the geosynthetic, as well as between the very front of the geosynthetic and the back of the sample. These values can then be compared to determine engagement of the sample in the confining soil and stress development during testing between the front and rear of the sample.

GENERAL PROCEDURE

Test Protocol

This project continued the study conducted by Cuelho and Perkins (2005) which modified the monotonic pullout standard by utilizing aspects from the resilient modulus of unbound aggregates test, in an effort to produce a test applicable to geosynthetics in roadbeds subject to repeated traffic loadings. The loading schedule consists of a series of sequence groups (SG) and confinements (σ). The geosynthetic specimen undergoes a conditioning step, and then is subjected to six loading sequences shown in Figure 20, based on a theoretical failure line.

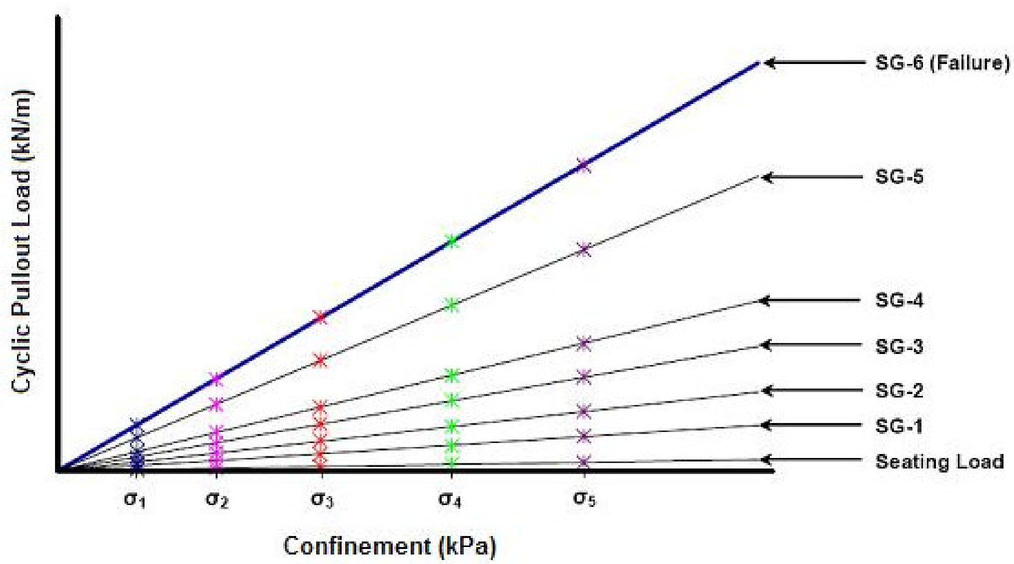

Figure 20. Cyclic pullout loading sequence (Cuelho and Perkins, 2005).

Each sequence group line is a certain percentage of an assumed ultimate failure line, SG-6, according to the percentages shown in Table 2. The line SG-6 is determined by an assumed interaction friction angle between the geosynthetic and the confining soil. Similar to a friction angle in unreinforced soil, an interaction friction angle is an estimate of the ability of the geosynthetic-aggregate interface to resist movement during shearing. Theoretically, each point on the failure line should be the combination of applied load and confinement that will produce gross pullout. Determination of this angle is mostly empirical, with an increase in estimated friction angle indicating an anticipation of greater pullout resistance between the aggregate and the geosynthetic.

Table 2. Sequence group loads (Cuelho and Perkins, 2005)

Load Level	Percentage of Estimated Failure Load
Seating Load	2.8
SG-1	9.7
SG-2	16.7
SG-3	30.6
SG-4	44.4
SG-5	72.2
SG-6	100

Five levels of confinement are used, (σ_1 to σ_5) equal to 15.5, 31.0, 51.7, 77.6, and 103.4 kPa. After cycling the geosynthetic through an initial load step, or conditioning step, the test begins at the point defined as (SG-1, σ_1). At this step, the load is cycled from the value at that confinement along the seating load line to the value on the SG-1 line. After the application of 1000 cycles, the confinement is increased to σ_2, and the loads are cycled between the seating load and SG-1 line corresponding to that confinement, and so forth. Once the σ_5 loading is completed for SG-1, confinement is then reduced back to σ_1. The loading process then begins again using values from the SG-2 line for the maximum cyclic load, followed by SG-3, 4, 5, and 6.

For each test, stresses were calculated for each load step according to the sequence group and confinement based on the estimated interface friction angle, sample length, and sample width. These stresses are then converted to force inputs for the testing apparatus. These force inputs are simply the applied shear stresses multiplied by the area of the geosynthetic sample. This is due to the fact that the load cylinder is designed to apply force, and does not calculate stress internally. Unless otherwise specified under individual test descriptions, a 0.2 second load pulse followed by a 0.5 second rest period for each load application was used for each cycle, with a total of 1000 load cycles per load step applied.

One polyester and one polypropylene geogrid, along with a woven polypropylene geotextile were used for testing, along with two confining aggregates. The first aggregate used was a graded Ottawa sand. A second, more angular aggregate designated as 'Golf Chips' was used. Sample length and width, interface friction angle, and attachment to the load cell were also varied within the testing regimen, with the specifics for each test series shown in Table 3.

Table 3. Test parameters and designations

Test Designation	Aggregate	Geo-synthetic Type	Interface Friction Angle (degrees)	Apertures/ Length	Width (mm)	Attachment to Load Cell
A-1 - A-6	1	PP	41	3	N	SP
B-1, B-2	1	PP	41	2	N	SP
B-3	1	PP	41	2	R	SP
B-4	1	PP	41	2	N	D
C-1 - C-3	1	PE	38	2	N	D
D-1, D-2	1	GT	41	80 mm	N	D
D-3 - D-5	1	GT	43	80 mm	N	D
E-1, E-2	2	PP	50	2	N	D
E-3, E-6	2	PP	53	2	N	D
Confinement	2	PP	N/A	2	N	D
Shear	2	PP	N/A	2	N	D
Intermediate	2	PP	53	2	N	D
Timing 1	1	PP	41	3	N	D
Timing 2	2	PP	53	2	N	D
Rest 1	1	PP	41	3	N	D
Rest 2	2	PP	53	2	N	D

Aggregate:	1= Ottawa Sand 2= Golf Chips
Geosynthetic Type:	PE= Polyester geogrid PP= Poly propylene geogrid GT= Woven geotextile
Width:	N= Normal, 486-502 mm R= Reduced, 246 mm
Attachment to Load Cell:	SP = Steel Plates (Load Transfer Plates) D= Direct

Data Analysis

Preliminary results were obtained by using the maximum and minimum (max/min) points for each cycle from the data acquisition system. However, it was found that these values were somewhat erratic at lower confinement and shear stresses. This was likely due to a source or sources of vibration and/or electronic interference during testing. It was observed during testing that the operation of the hydraulic system would propagate some vibration in the pullout box, which was likely transferred to the lead wires and the LVDTs. When measuring small displacements during rapid loadings, outside interference such as this vibration has the potential to greatly affect the data, as seen in Figure 21. In order to interpret the data, plots were made of applied shear stress versus displacement using timed data collected at 200 Hz. In other words, data was recorded once every 1/200 second.

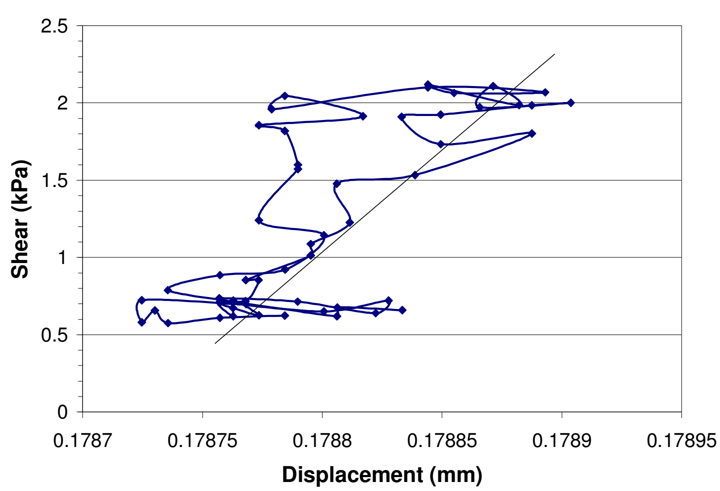

Figure 21. Timed data and Gi hand calculation at lower loads.

The timed data plots were then used to obtain an approximate slope between cyclic shear stress and displacement, which defines G_i. For load steps with low confinements and low applied shear stresses, an exact slope was difficult to determine, as noise and variability greatly affected the interpretation of the data. Figure 21 shows an example of these plots and a rough estimate of the slope from one cycle. As applied shear stress increased, the data began to reflect the expected loading and unloading curves, as shown in Figure 22.

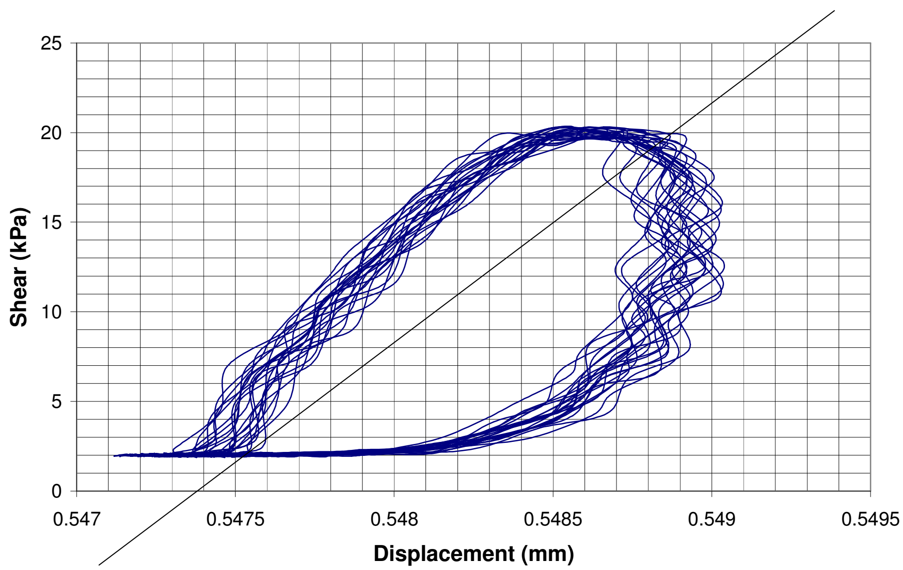

Figure 22. Timed data with higher applied shear stress.

Some variation was likely due to error from user interpretation by using the graphical method to determine G_i. However, this was more accurate than simply relying on the max/min values recorded by the data acquisition system. The max/min values did not reflect the behavior displayed by the 200 Hz timed data. During lower sequence groups and confinements, the data was much more susceptible to error from interference/disturbance, which is where the most erratic results occurred. At these lower levels, values for G_i obtained by hand were approximately between 5 to 45 times greater than those obtained from the max/min calculations. At higher sequence groups and confinements, the graphical values for G_i were closer (approximately 0.8 to 2.2 times greater) to those calculated using the recorded max/min values.

For each test, regression analyses were performed using the lab data to obtain k-values from the equation developed by Cuelho and Perkins (2005) presented earlier as Equation 6. These k-values were input into the equation for each load step to obtain a calculated value for G_i. R-squared (R^2) statistics were then applied to determine how well the equation predicted the measured values for each test. The R^2 statistic describes how well the predicted values reflect trends in the actual values measured from the lab data. An R^2 value close to 1 indicates a good relationship between the calculated and measured values, while values close to zero indicate very little relationship between the two. This statistic is calculated as follows:

$$R^2 = \left[\frac{\sum (x_i - \bar{x})(y_i - \bar{y})}{(n-1)s_x s_y} \right]^2 \tag{7}$$

Where, in this case, x_i is the measured value of G_i, for a particular load step, y_i is the calculated value of G_i, for a particular load step, $\bar{x}$ is the mean of the measured G_i for the test, $\bar{y}$ is the mean of the calculated G_i for the test, n is the number of values for the test, and s_x and s_y are the standard deviations for the measured and calculated G_i, respectively. The R^2 values only characterize the relationship between actual test data and theoretical values within a particular test.

To measure repeatability between test replicates, a Coefficient of Variation (Cv) was calculated for each k-value. This statistic is a measure of variation relative to the mean of a sample set, calculated as follows:

$$Cv = 100 * \frac{s_x}{\bar{x}} \tag{8}$$

Where s_x is the standard deviation and $\bar{x}$ is the mean of the specific k-value. Cv is expressed as a percentage, with a lower value indicating a higher amount of repeatability, or less variation between test replicates. A higher value indicates a lesser amount of repeatability, due to greater variation between replicates.

MODIFIED PROTOCOL TESTING

In order to evaluate the original test protocol itself, several modified tests were designed and executed. These tests consisted of restructuring the protocol in order to observe the influences of individual components. Single variables were identified, and then the tests were conducted with the goal of allowing only the specified variable to influence the geosynthetic's behavior. Whereas the majority of testing dealt with the materials in the test, several tests focused on the components of the protocol itself, such as confinement, and shear stress, and load pulse and rest period duration.

Confinement Testing

In order to observe the geosynthetic-aggregate interaction behavior due to change in confinement, uniform maximum and minimum cyclic shear stresses were applied to a polyester geogrid in confining aggregate 2. One test utilized an applied shear stress of 16 kPa akin to the load step SG2-C3, while the second test utilized a greater applied shear stress of 35 kPa, akin to the load step SG4-C3. Confining stress was then decreased from 159 kPa to 15.5 kPa in varying increments, with 250 applications of shear stress for each confinement step. By utilizing a consistent cyclic shear stress within each test, the influence of confining stress on G_i could be observed.

Figure 23 depicts the results from two tests where confinement was decreased while applied cyclic shear stresses were held constant. As expected,

G_i decreased as confining stress decreased. This is due to the stiffening effect of granular soil with increasing confinement. Higher applied shear stress yielded consistently lower values of G_i as a result of greater mobilized displacements of the geosynthetic. Based on these results, tests utilizing the original protocol should result in increasing G_i as confinements increase. With confinement as the only variable, this was the case.

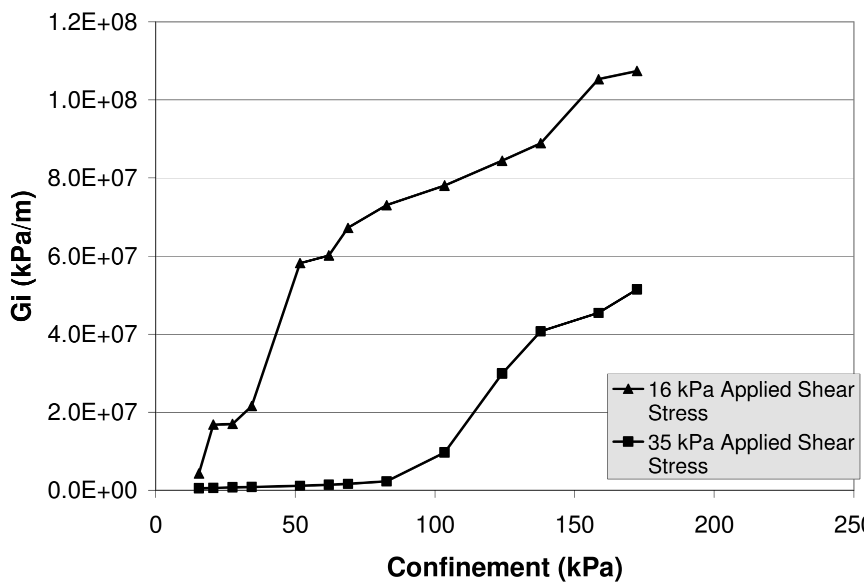

Figure 23. Confinement testing results.

Shear Testing

This series of tests involved maintaining a constant confinement while increasing the applied shear stress on a polyester geogrid confined by aggregate 2. Since the original protocol changed confinement stress and cyclic shear stress with each step, a possibility existed that the considerable decrease in confinement between sequence groups could have some effect on test results.

Therefore, the original protocol was rearranged by confinement as opposed to sequence group; i.e. instead of SG-1, C-1 followed by SG-1 C-2, the order would be C-1 SG-1, then C-1 SG-2.

Test results for two replicate tests are shown in Figure 24. The number in parentheses indicates the replicate number, 1 or 2. Except for the initial point for 15.5 kPa Confinement SG 1-3, the results displayed a decrease in G_i as shear stress increased. The shear stresses applied were derived from sequence groups 1 through 3 of the original protocol, with the first three confinements (15.5, 31.1, and 51.7 kPa). This makes it difficult to compare the results between confinements, as the applied shear stresses were different. However, results between each replicate were relatively consistent. G_i increases with increasing confinement, with the exception of the first point of the 15.5 kPa confinement test 1.

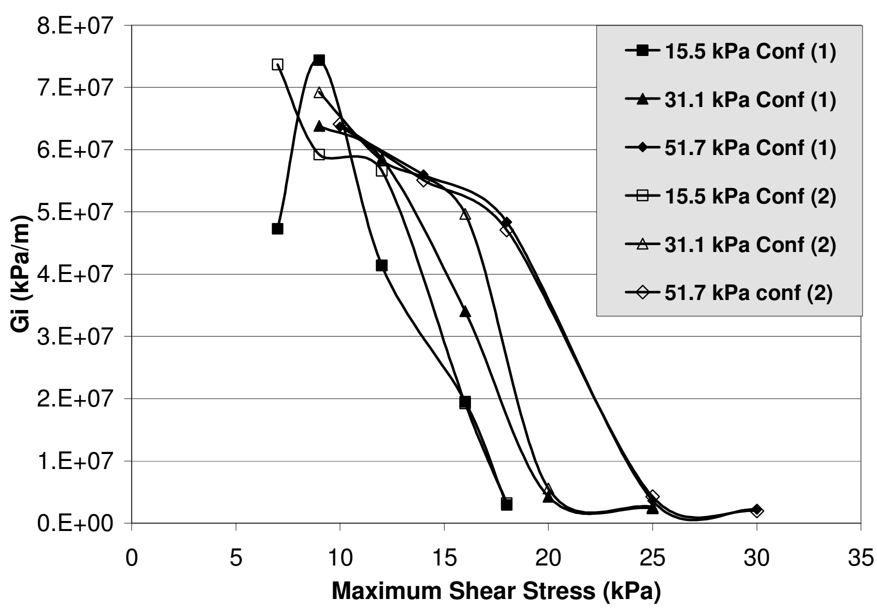

Figure 24. Shear testing results.

By focusing on the individual parameters of shear stress and confinement, it was shown that the geosynthetics behaved as expected. With increased shear stress, G_i decreased. Logically, as greater shear stresses are applied, greater displacements would occur within the geosynthetic sample, which would result in a decrease in G_i. Also, as confinement increases G_i should theoretically increase, due to less displacement occurring over the sample length. The overall results suggest that shear stress may have a greater effect on G_i than confinement, since G_i was observed to change more rapidly with changes in shear stress. Values of k_1, k_2, and k_3 were determined for each test using Equation 6. The results and the R-squared values (R^2) between the calculated and measured G_i are shown in Table 4.

Table 4. K-values for shear and confinement testing.

Test	k_1	k_2	k_3	R2
Confinement (16 kPa)	4.21E+07	0.707	-25.6	0.95
Confinement (35 kPa)	4.82E+07	0.754	-23.6	0.96
Shear (1)	4.72E+07	0.622	-28.8	0.95
Shear (2)	4.95E+07	0.632	-24.7	0.98
Cv (%)	6.9	9.3	8.6	

The R^2 statistics help to show how accurately the equation presented earlier for G_i predicted the actual values measured during testing. Both the confinement and shear tests showed a high level of correlation between the test results and the predicted behavior, with R^2 values greater than 0.95. K-values were also consistent between tests, with coefficients of variation (Cv) of 7%, 9%, and 9% for k1, k2, and k3, respectively between the four test replicates. Figure 25 displays a comparison between the calculated and measured values of G_i for the confinement testing, with a 1:1 line drawn for comparison. The same comparison is made in Figure 26 for the shear testing. As also shown by the R^2 values, the test results correlate well with the calculated results.

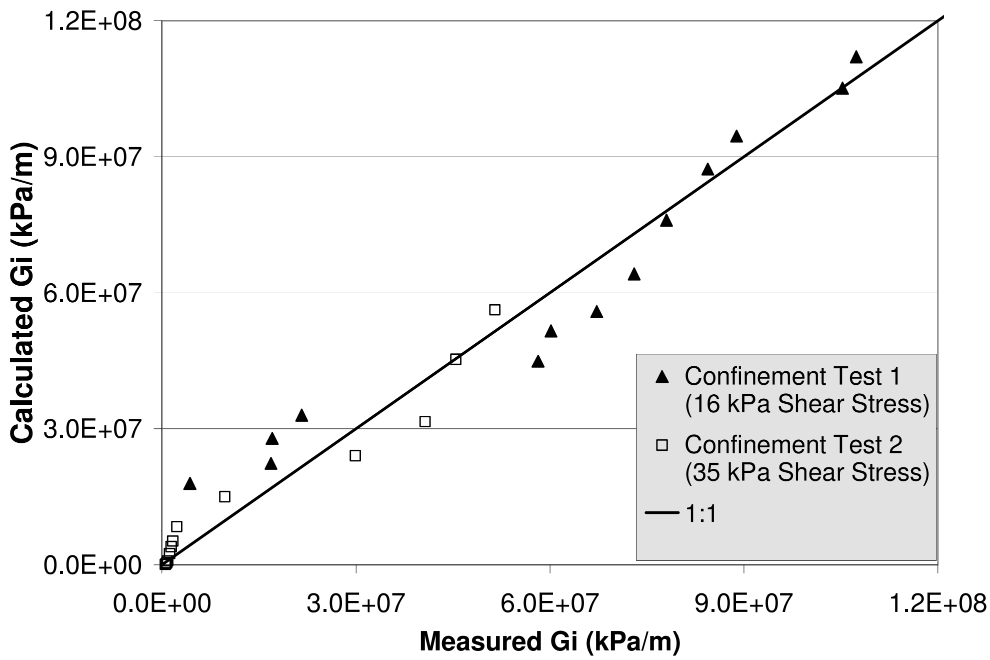

Figure 25. Calculated vs. Measured Gi for confinement testing.

From these results, it can be concluded that these types of tests where one parameter (shear stress or confinement) is held constant, while the other is varied show a high amount of repeatability and correlation to the adapted resilient modulus equation. Further testing of this type with other geosynthetics and confining aggregates should be conducted to determine if results are consistent with other geosynthetics and confining aggregates.

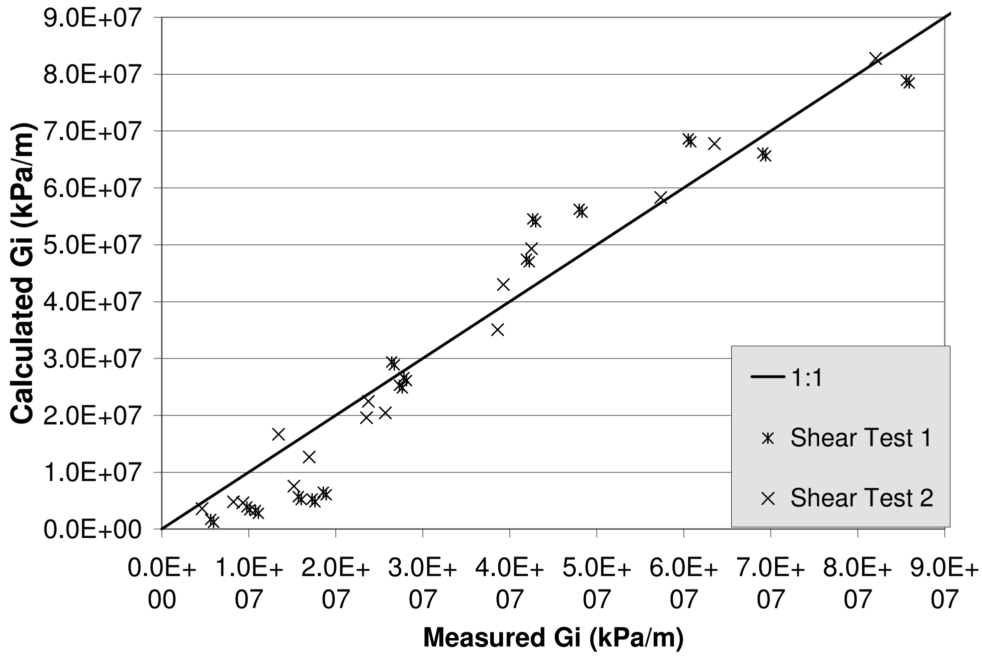

Figure 26. Calculated vs. Measured Gi for shear testing.

Intermediate Testing

Preliminary analysis of the overall test data seemed to suggest that G_i might increase with increased shear stress and confinement during early sequence groups, then reach a peak strength, at which point it would decrease with increased shear stress and confinement. In order to investigate the existence of this behavior in between sequence groups, an intermediate testing protocol was proposed that would use the same materials as the confinement and shear tests, a polyester geogrid confined by aggregate 2. The objective for this analysis was to investigate the geosynthetic-soil interaction at intermediate loads, and to compare the behavior with these loads to that of the earlier protocol. However, later analysis suggested that this behavior was likely due to the amount of noise in the data, and not reflective of a true material behavior.

This protocol consisted of combinations of shear stresses that lie in between the established protocol sequence groups. Two intermediate groups were added, labeled SG1.5 and SG2.5, and Sequence Groups 4, 5, and 6 were abandoned for these tests. SG 1.5 consisted of applied maximum shear stresses that were halfway between sequence groups 1 and 2. Likewise, applied shear stresses for SG2.5 were halfway between sequence groups 2 and 3.

Measured values of G_i from these tests are shown in Figure 27. Regression analysis for the k-values yielded 8.20 E+05, 0.502, and -16.2 for k_1, k_2, and k_3, respectively. These results and behaviors are similar to other series of tests conducted using the original protocol for this study. As shear stress increases, G_i decreases, and as confinement increases, G_i increases. Again, shear stress seems to have a greater influence on G_i than confinement. From this data, no apparent odd behaviors exist between sequence groups that would require further analysis. Therefore, use of the intermediate sequence groups 1.5 and 2.5 is not necessary and is not recommended for future testing. Utilizing the same sequence groups from the original protocol will give a broader range of loadings, which would be helpful in understanding the interaction behavior of the geosynthetic in the confining soil.

The R^2 value for this testing was 0.65, indicating that there is some relation between the equation for G_i and the measured results, though it is not a significantly strong one. Since the loads used in this series of test were relatively low, noise in the displacement data had a greater impact on the overall results. The calculated values (Calc) are also shown in Figure 27 and grouped by confinement. These results show a parabolic curve with a shallower slope at lower maximum shear stress than that of the measured values. The predicted behavior from Equation 6 reflects the general trend of the measured behavior, but is lacking in accuracy for predicting actual values.

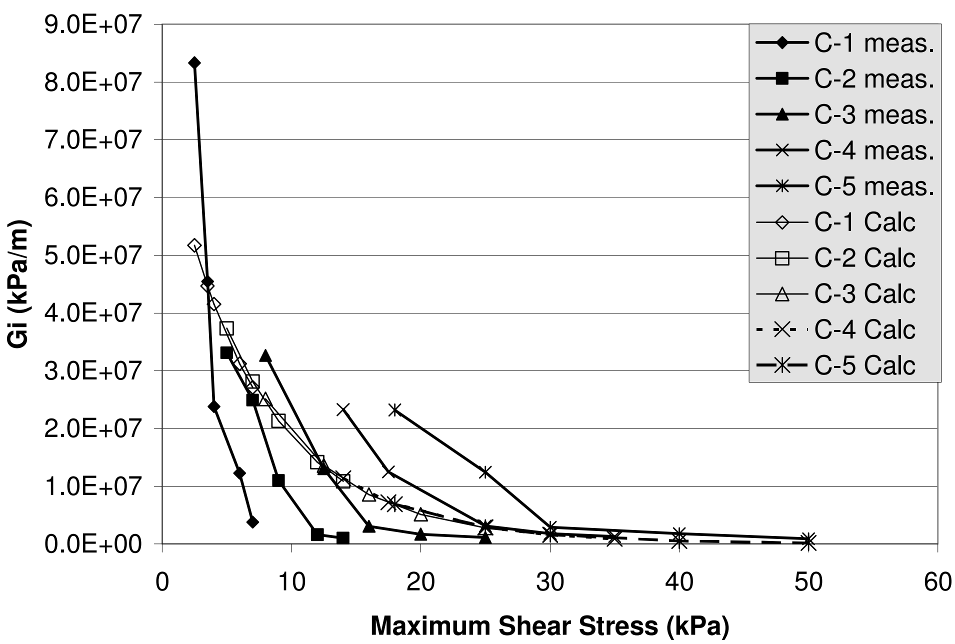

Figure 27. Intermediate testing protocol results.

A comparison of the measured and calculated values from this test is shown in Figure 28. The line extending from the origin represents a 1:1 ratio between the measured and calculated values. The most significant difference between measured and calculated values can be observed at SG-1, C-1, as shown as the point at approximately (8.30 E+07, 5.20 E+07). After this initial point, the data is less variable. Omitting values for this point increases the R^2 value to 0.70. With later testing, SG1-C1 presents itself as more of an outlying data point, and R^2 values were then calculated with this point omitted. The variation that is inherent in this particular load step is due to the low applied stress and very low displacements.

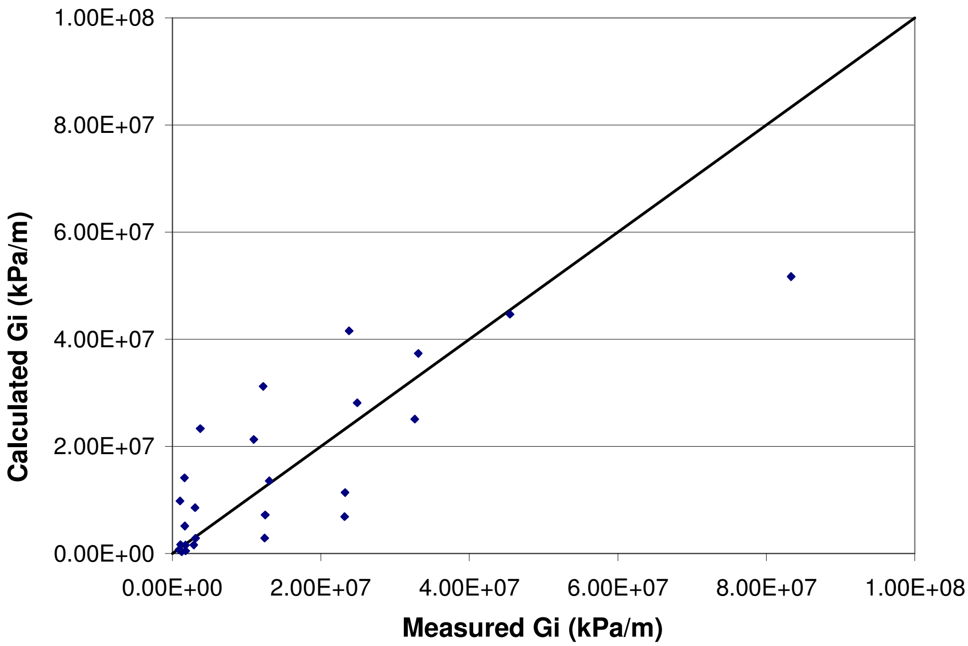

Figure 28. Calculated vs. measured Gi for intermediate test protocol.

AGGREGATE 1: OTTAWA SAND

Aggregate 1 utilized in this testing was an Ottawa Sand. It was hoped that this sand would minimize the variability of results due to the confining aggregate, mainly due to the small particle size and cohesionless characteristics of the sand. Ottawa Sand was selected due to its universal availability, and use for other types of soil property testing. The main drawback to this aggregate was that silica particles have low frictional characteristics, with a friction angle of approximately 30 degrees. All three geosynthetics were tested in this soil.

Three Aperture Geogrid (PET) (A-Series)

For this series, the PP geogrid was used, with three aperture lengths extending from the sheet metal into the confining soil. These tests were conducted to compare results with those of later tests that utilize a two aperture length sample. An estimated 41 degree interface friction angle was used after conducting a basic monotonic test utilizing the confining aggregate and geogrid. Six replicate tests were conducted for comparison. Steel load transfer plates were attached to the sheet metal and then attached to the load cell. Bungee cords supported the plates on the sides and middle. During the conditioning cycle, the cords were adjusted by tightening and loosening so that the plates did not move out of plane as load was applied.

Figure 29 depicts a representative graph for this series of tests. The results are grouped by confining stress, C-1 to C-5. Results for G_i exhibit a general decrease with increased shear stress. It is expected that G_i would decrease as shear stress increases for a particular confinement stress, due in part to the occurrence of greater displacement of the geosynthetic relative to the soil. As confinement increases, G_i should also increase, due to restricting the movement of the geosynthetic within the soil. However, with this test protocol, shear stress is increased simultaneously with confinement. It would appear that the influence of shear stress on G_i is greater than that of confinement.

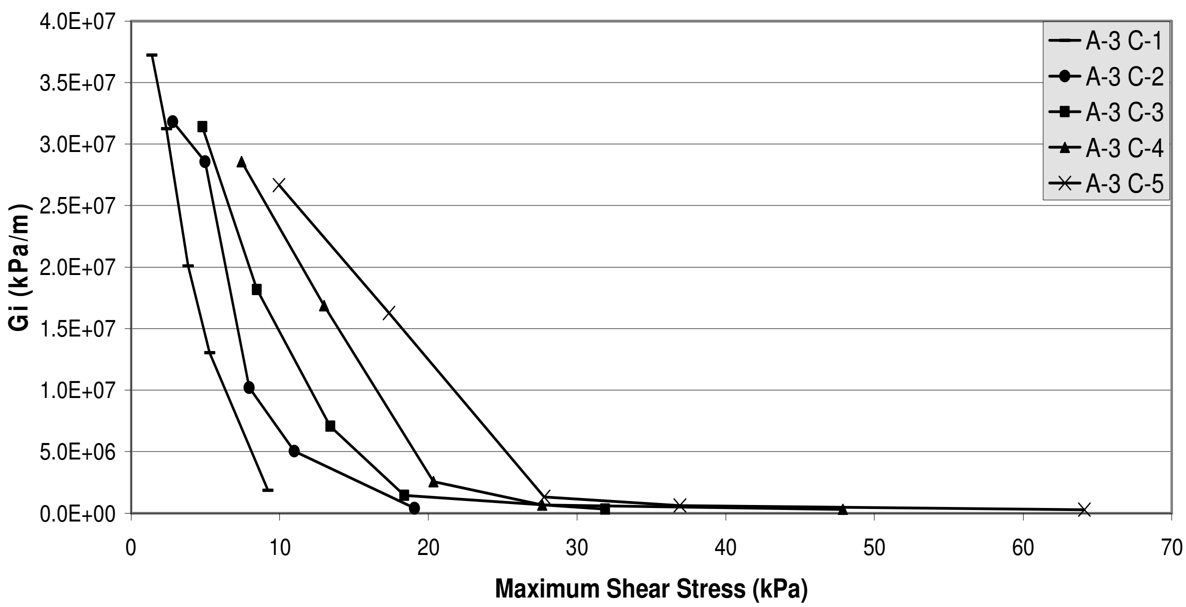

Figure 29. Representative graph for A-series tests.

Using Equation 6, values of k_1, k_2, and k_3 were determined for each test. As seen in Table 5, the results are relatively variable between replicates, with a coefficient of variation of 192% for k_1, and approximately 45% for k_2 and k_3. These coefficients of variation (Cv) were calculated between test replicates, and indicate moderate to low repeatability of replicate tests. By treating test A-1 as an outliner, due to the notable difference in k-values, and omitting these results yields Cv values of 39%, 26%, and 10% for k_1, $k_{2,}$ and $k_{3,}$ respectively.

Table 5. K-values for A-series tests

Test	k_1	k_2	k_3	R2
A-1	4.36E+07	1.741	-38.9	0.94
A-2	2.19E+06	0.943	-18.6	0.85
A-3	1.28E+06	0.651	-15.9	0.91
A-4	1.41E+06	0.582	-14.3	0.85
A-5	1.50E+06	1.095	-17.1	0.89
A-6	3.05E+06	0.791	-17.9	0.81

For sequence group 1 during test A-1, the data acquisition system did not collect data. This was found to be due to operator error through an improper configuration of the protocol. This may have affected the overall analysis of the results, due to the protocol being reconfigured between sequence groups one and two. Once this protocol was repaired, the test was continued. After test A-1 was finished, the data acquisition system inputs were reexamined to ensure that the error was corrected, so that data would be collected during sequence group 1.

This test series also displayed a lower level of repeatability as compared to the confinement and shear testing presented earlier. This suggests that reworking the test protocol so that only one parameter, either shear stress or confinement, is altered within a sequence group may result in a more accurate test method. However, since the shear and confinement testing was limited to a few load levels, further testing should be conducted that more closely reflects the complete test protocol in order to further investigate the feasibility and effectiveness of altering the protocol as such.

R^2 values for each test were relatively high for this series, indicating a good correlation of the calculated values to the measured values. Figure 30 depicts the relationship between calculated and measured results for all of the A-series tests. The line indicates a 1:1 ratio between calculated and measured values, which would indicate an exact dependent relationship between the two values. As displayed by this graph and an R^2 values of 0.81 to 0.95, there exists a significant relationship between calculated behavior and measured behavior.

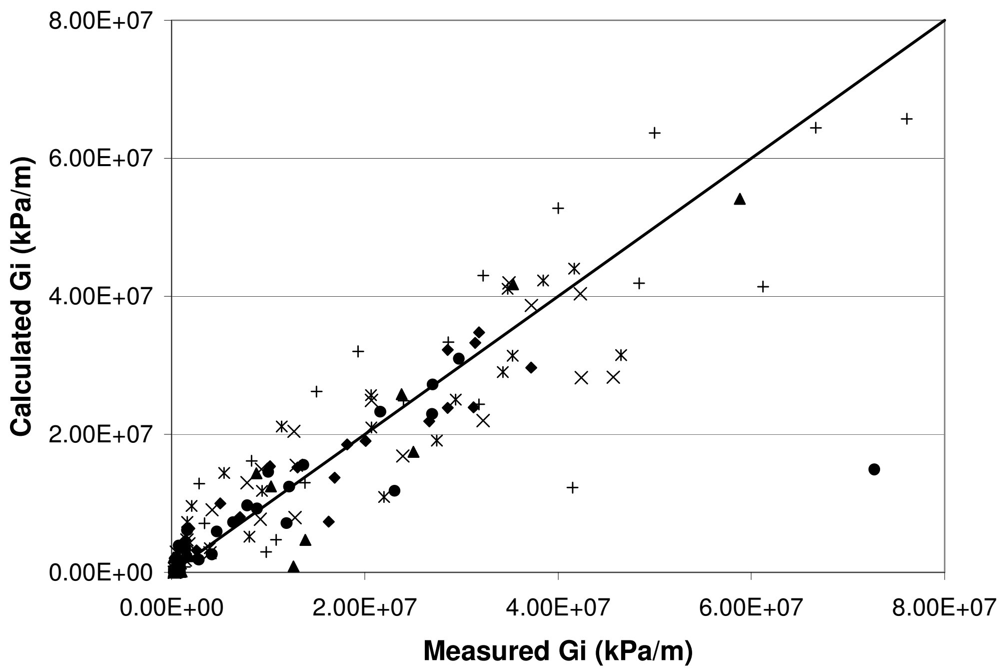

Figure 30. Calculated vs. measured Gi for A-series tests.

Two Aperture Geogrid (PET) (B-Series)

The B-Series of testing consisted of PP geogrid samples two apertures in length. B-1 and B-2, the first two tests, were conducted using an assumed interface friction angle of 41 degrees, and the steel load transfer plates as in the A-Series of testing. Test B-3 consisted of a reduced width sample, cut down to 246 mm to analyze the effects of a smaller sample. Test B-4 returned to a 486 mm sample width, but utilized a single hole drilled through the sheet metal to accommodate the load cell connections, avoiding use of the steel load transfer plates as an adapter.

Table 6. K-Values for B-Series tests

Test	k_1	k_2	k_3	R2
B-1	1.17E+06	0.344	-8.3	0.69
B-2	7.49E+05	0.702	-7.1	0.67
B-3	8.52E+05	0.552	-4.5	0.37
B-4	9.35E+05	0.362	-9.2	0.56

Tests B-1 and B-2 displayed varied results, despite being exact replicates of one another. Figure 31 displays the variability in these repeated tests. B-1 was plotted using black lines and closed point markers, while B-2 was shown as gray lines with open point markers. In general, G_i for test B-2 was less than B-1. This difference may have been due to variability inherent in this type of testing, or vibration or electrical interference that had an effect on the sensor signals. The R^2 values were similar for these two tests, indicating a moderate relation between the equation used to predict G_i and actual measured values. As mentioned previously, values for SG1-C1 were omitted, as the variability inherent in interpretation of the data for these points had a profound effect on the rest of the data. Omission of this point results in a more accurate portrayal of the test results. In general, G_i decreased as shear stress increased. As confinement increased, G_i also increased, as expected. This corresponds with the previous observations for other tests. The main issue with these tests is the variability in results.

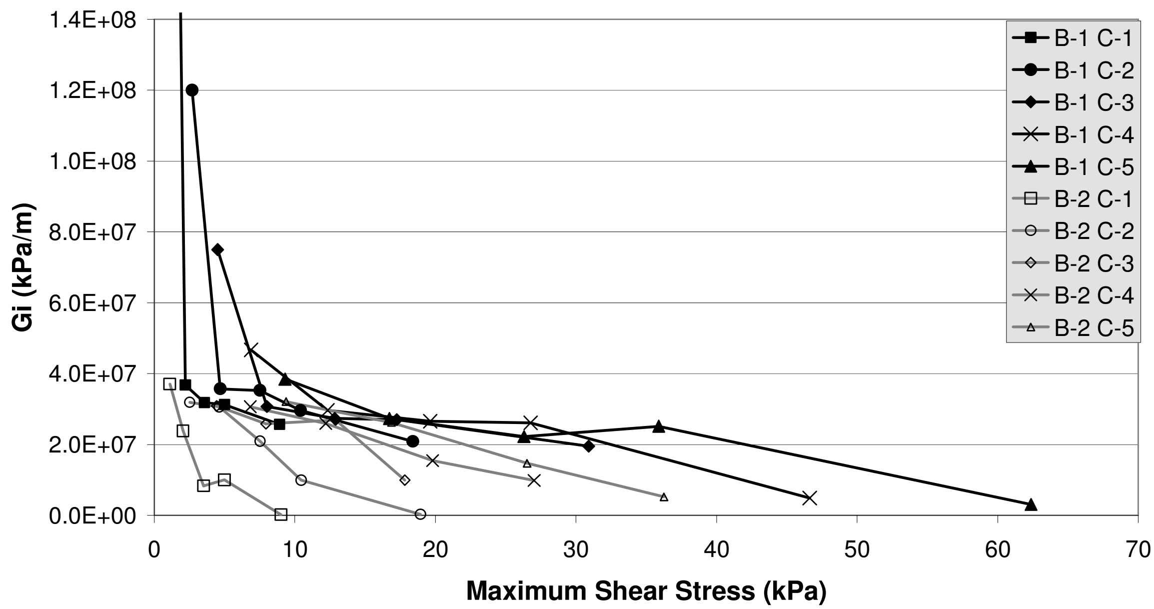

Figure 31. Results from tests B-1 and B-2.

Values of G_i for test B-3, the sole test conducted using a reduced-width sample, were erratic in behavior, as shown in Figure 32. Since the geosynthetic sample area was reduced significantly, loads applied by the equipment were less than previous tests. The load output was less consistent than the previous tests, as the equipment struggled to apply the lower loads. These results indicate that the shorter width can skew test results, as well as be problematic for the test equipment. Since the width increases the sample area, a greater force is necessary to achieve the specified shear stresses in a sample with wider width. The test equipment is better suited to apply greater loads (>0.1 kN) with more accuracy than the lesser loads (<0.1 kN). From these results, a wider sample width should be used in order to insure a more accurate load application. Values of G_i were also similar to those of the other tests.

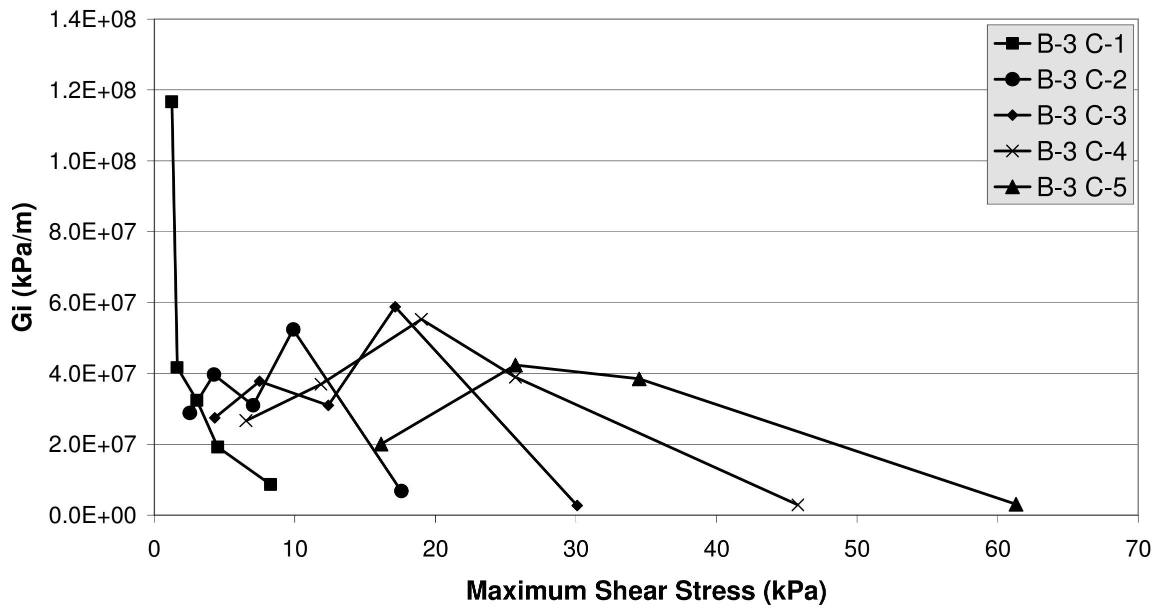

Figure 32. Results from test B-3.

During Test B-4, it was observed that the hydraulic cylinder was able to apply a direct horizontal load to the load transfer sheets without using the steel load transfer plates. Bungee cords were necessary to center the load cell and prevent sagging of the load transfer sleeves, due to their self-weight. These cords were adjusted during the conditioning step to ensure a uniform application of load to the geosynthetic, and to avoid affecting test results.

Test B-4's results are displayed as Figure 33. From these results, it does not appear that removal of the steel load transfer plates had any adverse effects on test results. Values for G_i obtained from this test display similar behavior to previous tests, in that as shear and/or confinement increased, G_i decreased slightly. Results were also generally similar in magnitude to the earlier tests overall. Since the omission of the steel load transfer plates did not reveal any significantly adverse effects on test results, it was determined that the direct connection method would be used for the remainder of testing. By eliminating the need for the steel load transfer plates, setup time for testing was significantly reduced.

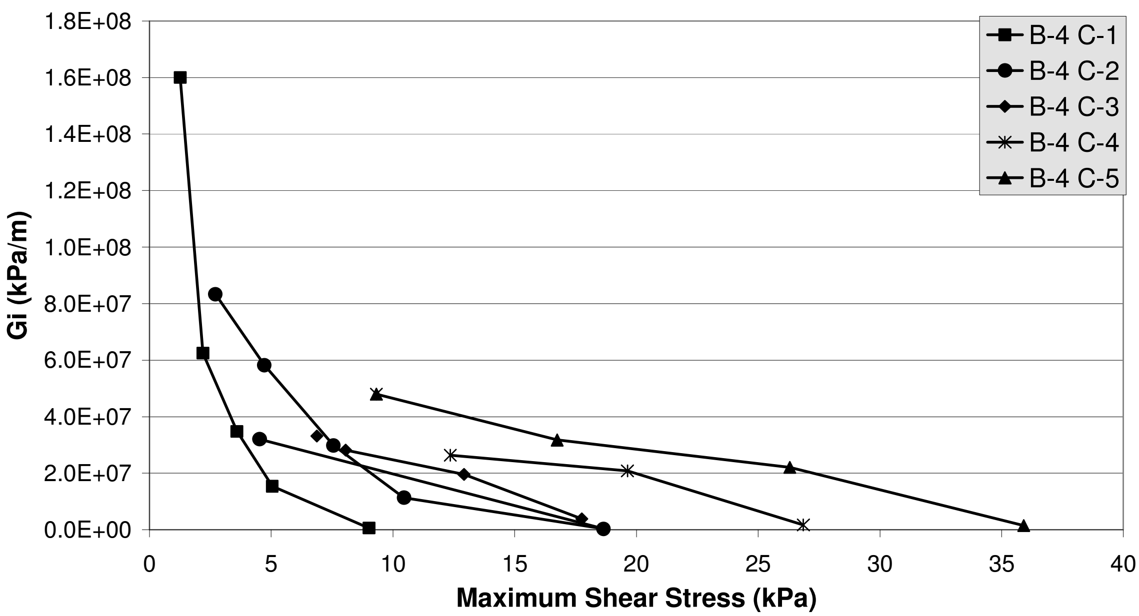

Figure 33. Results from test B-4.

Strain was calculated for the two-aperture (B-series) tests, and compared to that of the three aperture (A-series) tests. Analysis of this strain behavior and development during the two tests was conducted to gain a better understanding of the geosynthetic's behavior under cyclic loading. The strains were calculated along the center width of the geosynthetic sample. Figure 34 displays the sensor configuration for calculation of these strains. Two sections of length were used, between 0 (δ_8 and δ_7) and 3 mm (δ_6) at the front of the sample, then from the front (δ_8 and δ_7) to the back (δ_3) of the sample. It was observed that the very front of the sample from 0 to 3 mm experienced significantly greater strain than the overall sample.

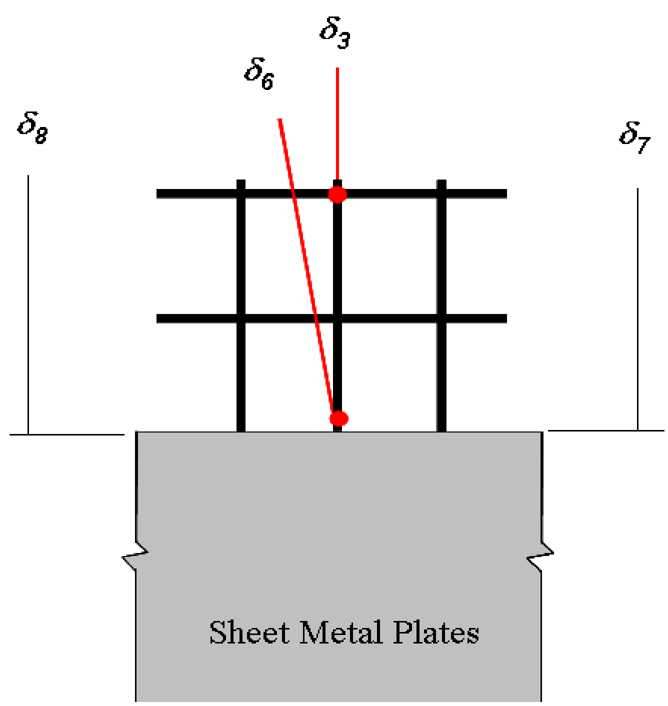

Figure 34. Sensor layout for strain calculations.

The three-aperture (A-series) tests experienced greater strains, especially at the very front of the sample. Figure 35 displays the strain at the very front of the sample for both types of test, with respect to number of cycles of loading applied. In the three-aperture sample, strain starts off higher (5%), and then decreases with repeated loadings.

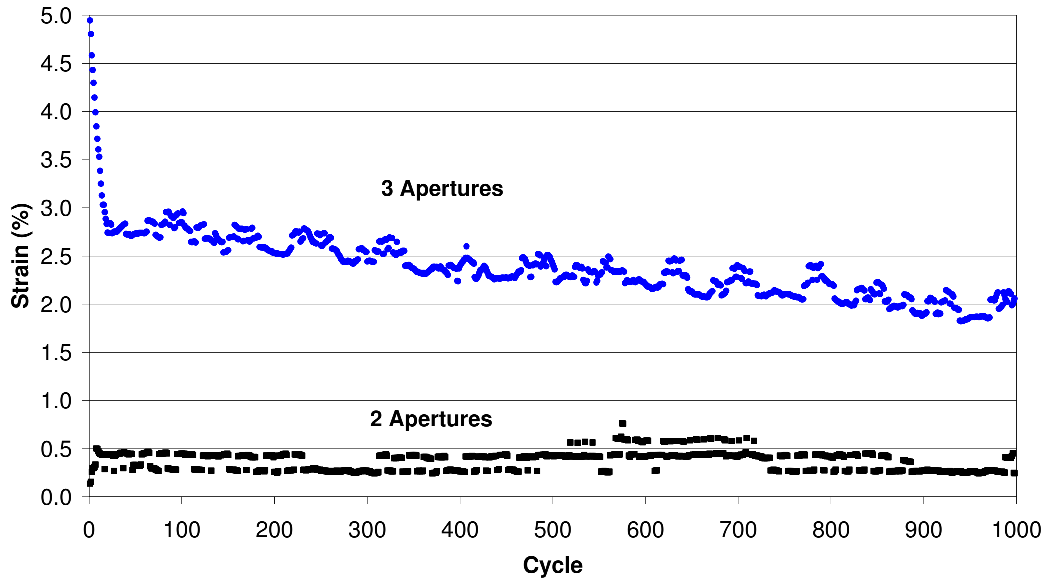

Figure 35. Strain near the front of sample.

Strain between the front and rear of the sample with respect to cycles is displayed in Figure 36. Again, the three aperture tests experienced more strain than the two-aperture tests. Unlike the very front of the sample, however, the overall sample experienced increasing strain after a rapid decrease within the first 30 cycles of the test. In general, strain between the front and rear of the sample was very low, indicating that the displacement at the front was relatively similar to that of the rear.

In both cases, the strain in the two-aperture tests is more consistent throughout the load step, and considerably less than those of the three-aperture tests. This suggests that the two-aperture tests could produce more consistent and accurate results based on the assumptions made in the analysis, as the behavior near the front of the sample should be more similar to that of the back of the sample. The three aperture tests' decrease in the near-front strain, combined with the increase in overall strain suggest that the longer sample length's behavior changes with the addition of more cycles.

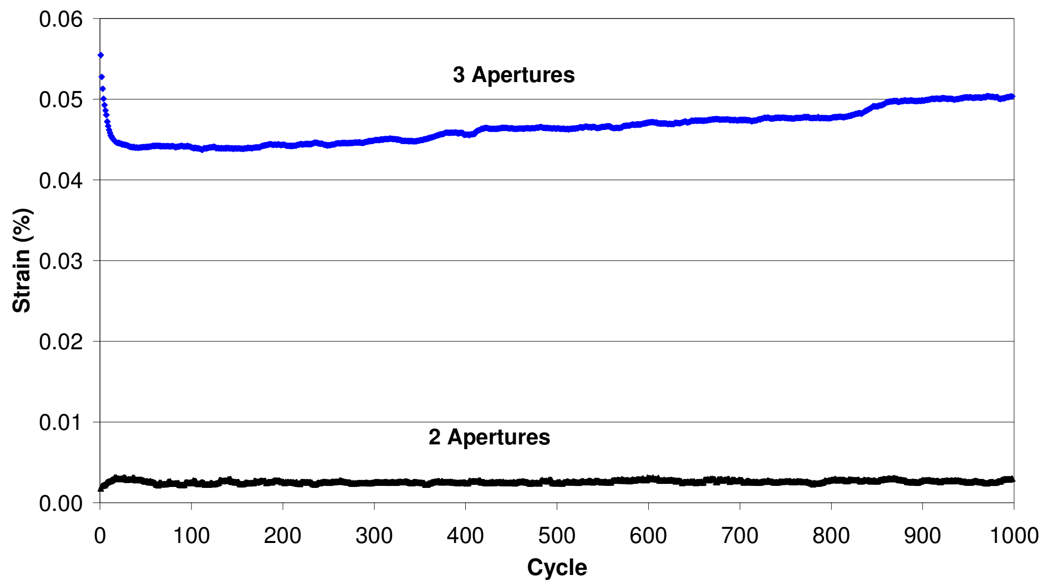

Figure 36. Strain of the entire sample.

At the beginning of cycling, the majority of the strain develops close to the front of the sample. As cycling progresses, the strain begins to distribute more rearward. This would result in a decrease over time in the near-front strain, and an increase over time in the overall strain. Since calculations of G_i account for the average overall behavior of the geosynthetic, a two aperture test should be more accurate than that of a test using a three aperture length sample, due to less variability in strain development. During testing, however, the three aperture length tests produced more consistent results than the two aperture tests, with respect to k-values between replicates, and R^2 values within each test, as shown in Table 7. This is likely a product of better accuracy in load application from the greater force required, and load effects averaged out through a greater surface area. Further testing should incorporate more two and three aperture tests in order to compare behaviors, as well as clarify the advantages or disadvantages of the differing sample lengths.

Table 7. K-values for A-series and B-series.

Test	k_1	k_2	k_3	R2
A-1	4.36E+07	1.741	-38.9	0.94
A-2	2.19E+06	0.761	-21.8	0.85
A-3	1.28E+06	0.651	-15.9	0.91
A-4	1.41E+06	0.582	-14.3	0.85
A-5	1.50E+06	1.095	-17.1	0.89
A-6	3.05E+06	0.791	-17.9	0.81
B-1	1.17E+06	0.344	-8.3	0.69
B-2	7.49E+05	0.702	-7.1	0.67
B-3	8.52E+05	0.552	-4.5	0.37
B-4	9.35E+05	0.362	-9.2	0.56

Two Aperture Length Geogrid (PP) C- Series

In this series, the PET geogrid with two apertures length was tested while confined by aggregate 1. The steel load transfer plates were not used, and a single hole drilled through the sheet metal which contained the specimen was used to attach to the load cell. The assumed interface friction angle was reduced to 38 degrees in hopes of avoiding gross pullout of the specimen prior to application of Sequence Group 5 loads.

This series of tests resulted in similar behavior to the tests run on the PET geogrid. In general, G_i decreased with increasing shear, and increased with increasing confinement. Values for G_i were similar to those obtained from the other series of tests. Test C-2, confinement 5 had a significant increase in G_i at the last point. The sample may have developed some additional frictional resistance at this end point if the confining aggregate became bound up in the slit at the front of the box that the sample is inserted through.

Table 8. K-values for C-series tests.

Test	k_1	k_2	k_3	R2
C-1	8.09E+05	0.343	-6.7	0.10
C-2	7.62E+05	0.339	-3.3	0.21
C-3	6.23E+05	0.314	-0.9	0.20

A high level of variation between measured and calculated G_i exists for this test series, as evidenced by the very low R^2 values. For this series of tests, the adapted resilient modulus equation for cyclic pullout does not seem to accurately portray the material's behavior. Values for k_1 and k_2 are relatively similar for these tests, while k_3. values seem to display more variation. Test C-1 displayed a lesser relationship between calculated and measured results, while tests C-2 and C-3 had considerably low, yet similar R^2 values. However, if the last point in confinement 5 for test C-2 is omitted as an outlier, the R^2 value for that test becomes 0.34. From these results, it appears that this polyester geogrid confined in Ottawa sand is not readily predictable using Equation 6.

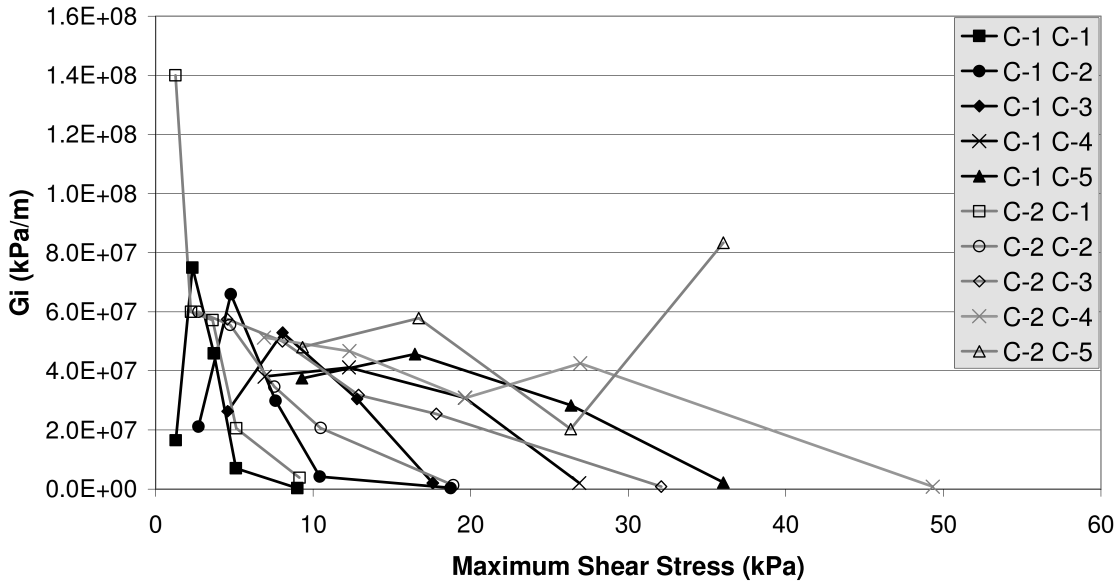

Figure 37. Results from tests C-1 and C-2.

A comparison of the calculated and measured values of G_i is shown in Figure 38. These results show that the calculated values have a lesser range (0.8 – 6 E+07 kPa/m) than the measured values (0.1 – 8.2 E+07 kPa/m). However, if the values for SG1-C1 and SG 4-C5 (1.40 E+08 and 8.1 E+07, respectively) are treated as outliers and omitted, the ranges for calculated and measured values are relatively similar. The outlying nature of the measured value at SG1-C1 is consistent with the other tests performed in this study. The cluster of data points with low measured G_i in the lower left hand corner are representative of points from higher sequence groups and confinements, mainly SG4-C4 and SG4-C5.

This geosynthetic exhibited lower values of G_i at lower shear stresses and confinements for the most part, as compared to the PP geogrid. This material also displayed more erratic behavior, as G_i occasionally decreased for a given shear stress with increased confinement, or increased with increased shear stress at a given confinement.

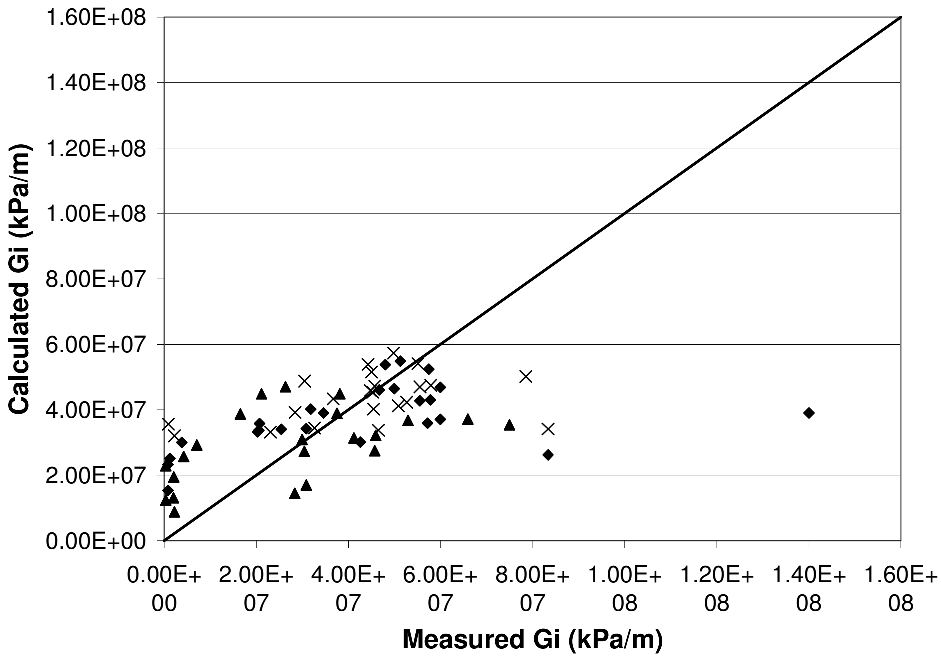

Figure 38. Calculated vs. measured Gi for C-series tests.

Geotextile (D- Series)

The D-Series of testing utilized the woven geotextile. Each sample used similar dimensions as the previous geogrid testing so that the same loading protocols could be utilized. After executing the first two tests, D-1 and D-2, it seemed that the estimated interface friction angle might be low. As the tests approached sequence group 5 loadings, it appeared that the displacements were still relatively low. The estimated interface friction angle was then increased to 43 degrees,in an effort to mobilize greater displacements during the later sequence groups.

Regression analyses performed on tests D-1 and D-3 yielded negative values for k_2, and positive values for k_3, as shown in Table 9. These two tests displayed the greatest deviation from the general trend of the other regression analyses. In general, k_2 values from earlier tests were positive, ranging from 0.3 to 1.5. Values for k_3 were generally negative with a value close to -10. This does not appear to be a behavior inherent in this geotextile, as tests D-2. D-4. and D-5 resulted in k-values similar to those of earlier tests. A high amount of variation was existent in this testing series in comparison to Equation 6, as evidenced by the low R^2 values.

Table 9. K-values for D-series tests.

Test	k_1	k_2	k_3	R2
D-1	2.63E+05	**-0.232**	**1.2**	0.10
D-2	2.47E+06	0.938	-11.6	0.47
D-3	3.72E+05	**-0.504**	**0.3**	0.56
D-4	2.27E+06	0.850	-11.3	0.10
D-5	2.47E+06	0.685	-12.1	0.11
Cv (%)	73	192	102	

The results for tests D-1 and D-3 are displayed in Figure 39. The slight increase in G_i during early sequence groups likely helped to contribute to the seemingly odd k-values. Since Equation 6 consistently depicts a decreasing slope with increasing shear stress, the increasing behavior at points for these tests may have produced the unexpected results. Also, G_i appeared to vary less for the D-series tests with increased shear than the previous tests on geogrid, which may have had an influence on the k-value results. Overall repeatability was low, with Cv between 73 and 192 percent. The negative results for tests D-1 and D-3 greatly affected the Cv of 192 for k_2. Tests D-2. D-4, and D-5 were relatively similar, with Cv of 5, 16, and 4% for k_1, k_2, and k_3, respectively.

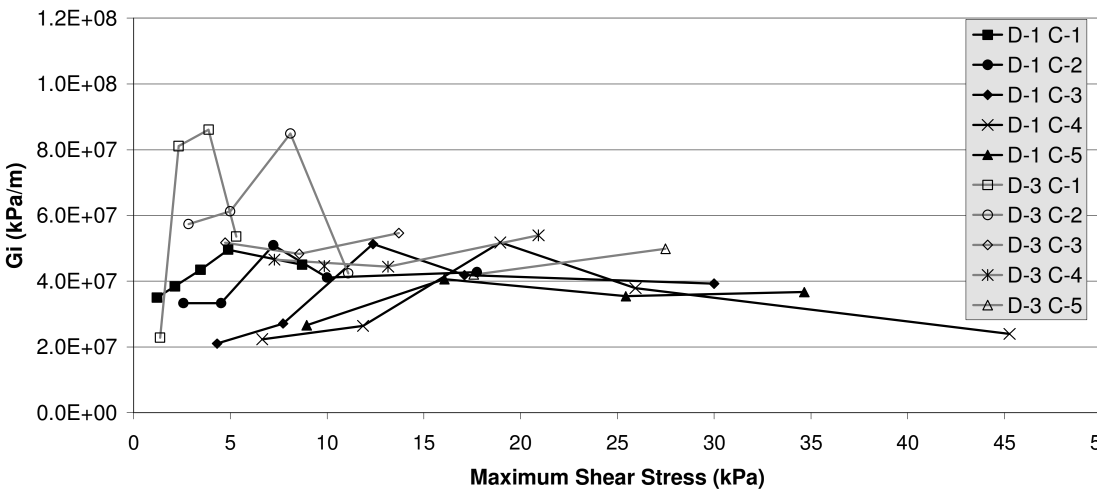

Figure 39. Results from tests D-1 and D-3.

Results obtained from tests D-2 and D-4 are displayed in Figure 40. These tests yielded similar parameters to each other during regression analyses. The values for G_i also seemed to vary less for these tests than those of D-1 and D-3. In comparison to the earlier tests that used geogrids, the tests using geotextile yielded less-varying results, and higher values for G_i at greater shear stresses. The geogrid may be better able to distribute loads through the entire sample, due to a more uniform or stiff structure.

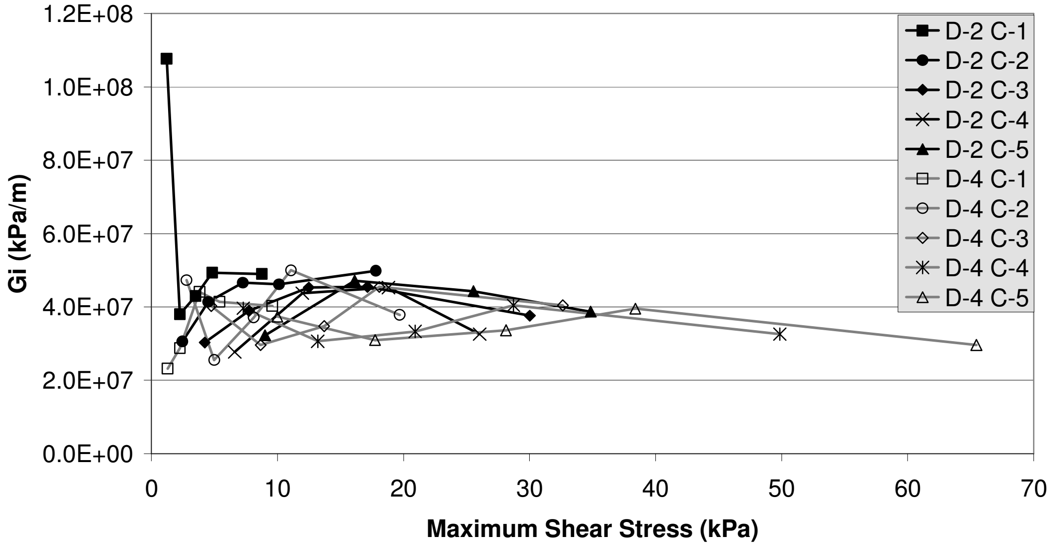

Figure 40. Results from tests D-2 and D-4.

Stress-strain behavior was also investigated for this series of tests, in order to further analyze the behavior of the geotextile under cyclic pullout loads. A typical graph for the D-series tests, obtained from test D-1, is shown in Figure 41. At lower confinements, strain increases noticeably with a slight increase in maximum shear stress. As confinement increases, greater shear stress is needed to mobilize strain in the geotextile. These strains are low, indicating a stiff response of the geotextile. For this test series, strain ranged from approximately 0.01 to 0.07 percent, with similar behavior as shown in Figure 41.

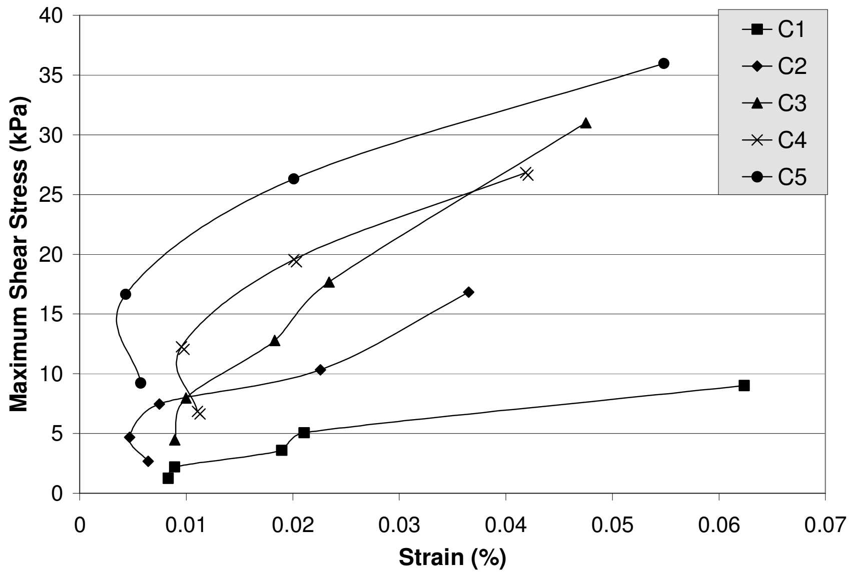

Figure 41. Representative stress-strain relationship for D-series tests.

Figure 42 displays a comparison of calculated versus measured values for the D-series testing, which had low R^2 values, indicating very little correlation between the calculated and measured values. This graph also shows that the measured values generally displayed a much narrower range, (approximately 3.00 E+07 to 6.00 E+07 kPa/m), than the calculated values (0.50 E+07 to 8.10 E+07 kPa/m). For these results, the equation for G_i both over-predicts and under-estimates the test values. The greatest outlying points were from test D-3. marked by the asterisks in Figure 42. A narrower range of measured results suggests that the actual behavior of the geotextile is less variable than the calculations predict. This may indicate that confinement and shear stress have a lesser effect on the interaction between a geotextile and confining aggregate than that of other geosynthetics. However, confinement stress seemed to have a greater effect, as G_i, generally decreased with increasing confinement more consistently than G_i was affected by changes in shear stress.

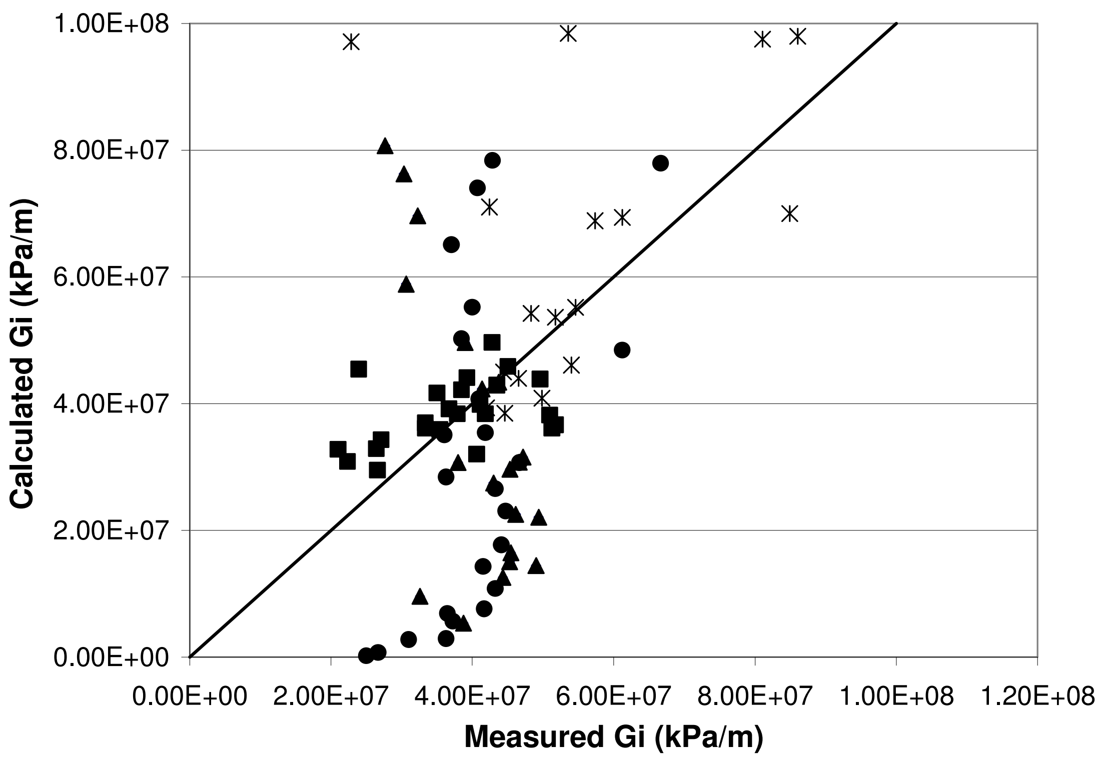

Figure 42. Calculated vs. measured Gi for D-series tests.

AGGREGATE 2 'GOLF CHIPS' (E-SERIES)

After the tests executed utilizing the Ottawa sand (Aggregate 1), a more angular, slightly larger aggregate was sought to continue testing. 'Golf chips,' a relatively uniformly graded coarse sand manufactured as a byproduct of golf sand, was selected for the second aggregate. Since this aggregate's particles consist mainly of coarse sand with some fines, it was hoped that the interface between the geosynthetics and the confining soil would be relatively uniform. A well graded soil would have the possibility of rendering a non-homogenous interface with the geosynthetic. This aggregate also consisted of more angular faces, as opposed to the roundness of the Ottawa sand particles. Tests utilizing this aggregate were conducted with PET geogrid samples, two apertures in length.

Initially, an interface friction angle of 50 degrees was utilized. Tests E-1 and E-2 were conducted consecutively, with no resetting of the sample and/ or LVDTs between tests. The goal of these consecutive tests was to analyze the effect of repeated sequence groups and confinements in order to determine if they impact the test results. For tests E-3 through E-6, the applied loadings were adjusted to reflect an interface friction angle of 53 degrees, thereby increasing the loads within each sequence group.

Tests E-4 and E-5 yielded similar results with the regression analysis for the k-values. These values, along with the values for the rest of the E-series tests, are shown in Table 10. Test E-2 was noticeably different from the other tests that were conducted in this series. E-1 and E-2 were executed seamlessly, and therefore, conducting tests consecutively without realigning the sample and recompacting the confining soil may induce greater error in test results. It appears that after cycling through the test protocol, the arrangement of the soil and geosynthetic are such that repeatability decreases significantly. Excavating the geosynthetic and realigning it, along with recompacting the confining soil helps to increase repeatability of the test results. The R^2 values, aside from E-5, showed only a moderate correlation between the calculated and measured values.

Table 10. K-values for E-series tests

Test	**k_1**	**k_2**	**k_3**	**R2**
E-1	2.47E+06	0.280	-16.7	0.52
E-2	1.08E+07	1.584	-34.8	0.58
E-3	2.90E+06	0.612	-9.6	0.65
E-4	1.98E+06	0.775	-8.8	0.67
E-5	1.86E+06	0.764	-8.3	0.90
E-6	1.80E+06	0.712	-10.9	0.62

Values of G_i, for tests E-4 and E-5 are noticeably different in value, but display similar trends as seen in Figure 43. For the most part, as shear stress increased, G_i decreased. Also, as confinement increased, G_i generally decreased. The early sequence groups show a slight fluctuation of results, somewhat similar to many of the other tests conducted during this study. This could be due to inherent variations that are part of the nature of the testing, and/ or differences in interpretation of data affected by interference. In both tests, between SG-1, C-1 and SG1, C-2 displayed an unexpected increase in G_i. It is possible that the influence of confinement was greater than that of shear stress at this point for this aggregate, since shear stresses at those load steps are relatively small.

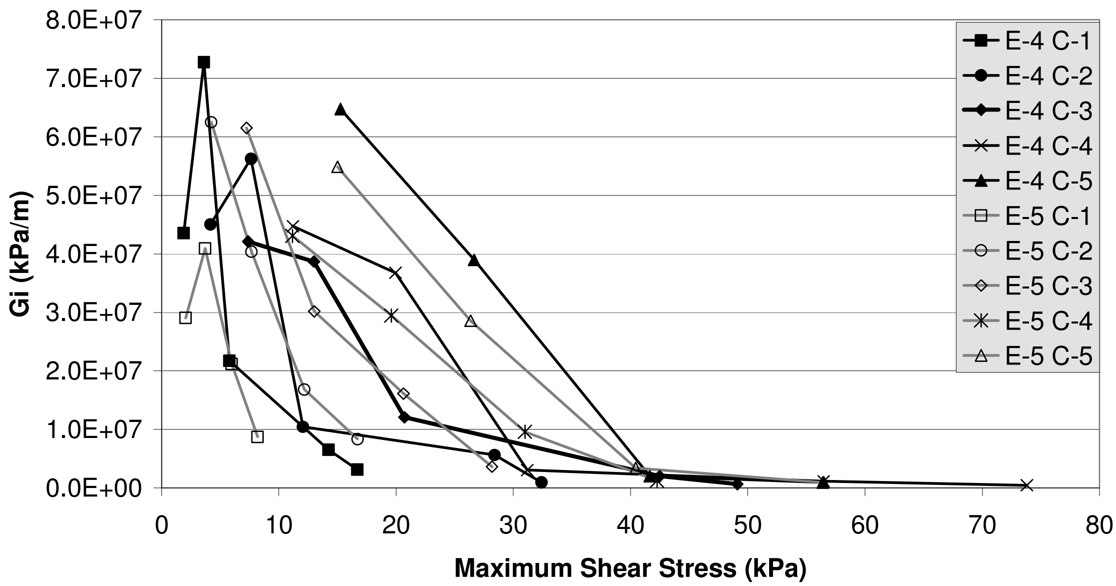

Figure 43. Results from tests E-4 and E-5.

From the plot of E-1 and E-2, shown in Figure 44, values of G_i for test E-2 are noticeably lower than those for E-1. The discrepancy in k-value regression is likely a result of these lower test values from E-2. Results from test E-1 range from 2 to 30 times greater than those of E-2, outside of the first point for Confinement 1. At this point, load step SG-1, C-1, G_i for E-1is actually 8 percent less than that of E-2.

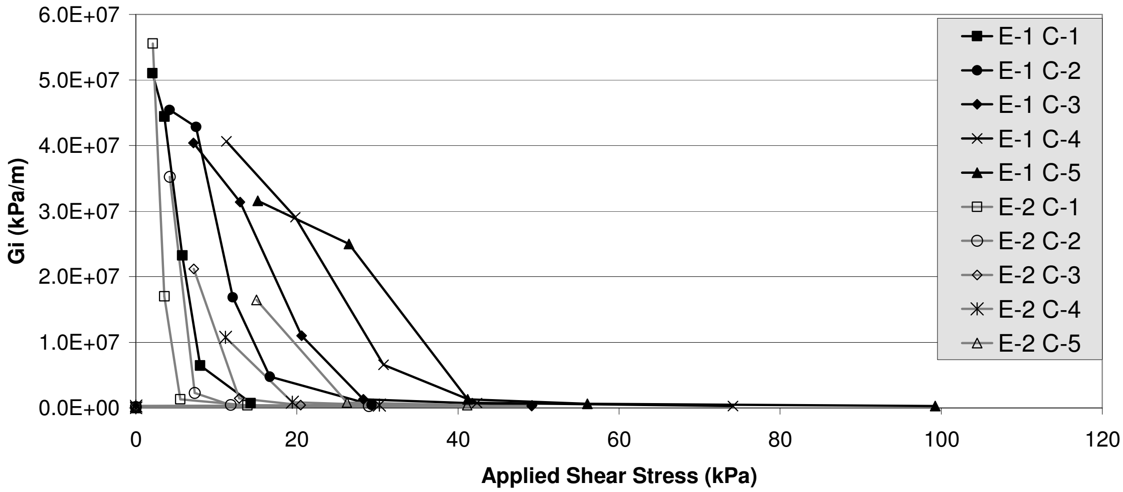

Figure 44. Results from tests E-1 and E-2.

TIMING TESTING

Load Pulse Analysis

Little is currently known about the influence of the load pulse duration on cyclic geosynthetic pullout testing. Therefore, tests were conducted to analyze this possible influence, with respect to G_i. This series of tests consisted of shear levels applied to the PP geogrid equivalent to Sequence Group 3, Confinement 3 (2.0 to 21.5 kPa shear stress at 51.7 kPa confinement stress). The geogrid was confined in aggregate 2, the golf chips. Load pulse was varied from 0.1 seconds to 0.9 seconds, in 0.1 second increments. A rest period of 0.5 seconds was added to reduce the potential effects due to the rest period. G_i was calculated for each load pulse duration and compared to one another.

Results for both load pulse and rest period are displayed in Figure 45. Values for G_i varied little between durations, as well as between load pulse and rest period tests. The variations in G_i portrayed in these results are likely due to human error (less than 5% for these results) in the manual interpretation of the slope between displacement and shear stress. This test had an R^2 value of 0.94, indicating a high correlation between the predicted and measured behaviors.

From this testing, a load pulse duration of 0.2 seconds is recommended for future testing. Since the load pulse duration did not have a significant affect on G_i, load pulses between 0.1 and 0.9 seconds would be acceptable. However, as the cyclic pullout test protocol has been developed based on the resilient modulus test, a 0.2 second load pulse would further align the two test methods.

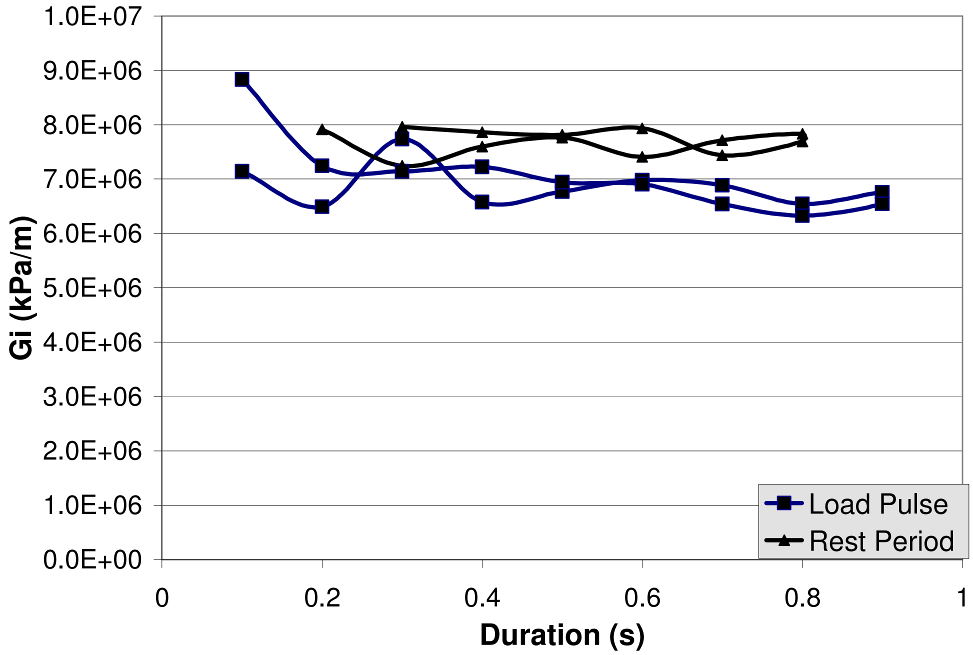

Figure 45. Load and rest period timing test results.

Rest Period Analysis

Tests were also conducted in order to assess the influence of the rest period portion of the load application cycle. Load pulse duration was held constant at 0.2 seconds, and rest period duration was varied from 0.2s to 0.8s in 0.1s increments, and then back from 0.8s to 0.2s. Shear stress was applied from 2 kPa to a maximum of 25 kPa for each cycle, with confinement held constant at 51.7 kPa, the same loading schedule used for the load pulse testing. The PP geogrid confined by aggregate 2 was utilized for this series of testing.

As shown previously in Figure 45, results for the different rest period durations are relatively similar. Coefficient of variation between these tests is at 3%, which indicates that there is not a considerable amount of difference between each duration. This test had an R^2 value of 0.99, indicating a very strong relationship between the predicted and actual values. The initial conclusions were reaffirmed that the load pulse and rest period duration did not have a significant effect on G_i values obtained during testing. From these results, a rest period of 0.5 seconds is recommended for tests conducted with dry sand as a confining aggregate. This will also align the cyclic pullout protocol with the resilient modulus, as the resilient modulus test allows for a rest period of 0.4 seconds when a free-draining sand is utilized.

CONCLUSIONS AND RECOMMENDATIONS

In general, test results with respect to G_i values possess a similar range of values, and for the most part reflect similar behaviors. At low shear stress and confinement levels, G_i can vary greatly. This is due to the profound impact that noise in displacement measurements can have, along with interpretation of these measurements. At lower loads and confinements, a small amount of interference or vibration can result in difficult interpretation of the data. Displacements at these lower sequence groups and confinements are very small, approximately from 5 x 10^{-5} mm to 1 x 10^{-4} mm. Interpretation errors of the displacement due to this affected data affect G_i up to an order of magnitude. Beyond these points, however, G_i had a general maximum around $8*10^7$ kPa/m. As shear stress increased, G_i generally decreased, as expected. Likewise. as confinement increased, G_i generally increased, which was also an expected behavior. It appears that G_i may be affected more greatly by change in applied shear stress.

Displacements at the back of the geosynthetic sample were quite small, along the order of thousandths of a millimeter. This extremely small displacement then requires instrumentation that can detect these movements, but can do so with minimal influence from outside disturbance and interference. As shown in this study, the instrumentation used has the ability to capture these small displacements. The instrumentation may have been affected by vibration or electrical interference, as evidenced by erratic displacement data. Due to the nature of this testing, with a large hydraulic cylinder applying shear stress to a geosynthetic embedded in soil, interference at low loads and displacements may be inherent.

For further study, further reduction of interference should be investigated. For instance, the instrumentation might be designed to incorporate some type of additional dampening, in order to reduce transfer of vibrations from the pullout box to the LVDTs. In the case that the interference appears to be due to electrical interference, filters or additional shielding may need to be added to reduce these effects.

Until the interference source(s) are further reduced so that less erratic data can be collected, data interpretation should be executed by manual analysis of the timed data. Shear stress should be plotted versus displacement, and a slope between the later cycles determined. A line should then be drawn representing this slope, and values for shear stress and displacement interpreted in order to calculate G_i. Visual inspection and manual calculation should be continued until it is determined that the data acquisition system produces max/min data that is representative of the actual behavior. Once the max/ min data reflects the maximum and minimum points from the timed data, the data analysis simplifies, and will expedite the testing process.

Omitting the steel load transfer plates for attaching the sheet metal load transfer sheets to the load cell did not seem to have any adverse effects on G_i. Therefore, future testing may utilize a direct connection between the load cell and the sheet metal load transfer sheets containing the geosynthetic sample. A single hole in the center width will allow for this type of connection.

Three aperture length tests seemed to have more consistent results for G_i., as well as correlating well to the equation presented by Cuelho and Perkins (2005). However, strain development in the three aperture tests resulted in higher strains, and increasing strain from the front to the back of the sample as more cycles of load were applied. From the strain analysis, two aperture length tests should yield a more accurate representation of the interaction between the soil and geosynthetic. For this reason, a two aperture sample length is desired. A sample width of 486-500 mm should be maintained so that the applied loads are greater in magnitude. The narrow width sample resulted in loads of smaller magnitude that seemed difficult for the servo-hydraulic actuator to produce consistently in a rapid fashion.

The geotextile yielded the most noticeable difference in results. The upper range of G_i was around $6.0*10^7$ kPa/m, similar to the other tests. As shear stress increased, G_i decreased, but not as greatly as observed in the other tests or as calculated using the adapted resilient modulus equation. After the first two sequence groups, G_i flattened out around $3.5*10^7$ kPa/m. This behavior seems to indicate that the geotextile used stabilized after loading progressions, resulting in a more consistent interaction with the confining soil.

The polypropylene geogrid displayed a low correlation to the Cuelho and Perkins equation, and a lack of repeatability with respect to values of k_3.

Additional testing could be conducted using different confining aggregates in order to determine if this behavior is a characteristic of the geosynthetic confined by aggregate 1, or more a characteristic of this geosynthetic, independent of the type of confining aggregate.

Consideration should be given to either removing Sequence Group 1, Confinement 1 (SG-1, C-1) from the protocol. The majority of variation in test data seemed to be produced by the lowest shear stresses, which occur at SG-1, C-1, as evidenced by outlying data points when measured and calculated G_i are compared. Several tests, such as the intermediate test, B and E series tests, etc. yielded low R^2 values (0.3-0.6) when all load steps were considered. However, when SG1-C1 was omitted, the R^2 values increased to approximately 0.65 to 0.8. The C and D series reflected low R^2 values of approximately 0.1, and omitting SG1-C1 had very little effect on the overall relationship of the measured data to the calculated data. Since the higher sequence groups generally produce greater displacement of the geosynthetic sample, the effect of interference on the measurements decreases. Also, as in the reduced width testing, the lower loads are more difficult for the actuator to produce consistently. Complete removal of SG-1 would also decrease the total test duration by approximately 1.25 hours.

Load pulse and rest period durations between 0.2 seconds and 0.8 seconds do not seem to have a significant effect on test results, with the granular aggregates used in this study. The test protocol should then incorporate a 0.2

second load pulse and 0.4 second rest period for granular confining aggregates, in order to further resemble the resilient modulus test.

Consideration should also be given to reworking the test protocol so that either confinement or shear stress remains constant between load steps. The shear and confinement testing displayed the best potential for repeatability with respect to k-values, and R^2 values for individual tests were high, In order to investigate the potential of modifying the protocol to reflect these types of tests, the shear and confinement tests should be expanded to reflect a complete test, as the tests conducted in this study were abbreviated versions of the current test protocol. Additional tests should be conducted with other geosynthetics and confining aggregates in order to determine the viability of the reworked protocol.

REFERENCES

Alfaro, M.C. Miura, N. Bergado, D.T. (1995), “Soil-Geogrid Reinforcement Interaction by Pullout and Direct Shear Tests.” *Geotechnical Testing Journal*, Vol. 18, No.2, pp.157-163.

Al-Qadi, I.L., Brandon, T.L., Valentine, R.J., Lacina, B.A. and Smith, T.E. (1994), “Laboratory Evaluation of Geosynthetic-Reinforced Pavement Sections.” *Transportation Research Record*, No. 1439, Durability of Geosynthetics, pp. 25-31.

Al-Qadi, I.L., Loulizi, A., Elseifi, M., and Lahouar, S. (2004), “The Virginia Smart Road: The Impact of Pavement Instrumentation on Understanding Pavement Performance.” *Journal of the Association of Asphalt Pavement Technologists*, Vol. 73

Alagiyawanna, A.M.N., Sugimoto, M., Sato, S., and Toyota, H. (2001), “Influence of Longitudinal and Transverse Members on Geogrid Pullout Behavior During Deformation.” *Geotextiles and Geomembranes* Vol 19, pp. 483-507

Alobaidi, I.M., Hoare, D.J., and Ghataora, G.S. (1997), “Load Transfer Mechanism in Pull-Out Tests.” *Geosynthetics International*, Vol. 4, No. 5 pp. 509-521.

Ashmawy, A.K. and Bourdeau, P.L. (1995), “Geosynthetic-Reinforced Soils Under Repeated Loadings: A Review and Comparative Study.” *Geosynthetics International*, Vol. 2, No. 4, pp. 643-678.

Ashmawy, A.K. and Bourdeau, P.L. (1996), “Response of a Woven and Nonwoven Geotextile to Monotonic and Cyclic Simple tension.” *Geosynthetics International*, Vol. 3, No. 4, pp. 493-515.

ASTM (2001), “Standard Test Method for Measuring Geosynthetic Pullout Resistance in Soil.” D 6706-01. In 2002 Annual book of ASTM standards, pp. 396-403.

Barksdale, R.D. (1971), “Compressive Stress Pulse Times in Flexible Pavements for use in Dynamic Testing.” *Highway Research Record*, No. 345, pp.32-44.

Cuelho, Eli (1998), “Determination of Geosynthetic Constitutive Parameters and Soil/Geosynthetic Interaction by In-Air and In-Soil experiments.” Thesis submitted in partial fulfillment of the requirements for the degree of Masters of Science, Montana State University, May 1998.

Cuelho, E.V., and Perkins, S.W., (2005), "Resilient Interface Shear Modulus from Short-Strip, Cyclic, Pullout Tests." *Proceedings of the Conference Geofrontiers, Geotechnical Special Publication 140, Slopes and Retaining Structures Under Seismic and Static Conditions*, ASCE, Austin, Texas.

Eiksund, G.; Hoff, I.; Perkins, S. (2004), "Cyclic triaxial tests on reinforced base course material." *Proceedings of EUROGEO 3, Geosynthetic Conference, Munich Germany,March 2004*

Farrag, K., Acar, Y.B., Juran, I. (1993), "Pull-out resistance of geogrid reinforcements." *Geotextiles and Geomembranes.* Vol. 12 No. 2, pp. 133-159.

Ingold, T.S. (1982), "Some Observations on the Laboratory Measurement of Soil-Geotextile Bond." *Geotechnical Testing Journal*, Vol. 5, No.3, pp.57-67.

Jewell, R.A., Milligan, G.W.E., Sarsby, R.W. and DuBois, D. (1984), "Interaction between soil and geogrids." *Proceedings: Science and Engineering Research Council Conference*, London, England, pp. 18-30.

Lee, K.M., and Manjunath, V.R. (2000), "Soil-Geotextile Interface Friction by Direct Shear Tests." *Canadian Geotechnical Journal*, Vol. 37, No. 1, pp.238-252.

Lopes, M.L. and Ladeira, M. (1996), "Influence of the Confinement, Soil Density and Displacement Rate on Soil-geogrid Interaction." *Geotextiles and Geomembranes*, Vol. 14, pp. 543-554.

Min, L., Leshchinsky, D., Kaliakin, V. and Ling, H.I. (1995), "Effects of sustained and repeated tensile loads on geogrid embedded in sand." *American Society for Testing and Materials*, pp. 204-225.

Moraci, N. and Recalcati, P. (2006), "Factors Affecting the Pullout Behavior of Extruded Geogrids Embedded in a Compacted Granular Soil." *Geotextiles and Geomembranes*, Vol. 24 pp. 220-242.

Moraci, N., Gioffre, D., Romano, G., Montanelli, F. and Rimoldi, P. (2002), "Pullout behaviour of geogrid embedded in granular soils." *Geosynthetics – 7th ICG*, Nice, France, pp. 1345-1348.

NCHRP (2003), NCHRP Project 1-37A, Development of NCHRP 1-37A Design Guide, Using Mechanistic Principles to Improve Pavement Design.

NCHRP (2004), "Laboratory Determination of Resilient Modulus for Flexible Pavement Design." *NCHRP Research Results Digest*, No. 285.

Nejad, F.M., and Small, J.C. (2005), "Pullout Behavior of Geogrids." *Iranian Journal of Science and Technology*, Vol. 29, No.3 pp. 301-310

Ochiai, H., Otani, J., Hayashic, S. and Hirai, T. (1996), "The Pull-out Resistance of Geogrids in Reinforced Soil." *Geotextiles and Geomembranes*, Vol. 14, pp. 19-42.

Palmeira, E.M., and Milligan, G.W.E. (1989), "Scale and Other Factors Affecting the Results of Pull-out Tests of Grids Buried in Sand." *Geotechnique*, Vol. 39, No. 3, pp. 511-524.

Perkins, S.W., Cuelho, E.V., Eiksund, G., Hoff, I., Svano, G., Watin, A.W., Schwartz, C.W., and Christopher, B.R. (2002), "Mechanistic-empirical models for reinforced pavements." *Geosynthetics – 7th ICG*, Nice, France, pp. 951-954.

Perkins, S.W., Christopher, B.R., Cuelho, E.L., Eiksund, G.R., Hoff, I.,Schwartz, C.W., Svanø, G. and Watn A. (2004), "Development of Design Methods for Geosynthetic Reinforced Flexible Pavements", Federal Highway Administration Report DTFH61-01-X-00068.

Raju, D.M., and Fannin, R.J. (1998), "Load-Strain-Displacement Response of Geosynthetics in Monotonic and Cyclic Pullout." *Canadian Geotechnical Journal*, Vol. 35, No. 2, pp. 183-193.

Voottipruex, P. Bergado, D.T. Ounjaichon, P. (2000), "Pullout and Direct Shear Resistance of Hexagonal Wire Mesh Reinforcement in Weathered Bangkok Clay." *Geotechnical Engineering*, Vol. 31, No. 1 pp. 43-62.

Wilson-Fahmy, R.F. (1994), "Experimental Behavior of Polymeric Geogrids in Pullout." *Geotechnical Engineering*, Vol. 120, No. 4, pp.661-667.

Yasuda, S., Nagase, H. and Marui, H. (1992), "Cyclic pull-out tests of geogrids in soils." *Earth Reinforcement Practice*, Balkema, Rotterdam, pp. 185-190.

APPENDIX A

INDIVIDUAL GRAPHS FOR LETTERED SERIES TESTS

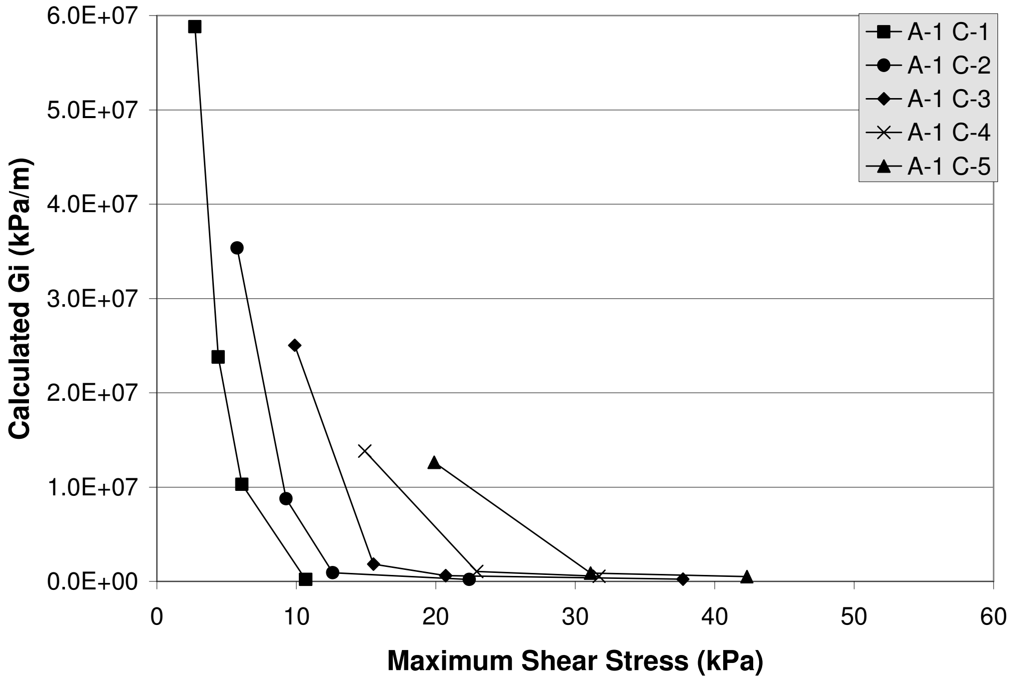

Figure 46. Test A-1 Gi.

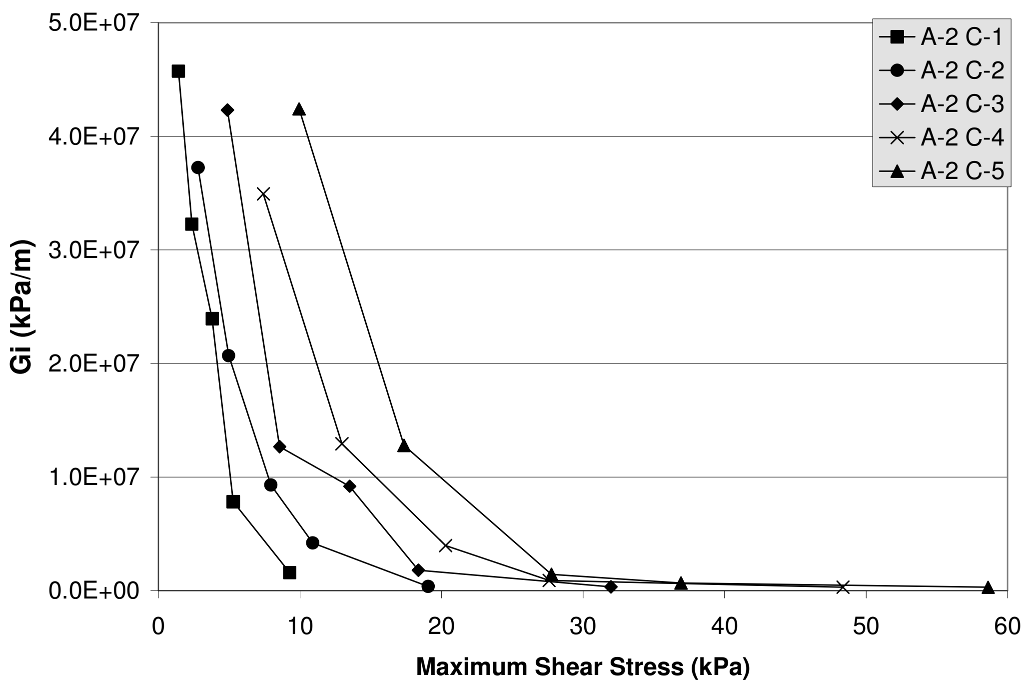

Figure 47. Test A-2 Gi.

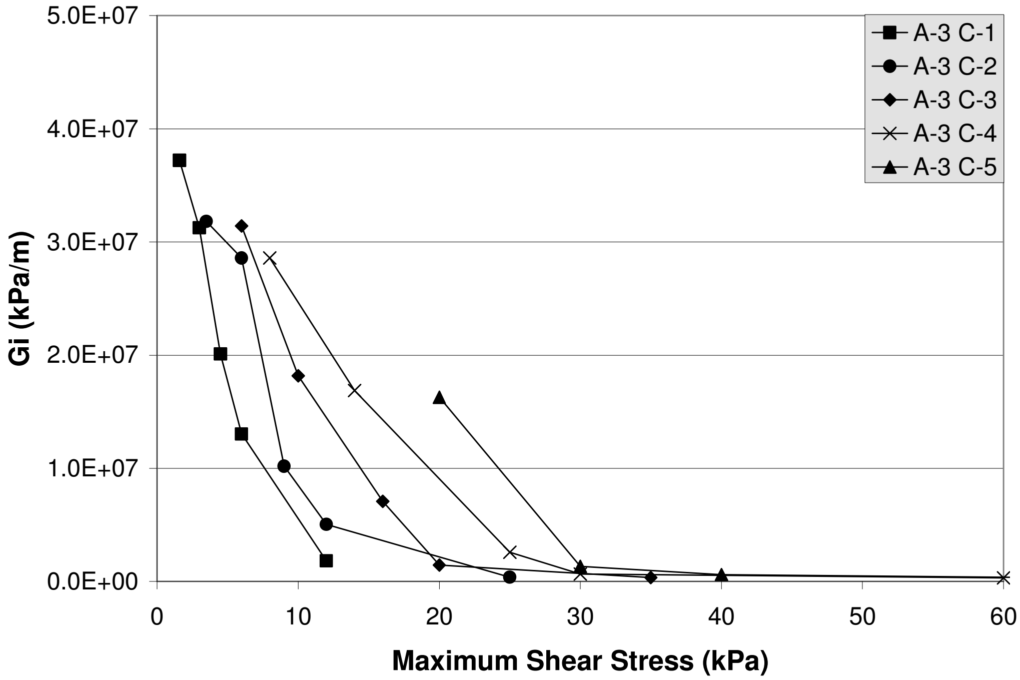

Figure 48. Test A-3 Gi

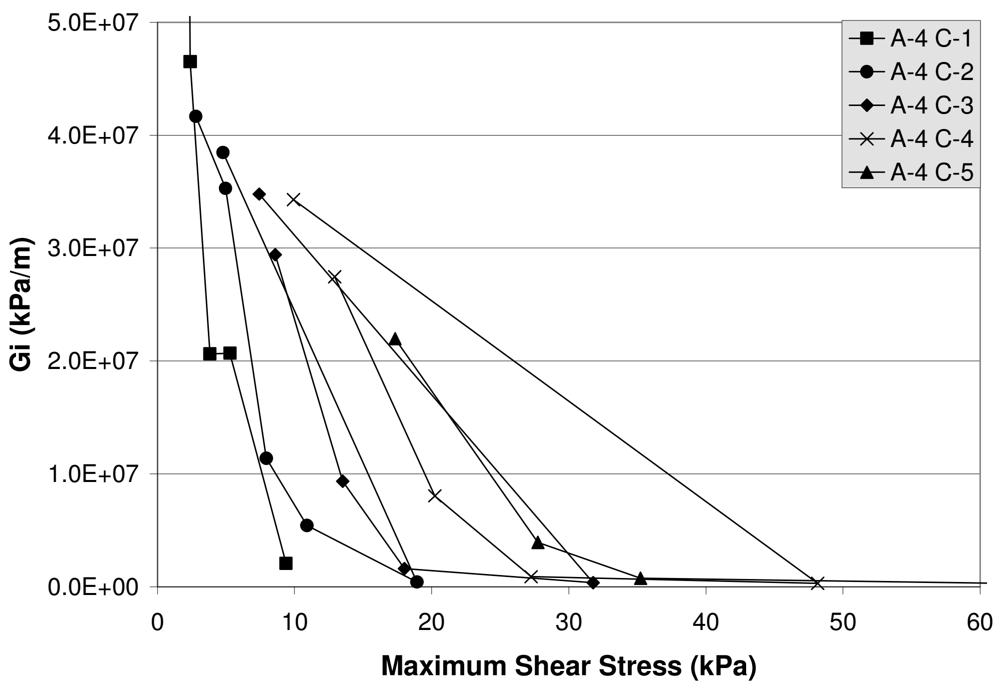

Figure 49. Test A-4 Gi.

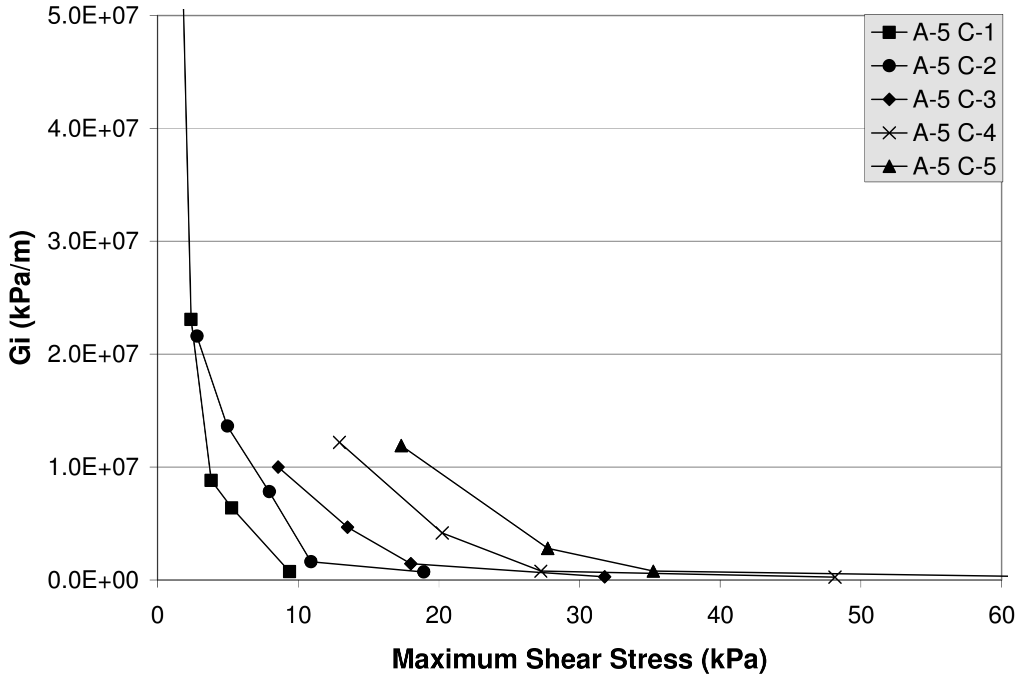

Figure 50. Test A-5 Gi.

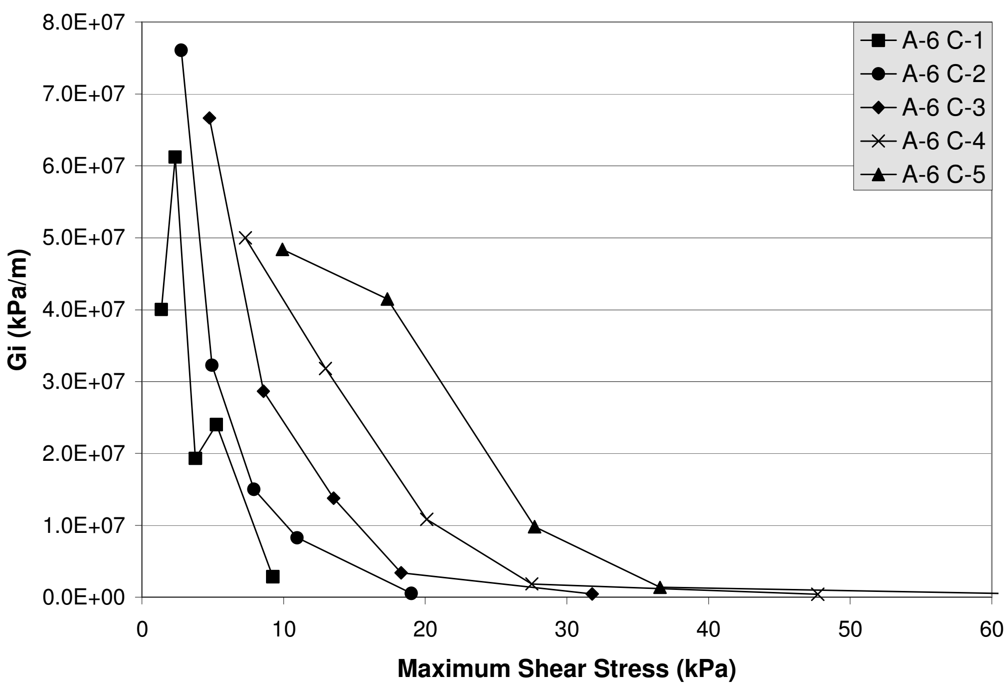

Figure 51. Test A-6 Gi.

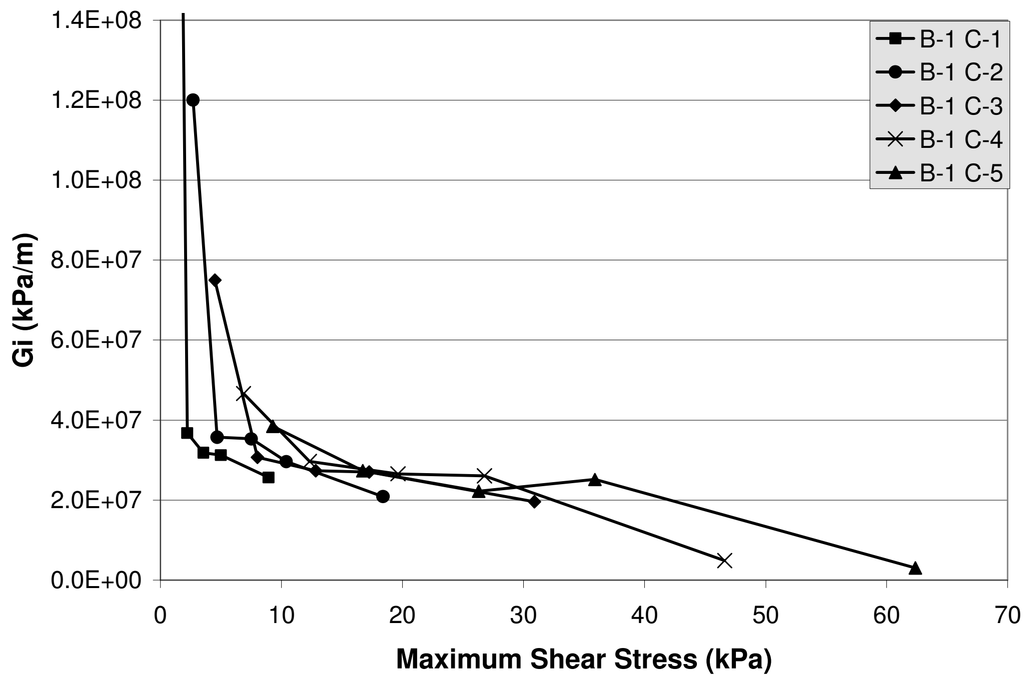

Figure 52. Test B-1 Gi.

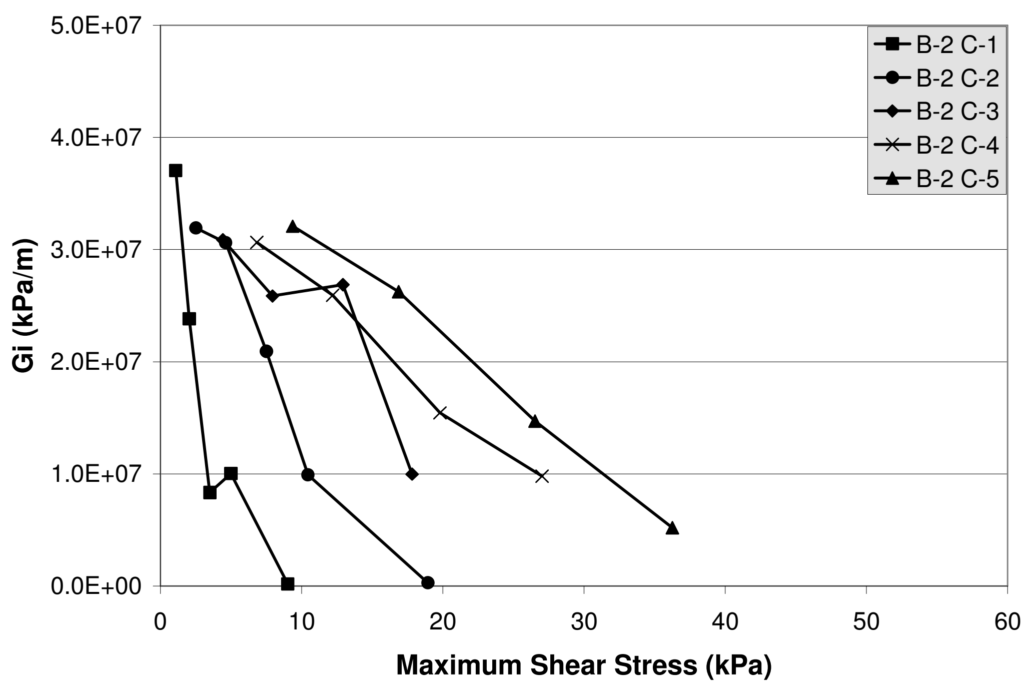

Figure 53. Test B-2 Gi.

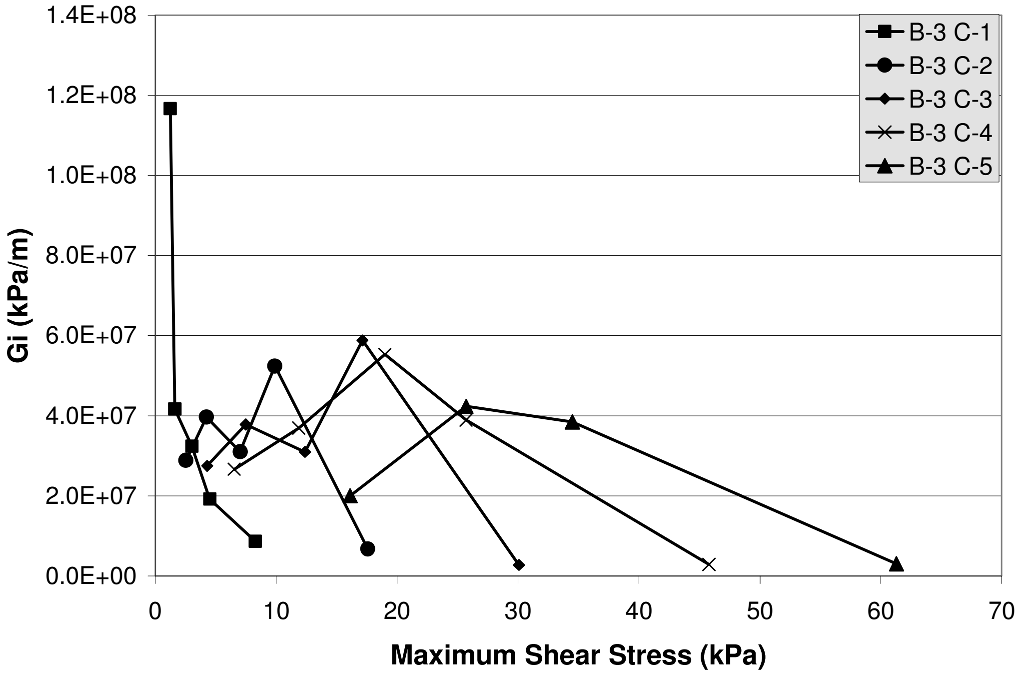

Figure 54. Test B-3 Gi.

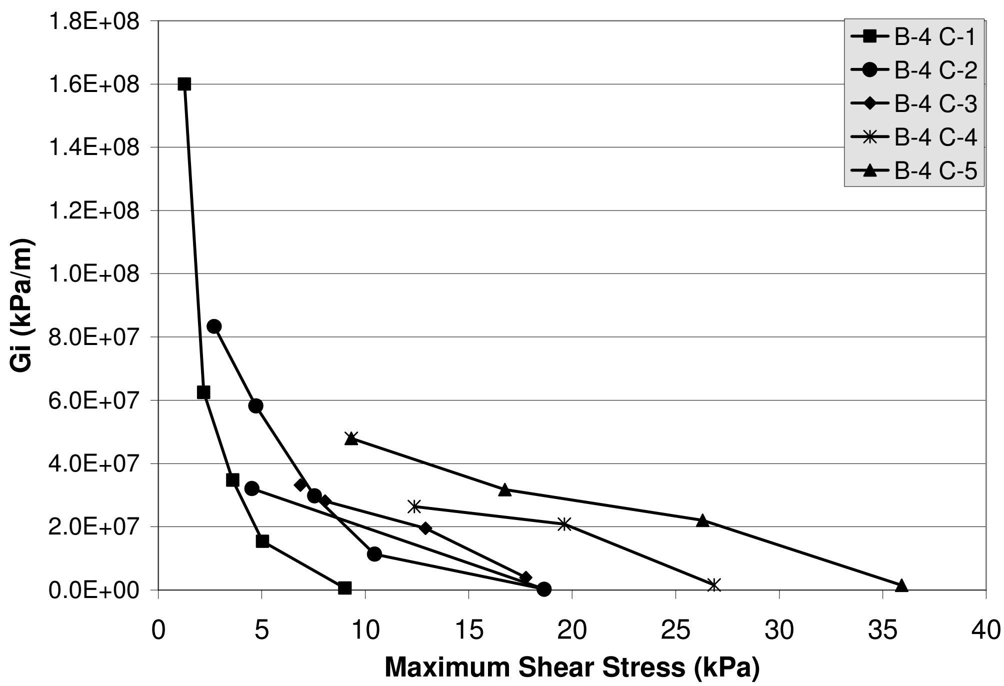

Figure 55. Test B-4 Gi.

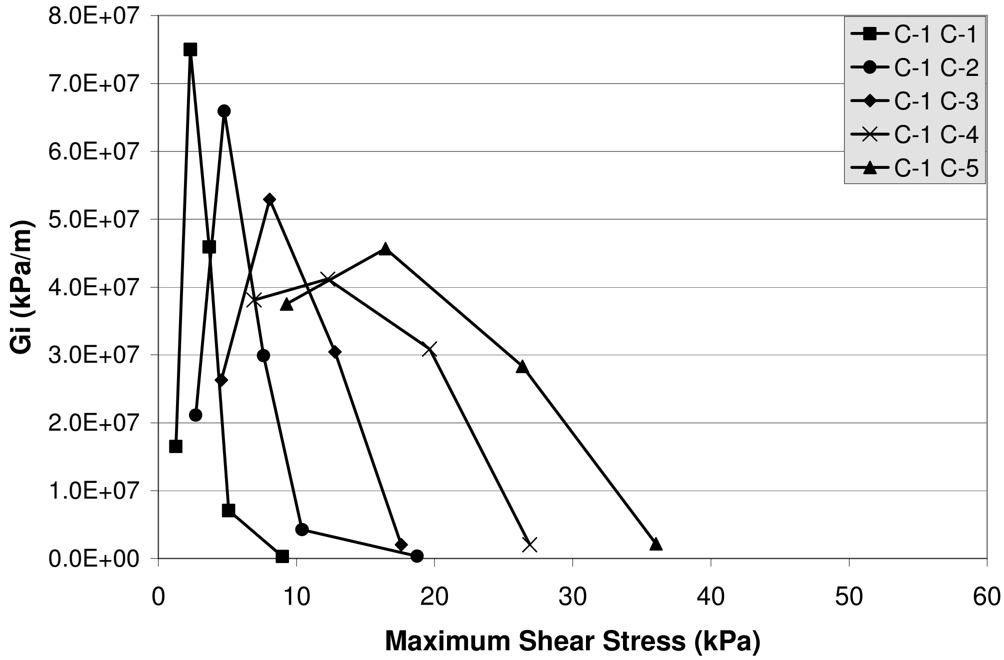

Figure 56. Test C-1 Gi.

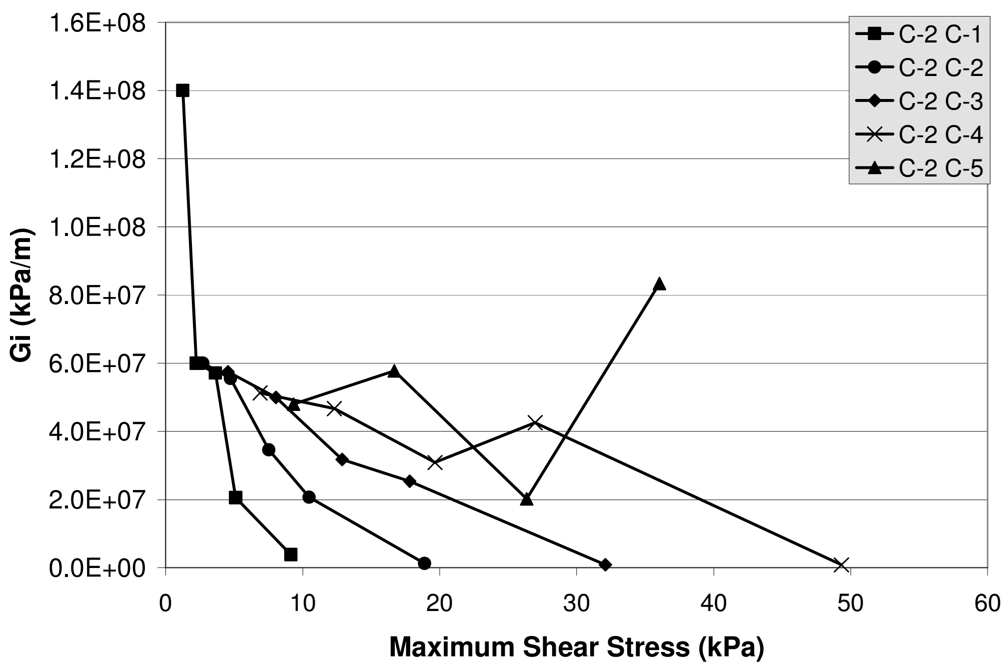

Figure 57. Test C-2 Gi.

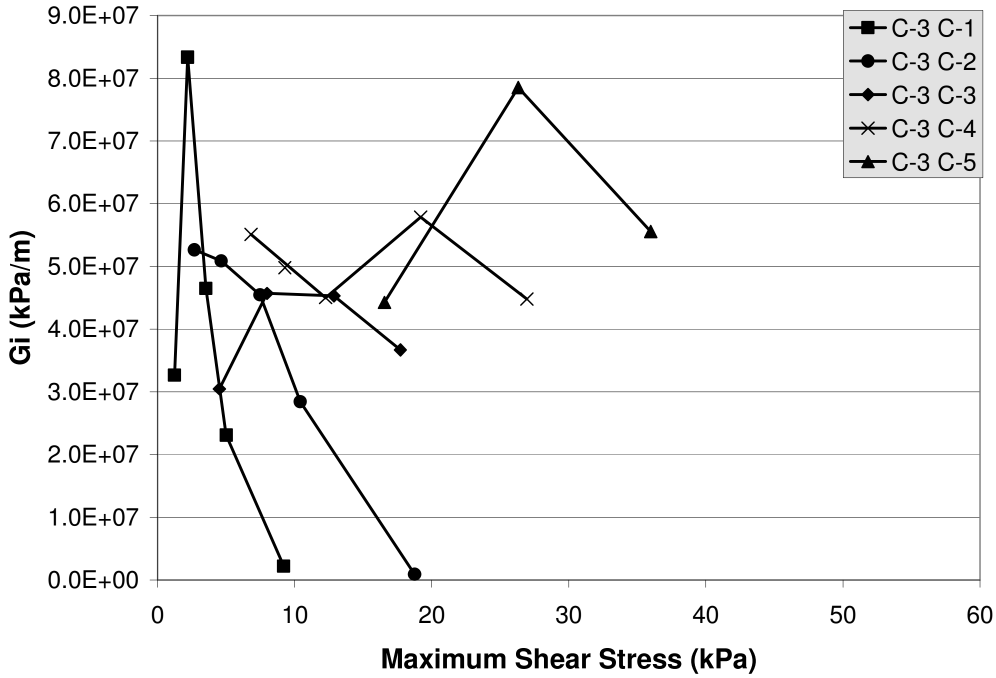

Figure 58. Test C-3 Gi.

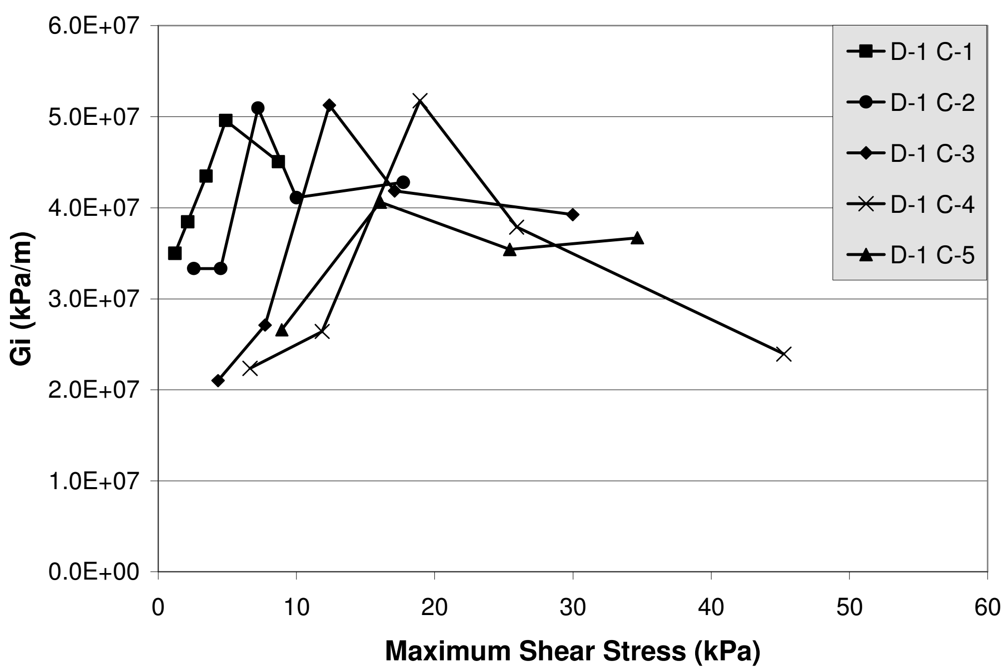

Figure 59. Test D-1 Gi.

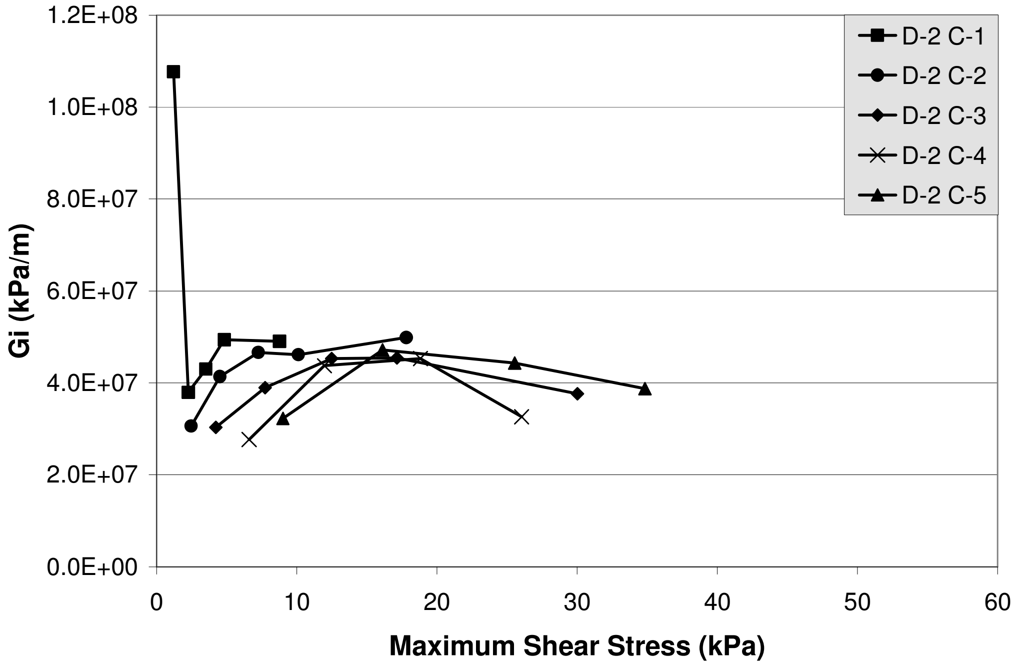

Figure 60. Test D-2 Gi.

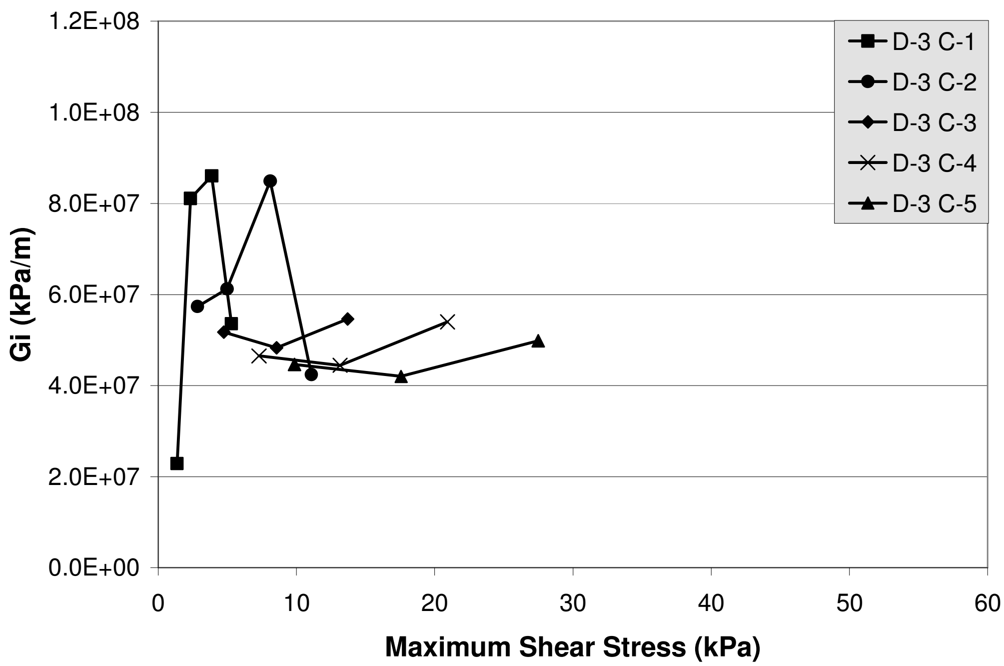

Figure 61. Test D-3 Gi.

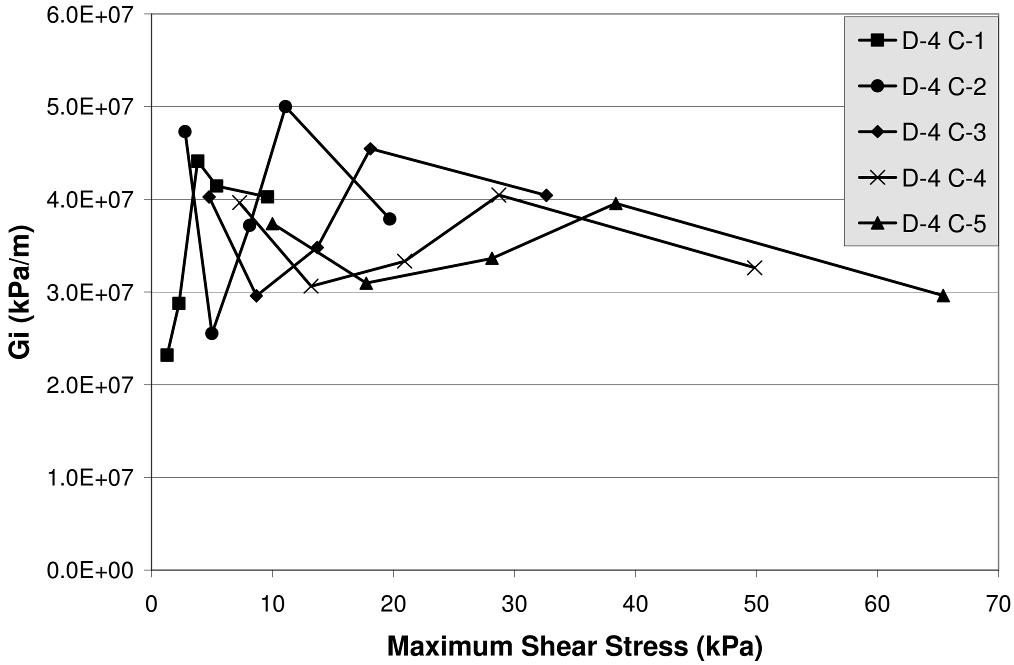

Figure 62. Test D-4 Gi.

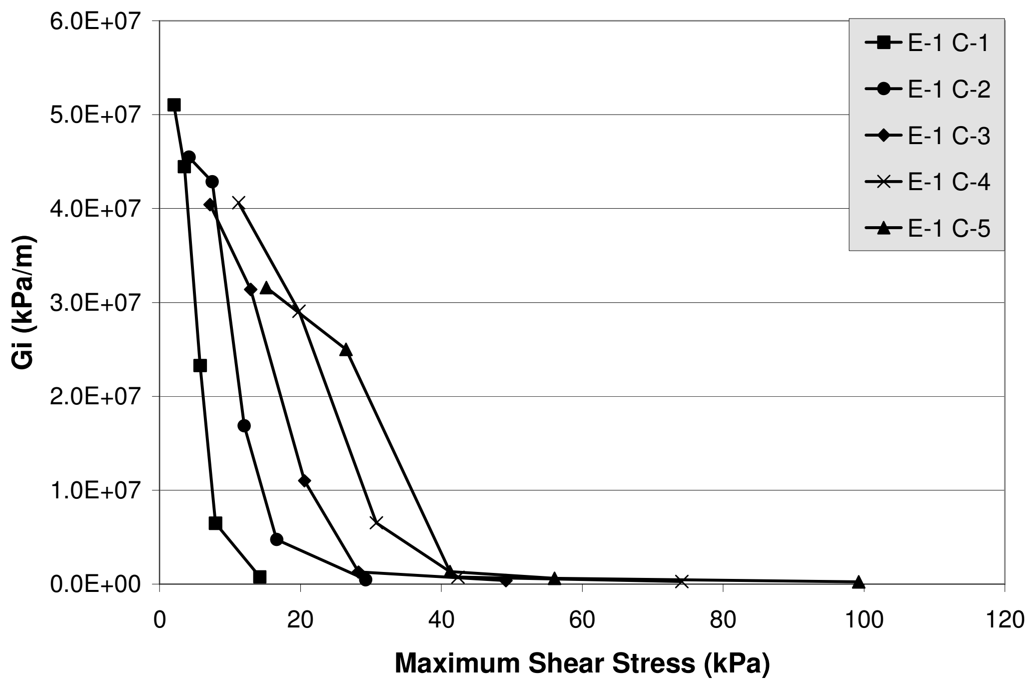

Figure 63. Test E-1 Gi.

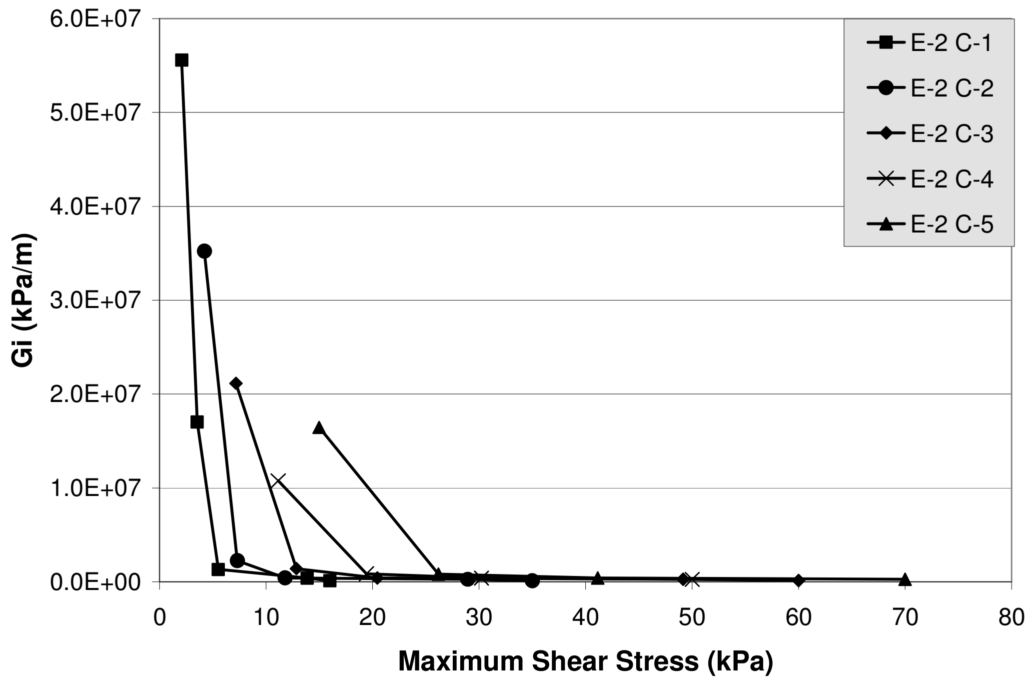

Figure 64. Test E-2 Gi.

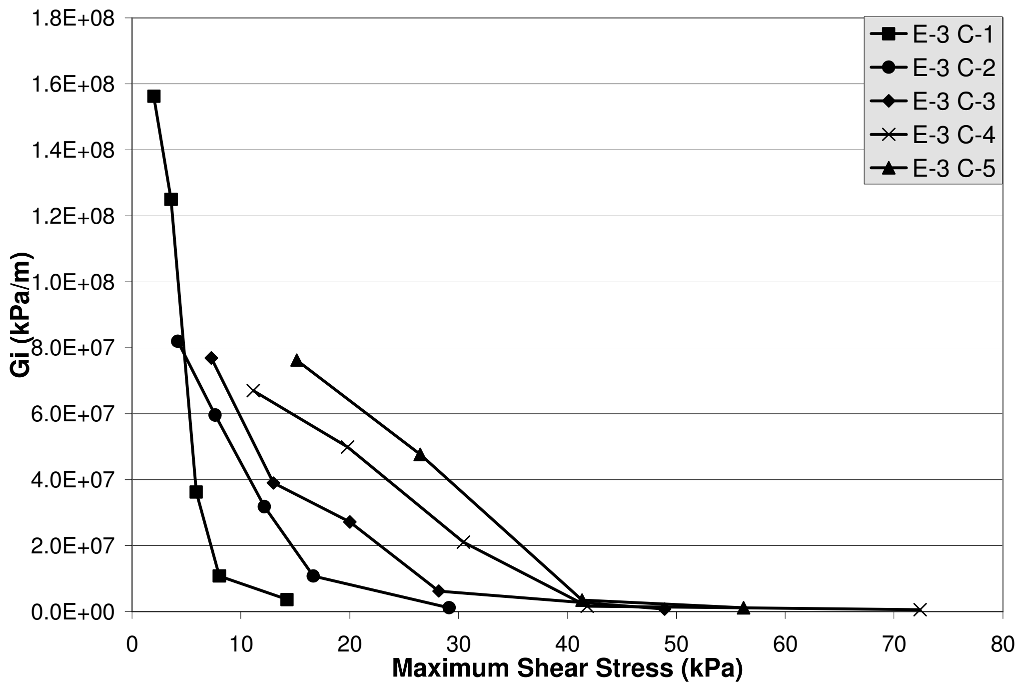

Figure 65. Test E-3 Gi.

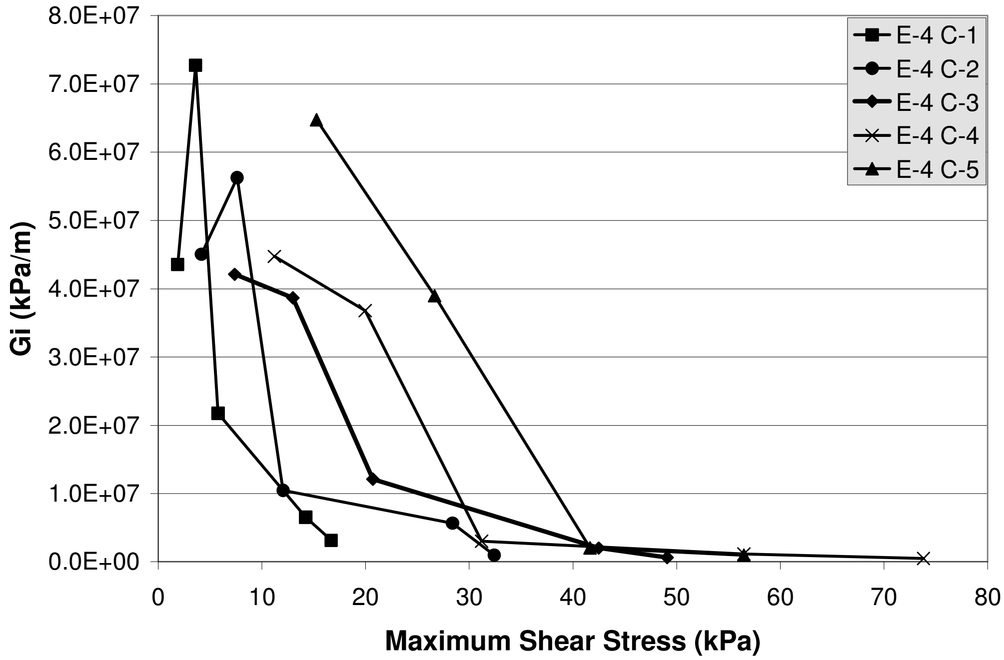

Figure 66. Test E-4 Gi.

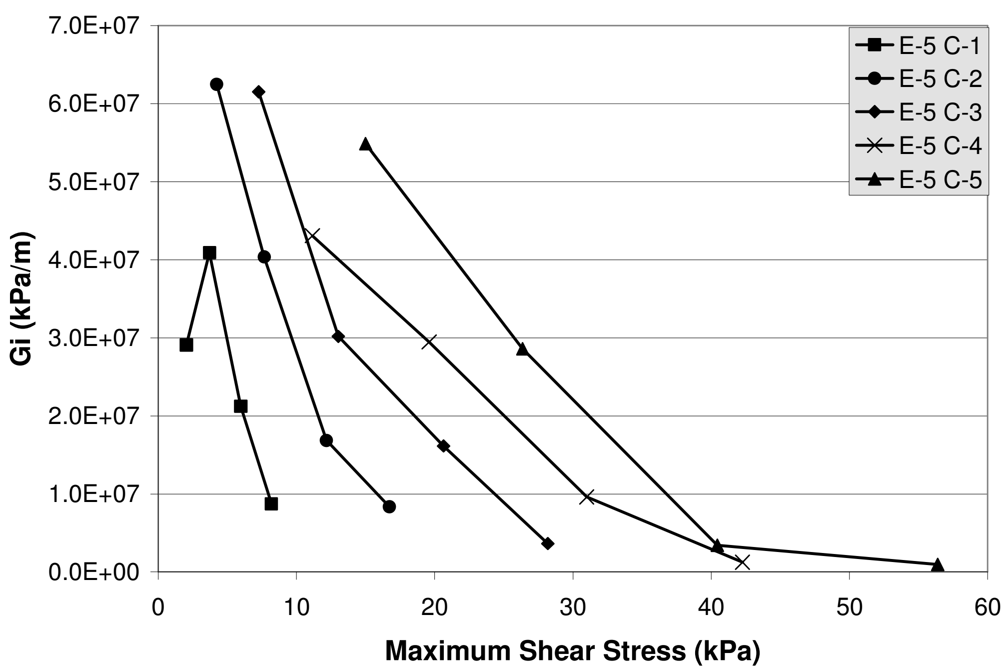

Figure 67. Test E-5 Gi.

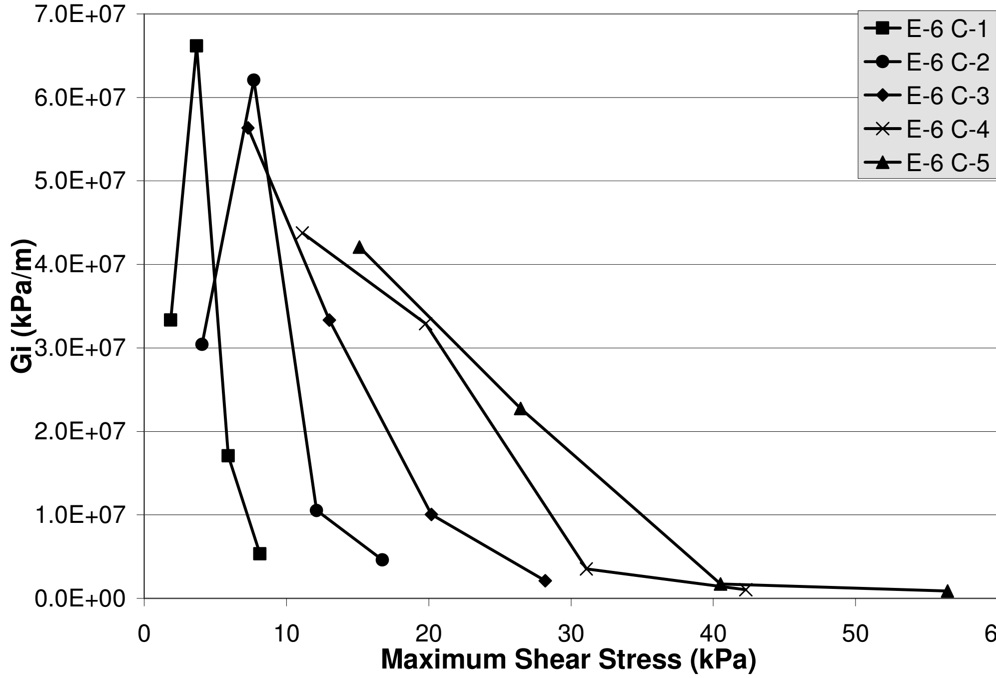

Figure 68. Test E-6 Gi.